

**OFFICE OF CIVILIAN RADIOACTIVE WASTE MANAGEMENT
ANALYSIS/MODEL COVER SHEET
Complete Only Applicable Items**

1. QA: QA
Page: 1 of 70

2. Analysis Engineering
 Performance Assessment
 Scientific

3. Model Conceptual Model Documentation
 Model Documentation
 Model Validation Documentation

4. Title:
Drift Degradation Analysis

5. Document Identifier (including Rev. No. and Change No., if applicable):
ANL-EBS-MD-000027 REV 00

6. Total Attachments:
Six

7. Attachment Numbers - No. of Pages in Each:
I-9, II-5 (plus 1 CD), III-9, IV-6, V-6, VI-4

	Printed Name	Signature	Date
8. Originator	Dwayne C. Kicker	<i>Dwayne C. Kicker</i>	11/4/99
9. Checker	Marek J. Mrugala	<i>Marek J. Mrugala</i>	11/4/99
10. Lead/Supervisor	Dwayne A. Chesnut	<i>for Randolph J. Schuiri</i>	11/4/99
11. Responsible Manager	Dwayne A. Chesnut	<i>for Randolph J. Schuiri</i>	11/4/99

2. Remarks:

This Analysis and Model Report (AMR) was prepared by the Engineered Barrier System Operations (EBSO) as an internal input to the activities related to the Process Model Report (PMR) within the EBSO. No external organization that may be affected by this document was identified. Therefore, a technical review under procedure AP-2.14Q is not required.

Supervisor: Dwayne A. Chesnut

Randolph J. Schuiri
11/4/99

Ming Lin provided a significant contribution to the development of Sections 6.3 and 6.4 of this analysis.

John Kemeny provided support in the analysis of seismic and thermal effects on drift degradation, and in the rock fall frequency assessment (Section 6.4.2)

TBV-1290 applies to the DRKBA Version 3.3 software used in this analysis.

TBV-3472 applies to the unqualified fracture data inputs used in this analysis.

Data confirmation TBVs as documented in Attachment I apply to this analysis.

**OFFICE OF CIVILIAN RADIOACTIVE WASTE MANAGEMENT
ANALYSIS/MODEL REVISION RECORD**

Complete Only Applicable Items

1. Page: 2 of 70

2. Analysis or Model Title:

Drift Degradation Analysis

3. Document Identifier (including Rev. No. and Change No., if applicable):

ANL-EBS-MD-000027 REV 00

4. Revision/Change No.

5. Description of Revision/Change

00

Initial issue.

CONTENTS

	Page
ACRONYMS.....	9
1. PURPOSE.....	11
1.1 BACKGROUND.....	11
1.2 OBJECTIVES.....	11
1.3 WORK SCOPE.....	12
1.4 ANALYSIS APPLICABILITY.....	12
2. QUALITY ASSURANCE.....	13
3. COMPUTER SOFTWARE.....	14
3.1 QUALIFIED COMPUTER SOFTWARE.....	14
3.2 UNQUALIFIED SOFTWARE.....	14
3.3 OTHER SOFTWARE.....	14
4. INPUTS.....	15
4.1 DATA AND PARAMETERS.....	15
4.2 CRITERIA.....	18
4.3 CODES AND STANDARDS.....	18
5. ASSUMPTIONS.....	19
6. ANALYSIS.....	20
6.1 INTRODUCTION.....	20
6.2 FIELD OBSERVATION OF KEY BLOCKS.....	20
6.3 APPROACH.....	20
6.3.1 DRKBA Approach.....	24
6.3.2 Statistical Representation of Joint Data.....	24
6.3.3 Excavation Modeling.....	29
6.3.4 Seismic Consideration.....	32
6.3.5 Thermal and Fracture-Degradation Consideration.....	32
6.4 ANALYSIS RESULTS.....	33
6.4.1 Prediction of Key Block Size and Distribution.....	34
6.4.1.1 Static Condition.....	34
6.4.1.2 Quasi-Static Seismic Analysis Results.....	34
6.4.2 Rock Fall Related to Time-Dependent and Thermal Effects.....	52
6.4.3 Drift Profile Prediction.....	52
7. CONCLUSIONS.....	63
7.1 SUMMARY.....	63
7.2 ASSESSMENT.....	63

CONTENTS (Continued)

	Page
7.3 TBV IMPACT	64
7.4 RECOMMENDATIONS.....	64
8. REFERENCES	65
8.1 DOCUMENTS CITED	65
8.2 CODES, STANDARDS, REGULATIONS, AND PROCEDURES.....	66
8.3 SOURCE DATA, LISTED BY DATA TRACKING NUMBER	67
 ATTACHMENT I –	 DOCUMENT INPUT REFERENCE SHEET I-1
 ATTACHMENT II –	 DRIFT DEGRADATION ANALYSIS COMPUTER FILES II-1
 ATTACHMENT III –	 CALCULATION EXAMPLE FOR JOINT PARAMETERS USED IN DRKBA ANALYSIS..... III-1
 ATTACHMENT IV – DETERMINATION OF THE NUMBER OF DRKBA MONTE CARLO SIMULATIONS IV-1
 ATTACHMENT V – QUASI-STATIC APPROACH FOR SIMULATION OF SEISMIC EFFECT.....	 V-1
 ATTACHMENT VI – TIME DEPENDENT AND THERMAL EFFECTS ON JOINT COHESION.....	 VI-1

FIGURES

	Page
Figure 1. Illustration of a Typical Key Block and Associated Fracture Planes	21
Figure 2. Evidence of Key Block Occurrence in the ECRB Cross Drift, Station 11+55	22
Figure 3. Opening Profile at ESF Station 60+24.70 (Steel Set #1272, Tptpmn Lithostratigraphic Unit) Based on Field Survey Data.....	23
Figure 4. Determination of Primary Joint Sets, Tptpul	25
Figure 5. Determination of Primary Joint Sets, Tptpmn	26
Figure 6. Determination of Primary Joint Sets, Tptpll	27
Figure 7. Determination of Primary Joint Sets, Tptpln	28
Figure 8. Degradation of Joint Cohesion with Respect to Time	33
Figure 9. Cumulative Block Size Distribution for Various Drift Orientations in the Tptpul Unit, Static Condition	35
Figure 10. Cumulative Block Size Distribution for Various Drift Orientations in the Tptpmn Unit, Static Condition	36
Figure 11. Cumulative Block Size Distribution for Various Drift Orientations in the Tptpll Unit, Static Condition	37
Figure 12. Cumulative Block Size Distribution for Various Drift Orientations in the Tptpln Unit, Static Condition	38
Figure 13. Block Size vs. Drift Orientation, Tptpul Unit	40
Figure 14. Block Size vs. Drift Orientation, Tptpmn Unit	41
Figure 15. Block Size vs. Drift Orientation, Tptpll Unit	41
Figure 16. Block Size vs. Drift Orientation, Tptpln Unit	42
Figure 17. Maximum Block Size vs. Drift Orientation	42
Figure 18. Cumulative Key Block Size Distribution for Seismic Consideration in the Tptpul Unit	44
Figure 19. Cumulative Key Block Size Distribution for Seismic Consideration in the Tptpmn Unit	45

FIGURES (Continued)

	Page
Figure 20. Cumulative Key Block Size Distribution for Seismic Consideration in the Tptpll Unit	46
Figure 21. Cumulative Key Block Size Distribution for Seismic Consideration in the Tptpln Unit	47
Figure 22. Block Size vs. Seismic Category, Tptpul Unit	49
Figure 23. Block Size vs. Seismic Category, Tptpmn Unit	50
Figure 24. Block Size vs. Seismic Category, Tptpll Unit	50
Figure 25. Block Size vs. Seismic Category, Tptpln Unit	51
Figure 26. Backfill Configuration and Simplified Opening Geometry	54
Figure 27. Emplacement Drift Profiles Considering Seismic Effects on Rock Fall for the Tptpul Unit	55
Figure 28. Emplacement Drift Profiles Considering Seismic Effects on Rock Fall for the Tptpmn Unit	56
Figure 29. Emplacement Drift Profiles Considering Seismic Effects on Rock Fall for the Tptpll Unit	57
Figure 30. Emplacement Drift Profiles Considering Seismic Effects on Rock Fall for the Tptpln Unit	58
Figure 31. Emplacement Drift Profiles Considering Time-Dependent and Thermal Effects on Rock Fall for the Tptpul Unit	59
Figure 32. Emplacement Drift Profiles Considering Time-Dependent and Thermal Effects on Rock Fall for the Tptpmn Unit	60
Figure 33. Emplacement Drift Profiles Considering Time-Dependent and Thermal Effects on Rock Fall for the Tptpll Unit	61
Figure 34. Emplacement Drift Profiles Considering Time-Dependent and Thermal Effects on Rock Fall for the Tptpln Unit	62

TABLES

	Page
Table 1. Origin of Data for Joint Geometrical Parameters	15
Table 2. Geotechnical Data Sources for the Drift Degradation Analysis	16
Table 3. Inputs for Joint Strength Parameters	17
Table 4. Selected Peak Ground Accelerations for Seismic Analysis	17
Table 5. Joint Set Orientation Data and Concentration Factors	30
Table 6. Beta Distribution Parameters for Ttpul Unit	30
Table 7. Beta Distribution Parameters for Ttpmn Unit	31
Table 8. Beta Distribution Parameters for Ttpll Unit	31
Table 9. Beta Distribution Parameters for Ttpln Unit	31
Table 10. Reduced Joint Strength Parameters to Account for Seismic Effect	32
Table 11. Block Volume (in cubic meter) Corresponding to Various Levels of Predicted Cumulative Frequency of Occurrence, Performance Confirmation Drift in Ttpul Unit	39
Table 12. Block Volume (in cubic meter) Corresponding to Various Levels of Predicted Cumulative Frequency of Occurrence, Emplacement Drift in Ttpmn Unit	39
Table 13. Block Volume (in cubic meter) Corresponding to Various Levels of Predicted Cumulative Frequency of Occurrence, Emplacement Drift in Ttpll Unit	39
Table 14. Block Volume (in cubic meter) Corresponding to Various Levels of Predicted Cumulative Frequency of Occurrence, Emplacement Drift in Ttpln Unit	40
Table 15. Predicted Number of Key Blocks per Unit Length (km) along Emplacement Drift	43
Table 16. Block Volume (in cubic meter) Corresponding to Various Level of Predicted Cumulative Frequency of Occurrence, Performance Confirmation Drift in Ttpul Unit, with Seismic Consideration	48
Table 17. Block Volume (in cubic meter) Corresponding to Various Level of Predicted Cumulative Frequency of Occurrence, Performance Confirmation Drift in Ttpmn Unit, with Seismic Consideration	48

TABLES (Continued)

	Page
Table 18. Block Volume (in cubic meter) Corresponding to Various Level of Predicted Cumulative Frequency of Occurrence, Performance Confirmation Drift in Tptpll Unit, with Seismic Consideration	48
Table 19. Block Volume (in cubic meter) Corresponding to Various Level of Predicted Cumulative Frequency of Occurrence, Performance Confirmation Drift in Tptpln Unit, with Seismic Consideration	49
Table 20. Predicted Number of Key Blocks per Unit Length (km) along Emplacement Drift, with Seismic Consideration	51
Table 21. Predicted Average Volume of Key Blocks per Unit Length along Emplacement Drift, with Seismic Consideration	52
Table 22. Reduced Joint Cohesion to Account for Time-Dependent and Thermal Effects	53
Table 23. Predicted Number of Key Blocks per Unit Length (km) along Emplacement Drift, with Time-Dependent and Thermal Consideration	53
Table 24. Predicted Average Volume of Key Blocks per Unit Length (km) along Emplacement Drift, with Time-Dependent and Thermal Consideration	53

ACRONYMS

ACC	Records Processing Center accession number
AMR	analysis and modeling report
AP	administrative procedure
CD	compact disc
CFR	Code of Federal Regulations
CRWMS M&O	Civilian Radioactive Waste Management System Management and Operating Contractor
DLS	detailed line survey
DOE	U.S. Department of Energy
DRKBA	Discrete Region Key Block Analysis
DTN	data tracking number
ECRB	Enhanced Characterization of the Repository Block
ESF	Exploratory Studies Facility
FPGM	full periphery geologic map
LADS	License Application Design Selection
M&O	Management and Operating Contractor
MCS	Monte Carlo simulation
MGR RD	Monitored Geologic Repository Requirements Document
NLP	Nevada line procedure
NRG	North Ramp geotechnical borehole
PGA	peak ground acceleration
PMR	process model report
QA	quality assurance
QAP	quality administrative procedure
SD	systematic drilling borehole
SNL	Sandia National Laboratories
TBD	to be determined
TBV	to be verified
TCw	Tiva Canyon welded tuff thermal mechanical unit
TIC	Technical Information Center
Tptpll	Topopah Spring Tuff crystal poor lower lithophysal zone
Tptpln	Topopah Spring Tuff crystal poor lower nonlithophysal zone
Tptpmn	Topopah Spring Tuff crystal poor middle nonlithophysal zone

ACROYNMS (Continued)

Tptpul	Topopah Spring Tuff crystal poor upper lithophysal zone
TSw2	Topopah Spring welded, lithophysal-poor thermal mechanical unit
UDEC	Universal Distinct Element Code
USBR	U.S. Bureau of Reclamation
USGS	U.S. Geological Survey

1. PURPOSE

The purpose of this analysis and modeling report (AMR) is to analyze the deterioration of the rock mass surrounding the potential repository emplacement drifts, and provide data to the Engineered Barrier System (EBS) post-closure performance assessment. This analysis has been developed according to the guidance provided by the *Development Plan for Drift Degradation Analysis* (CRWMS M&O 1999a). The output of this analysis documents expected drift deterioration for the License Application Design Selection (LADS) for the repository (Wilkins and Heath 1999). The analysis will provide input data to two EBS AMRs: the Physical and Chemical Environment Model, and the Water Distribution and Removal Model.

1.1 BACKGROUND

A probabilistic key block analysis was initially proposed as part of the Exploratory Studies Facility (ESF) design confirmation activities. These plans included an analysis of geotechnical mapping data from the ESF to identify the size of potential key blocks, assess specific key blocks occurring in the field, and conduct a stability analysis on these blocks, if necessary, to confirm the effectiveness of the existing ground support. Large key blocks are significant because they have the potential to increase ground support loads, and if disturbed by a seismic event, could potentially fail if the ground support is not adequate.

As part of this initial planning, technical literature sources were reviewed for the purpose of determining the most appropriate approach to be used in the development of a key block analysis for the Yucca Mountain Site Characterization Project. As a result, the Discrete Region Key Block Analysis (DRKBA) software was purchased. The DRKBA probabilistic approach is unique and is distinguished from traditional key block analyses in that it not only assesses the maximum size of key blocks, but it also predicts the number of potential key blocks that will be formed within a referenced length of tunnel. The DRKBA approach also allows for a variety of tunnel and jointing configurations.

It was recognized that this key block analysis has the potential to provide necessary information to support several key project documents, including the Site Recommendation Report and the License Application. The potential users of the key block analysis include Waste Package Operations, Repository Systems Operation, Performance Assessment Operations, and Engineered Barrier Systems Operations.

1.2 OBJECTIVES

The specific objectives of the Drift Degradation Analysis are:

- to provide a statistical description of block sizes formed by fractures around the emplacement drifts for the lithologic units of the repository host horizon
- to estimate changes in drift profiles resulting from progressive deterioration of the emplacement drifts both with and without backfill
- to provide an estimate of the time required for significant drift deterioration to occur.

1.3 WORK SCOPE

These activities involve using analytical methods, including both a distinct element numerical code and the DRKBA (key block) numerical code, and performing calculations and statistical analyses to determine the expected quantities, locations, size distributions and frequencies of rock fall, based on the LADS for the repository (CRWMS M&O 1997a; Wilkins and Heath 1999). Deteriorated drift profiles as a result of rock fall have been determined. This analysis has considered various emplacement drift orientations, with the drift azimuth varied in appropriate increments to examine the effect of orientation on key block size and frequency. This analysis has examined unsupported drifts, both with and without backfill, and applied static, thermal, and seismic loading conditions.

1.4 ANALYSIS APPLICABILITY

The drift degradation results, including the drift profiles, are applicable for the LADS for the repository (CRWMS M&O 1997a, pp. 22 and 33; Wilkins and Heath 1999), which includes 5.5-m-diameter emplacement drifts oriented at a bearing of N72W. The key block analysis is constrained by various joint configuration assumptions as identified in Section 5.

2. QUALITY ASSURANCE

This AMR has been developed in accordance with AP-3.10Q as an implementing document of Work Package 12012383MX. A Development Plan (CRWMS M&O 1999a) was used, and a Technical Change Request was processed in accordance with AP-2.13Q and AP-3.4Q, respectively.

A QAP-2-0 activity evaluation was performed for the preparation of this report, which showed that this analysis activity is subject to the controls of a QA program (CRWMS M&O 1999b). There are no QAP-2-3 Classification of Permanent Items and NLP-2-0 Determination of Importance Evaluations directly applicable to the development of this document. Unverified and undetermined data are identified and tracked in accordance with AP-3.15Q.

All computer software used in this analysis are identified in Section 3. Qualified codes include Universal Distinct Element Code (UDEC) Version 2.0. Unqualified codes include DRKBA Version 3.3. DRKBA is expected to be qualified by the end of November 1999. The data generated using DRKBA has been identified as to be verified (TBV). Output data/results developed in this AMR have been submitted to the TDMS in accordance with AP-SIII.3Q.

In addition to the procedures cited above, the following procedures are applicable to this document: AP-6.1Q, AP-3.14Q, AP-3.17Q, AP-SI.1Q, AP-SIII.2Q, and YAP-SV.1Q.

3. COMPUTER SOFTWARE

3.1 QUALIFIED COMPUTER SOFTWARE

UDEC Version 2.0 (CRWMS M&O 1994) was used in parts of this drift degradation analysis. UDEC was used to analyze the seismic and thermal effects on block movement. The analyses were performed on a computer with a Pentium microprocessor. UDEC software is appropriate for the applications used in this drift degradation analysis. UDEC was obtained from the Configuration Management in accordance with the applicable M&O procedures. UDEC software was used only within the range of validation as specified in the software qualification documentation (CRWMS M&O 1994). A complete listing of UDEC input files used in this analysis is provided in [Attachment II](#). The outputs are described in [Attachment V](#). A complete listing of output files is also provided in [Attachment II](#).

3.2 UNQUALIFIED SOFTWARE

DRKBA Version 3.3 (software tracking number: 10071-3.3-00) was used in parts of this drift degradation analysis. DRKBA was used to simulate the formation of blocks formed in the rock mass based on tunnel mapping data, and to analyze these blocks to determine if they are stable. DRKBA is currently unqualified due to resource and schedule constraints. DRKBA calculations reported in this AMR are considered unqualified and carry TBV-1290. DRKBA Version 3.3 is expected to be qualified by the end of November 1999. A complete listing of DRKBA input files used in this analysis is provided in [Attachment II](#). The outputs are described in Section 6. A complete listing of output files is also provided in [Attachment II](#).

3.3 OTHER SOFTWARE

In addition to the above listed items, both *Microsoft Excel 97* and *Mathcad 7 Professional* were also used. These software items were used to perform support activities and are not the controlled source of information in this drift degradation analysis, and thus not subject to software management per AP-SI.1Q.

Excel is a commercial spreadsheet program designed to assist in routine calculations. The program provides built-in mathematical functions together with user-defined formulas to automate the calculation process. Output formulas are automatically updated as input data are added or changed. *Excel* also includes a graphical package to assist in data presentation. *Excel* was used to calculate excavation orientation inputs, to assist in the summary of the block size data, and to provide graphical presentation of the block size distribution data.

Mathcad is an all-purpose program for performing and documenting mathematical calculations. *Mathcad* has many built-in functions for conducting mathematical calculations. *Mathcad* was used to calculate both excavation orientation and joint description input parameters.

4. INPUTS

4.1 DATA AND PARAMETERS

The geotechnical parameters include data and information collected either by field mapping or by laboratory testing. Two sets of geometrical data for joints were used in this analysis. The first set, collected from the Exploratory Studies Facility (ESF) Main Loop (i.e., the North Ramp, Main Drift, and South Ramp), is referred to as the ESF data in this report. The second set, collected from the Enhanced Characterization of the Repository Block (ECRB) Cross Drift, is called the ECRB data. Qualified joint mapping data for the Topopah Spring Tuff crystal poor upper lithophysal zone (Tptpul) and Topopah Spring Tuff crystal poor middle nonlithophysal zone (Tptpmn) lithologic units are available from the ESF data. Qualified joint mapping data for the Tptpul, Tptpmn, Topopah Spring Tuff crystal poor lower lithophysal zone (Tptpll), and Topopah Spring Tuff crystal poor lower nonlithophysal zone (Tptpln) lithologic units are available from the ECRB data. It should be noted that a study of small trace length fractures has been initiated in the ECRB Cross Drift. The data collected from the small trace length fracture study have not been finalized and were not available for this analysis. A future revision of this work may include this additional data.

Mapping data from the ESF being used in the analysis includes both U.S. Geological Survey/U.S. Bureau of Reclamation (USGS/USBR) Full Periphery Geologic Maps (FPGMs) and the Detailed Line Survey (DLS). Developed fracture data, including joint set orientation, joint spacing, joint trace length, and joint offset from the DLS, have been provided by the CRWMS M&O (1999d). The developed fracture data are based on final, qualified fracture data as listed in [Tables 1 and 2](#). However, the developed fracture data are preliminary and are in the process of being documented according to a qualified procedure. These data therefore carry TBV-3472. Fracture strike and dip data contained in the electronic files of the FPGMs were used to determine fracture set orientation, while fracture set spacing and trace length data were obtained from the DLS. All fracture spacing information for the primary joint sets has been converted to “true spacing”. Details for the determination of fracture set orientations, the identification of joint sets, and fracture spacing and trace length data are provided in Section 6.

The origin of the data for specific joint geometrical parameters is listed in [Table 1](#), with the data sources for FPGMs and DLSs provided in [Table 2](#).

[Table 1. Origin of Data for Joint Geometrical Parameters](#)

Lithologic Unit	Origin of Joint Geometrical Parameters		
	Joint Set Orientation	Joint Spacing	Joint Trace Length
Tptpul	ESF FPGM & ECRB FPGM	ESF DLS & ECRB DLS	ESF DLS & ECRB DLS
Tptpmn	ESF FPGM & ECRB FPGM	ESF DLS & ECRB DLS	ESF DLS & ECRB DLS
Tptpll	ECRB FPGM	ECRB DLS	ECRB DLS
Tptpln	ECRB FPGM	ECRB DLS	ECRB DLS

Table 2. Geotechnical Data Sources for the Drift Degradation Analysis¹

Description of Data	Data Tracking Number	Organizational Responsibility
ESF DLS, Stations 18+00 through 26+00, Rev. 01	GS971108314224.024	USGS/USBR
ESF DLS, Stations 26+00 through 30+00, Rev. 01	GS971108314224.025	USGS/USBR
ESF DLS, Stations 30+00 through 35+00, Rev. 00	GS960708314224.008	USGS/USBR
ESF DLS, Stations 35+00 through 40+00, Rev. 00	GS960808314224.011	USGS/USBR
ESF DLS, Stations 40+00 through 45+00, Rev. 00	GS960708314224.010	USGS/USBR
ESF DLS, Stations 45+00 through 50+00, Rev. 01	GS971108314224.026	USGS/USBR
ESF DLS, Stations 50+00 through 55+00, Rev. 00	GS960908314224.014	USGS/USBR
ESF DLS, Stations 55+00 through 60+00, Rev. 01	GS971108314224.028	USGS/USBR
ESF DLS, Stations 60+00 through 65+00, Rev. 00	GS970208314224.003	USGS/USBR
ESF DLS, Stations 70+00 through 75+00, Rev. 00	GS970808314224.010	USGS/USBR
ESF FPGM, Station 04+00 to 26+00 Revision 1	GS960908314224.020	USGS/USBR
ESF FPGM, Station 26+00 to 30+00 Revision 0	GS960808314224.012	USGS/USBR
ESF FPGM, Station 30+00 to 40+00 Revision 0	GS960908314224.015	USGS/USBR
ESF FPGM, Station 40+00 to 50+00 Revision 0	GS960908314224.016	USGS/USBR
ESF FPGM, Station 50+00 to 55+00 Revision 0	GS960908314224.017	USGS/USBR
ESF FPGM, Station 55+00 to 60+00 Revision 0	GS970108314224.002	USGS/USBR
ESF FPGM, Station 60+00 to 65+00 Revision 0	GS970208314224.004	USGS/USBR
ESF FPGM, Station 65+00 to 70+00 Revision 0	GS970808314224.009	USGS/USBR
ESF FPGM, Station 70+00 to 75+00 Revision 0	GS970808314224.011	USGS/USBR
ECRB DLS, Station 00+00 to 15+00	GS990408314224.001	USGS/USBR
ECRB DLS, Station 15+00 to 26+64	GS990408314224.002	USGS/USBR
ECRB FPGM, Station 00+00 to 10+00	GS990408314224.003	USGS/USBR
ECRB FPGM, Station 10+00 to 15+00	GS990408314224.004	USGS/USBR
ECRB FPGM, Station 15+00 to 20+00	GS990408314224.005	USGS/USBR
ECRB FPGM, Station 20+00 to 26+00	GS990408314224.006	USGS/USBR
Summary of bulk properties measurements from borehole data	SNL02030193001.027	SNL
Fracture shear strength from NRG-7	SNL02112293001.002	SNL
Fracture shear strength from NRG-4 & NRG-6	SNL02112293001.003	SNL
Fracture shear strength from SD-9	SNL02112293001.005	SNL
Fracture shear strength from NRG-7/7A and SD-12	SNL02112293001.007	SNL
Intact rock elastic properties from the TSw2 unit from NRG-5	SNL02030193001.012	SNL
Intact rock elastic properties from the TSw2 unit from NRG-6	SNL02030193001.004	SNL
Intact rock elastic properties from the TSw2 unit from NRG-7/7A	SNL02030193001.019	SNL
Intact rock elastic properties from the TSw2 unit from NRG-7/7A	SNL02030193001.020	SNL
Intact rock elastic properties from the TSw2 unit from NRG-7/7A	SNL02030193001.021	SNL
Intact rock elastic properties from the TSw2 unit from SD-9	SNL02030193001.026	SNL
Intact rock elastic properties from the TSw2 unit from SD-12	SNL02030193001.023	SNL

¹Developed DLS and FPGM fracture data are provided by CRWMS M&O (1999d).

Joint strength parameters, including cohesion and friction angle, were developed in CRWMS M&O (1997b, p. 5-143) based on laboratory shear strength test data from core specimens (see Table 2 for source data tracking number (DTN)). Mean value and standard deviation are required as the inputs for the key block analysis (Table 3).

Table 3. Inputs for Joint Strength Parameters (CRWMS M&O 1997b, p. 5-143)¹

Parameter	Cohesion (MPa)	Friction Angle (degree)
Mean	0.86	41
Standard Deviation	0.81	3

¹Source DTNs provided in Table 2.

Rock density data and intact rock elastic properties were obtained from the laboratory tests performed on the rock cores from the North Ramp geotechnical (NRG) and the systematic drilling (SD) boreholes (CRWMS M&O 1997b, pp. 5-26, 5-88, and 5-96). The DTN for the rock properties data is provided in Table 2. The saturated bulk density (ρ) of 2.41 g/cc for Tptpln unit was used in the analysis (CRWMS M&O 1997b, pp. 5-26). This value was selected for conservatism since the value is the highest of the examined units. Mean elastic rock properties from the TSw2 thermal mechanical unit, including an elastic modulus of 33.03 GPa and a Poisson's ratio of 0.21 (CRWMS M&O 1997b, pp. 5-88 and 5-96), were used in this analysis as described in Attachment V.

Design basis seismic ground motion parameters are provided by CRWMS M&O (1999e) for both Category 1 and Category 2 design basis events. A Category 1 design basis event means "those natural and human-induced events that are reasonably likely to occur regularly, moderately frequently, or one or more times before permanent closure of the geologic repository operations area." A Category 2 design basis event is defined as "other natural and man-induced events that are considered unlikely, but sufficiently credible to warrant consideration, taking into account the potential for significant radiological impacts on public health and safety." The return periods for the occurrence of Category 1 and Category 2 design basis events are 1,000 years and 10,000 years, respectively. In addition to the two categories, an intermediate category with a 5,000-year event was also considered in this analysis.

The peak ground accelerations (PGAs) for the horizontal motion in the frequency range of 5 to 10 Hz were selected for this analysis. The values are listed in Table 4. Three levels of seismic events are included: Level 1 corresponding to a 1,000-year event (Category 1), Level 2 corresponding to a 5,000-year event, and Level 3 corresponding to a 10,000-year event (Category 2).

Table 4. Selected Peak Ground Accelerations for Seismic Analysis (CRWMS M&O 1999e)

Seismic Event	Peak Ground Acceleration (g) ¹
Level 1 (1,000-year event, Category 1)	0.14
Level 2 (5,000-year event)	0.30
Level 3 (10,000-year event, Category 2)	0.43

¹The Level 2 (5,000-year event) PGA value was estimated based on the Category 1 and Category 2 PGA values. See assumption 5.5.

4.2 CRITERIA

There are no criteria from either requirements documents or System Description Documents that are applicable to this drift degradation analysis.

4.3 CODES AND STANDARDS

There are no codes and standards applicable to this drift degradation analysis.

5. ASSUMPTIONS

The following assumptions have been used in this drift degradation analysis.

- 5.1 Joints are represented as circular discs with radii equal to twice the mapped trace length. This is considered conservative since the diameter of the joint disc developed from mean trace length is much greater than the emplacement drift diameter. This assumption is used in Section 6.3.2.
- 5.2 The positioning parameter required as joint parameter input is assumed to be the offset measured from the center of the trace length to the scan line of the detailed line survey. This is the best available way to represent the positioning parameter since the determination of the true positioning parameter requires the three dimensional information of the joint plane that is not available. This approach is considered conservative because the offset measured from the one dimensional scan line is smaller than the true offset in three dimensional space (The probability of forming key block is higher with smaller offset value). This assumption is used in Section 6.3.2.
- 5.3 The key block analysis simulated in the DRKBA software does not include a ground support element. All key blocks predicted in this analysis are therefore the blocks that fail in an unsupported opening. This assumption is necessary due to the limitation of the DRKBA program. The assumption apparently will lead to a conservative prediction of key blocks for the pre-closure period and is considered adequate for the post-closure period. The assumption is used in Section 6.3.
- 5.4 This analysis uses an alternative method for joint strength reduction to simulate the seismic effect on the occurrence key blocks. This method is verified using the distinct element code UDEC (CRWMS M&O 1994). The dynamic analysis result was compared to the quasi-static analysis result adopting the alternative method. The process of verification is documented in [Attachment V](#). This assumption is used in Sections 6.3.4 and 6.4.
- 5.5 A PGA value of 0.30 g was assumed for a 5,000-year seismic event. This value is based on an interpolation from the PGA values provided for 1,000-year and 10,000-year seismic events (CRWMS M&O 1999e). This assumption is used in Section 6.4.
- 5.6 Subcritical crack growth parameters A and n were used in the analysis of time-dependent and thermal effects on joint cohesion. Conservative values of $n = 25$ and $A = 10^{-5}$ meters/second were assumed based on previous Yucca Mountain studies (Kessler and McGuire 1996). This assumption was used in Section 6.4.2 and in [Attachment VI](#).

6. ANALYSIS

6.1 INTRODUCTION

Key blocks are formed at the surrounding rock mass of an excavation by the intersection of three or more planes of structural discontinuities as shown in [Figure 1](#). This analysis provides an assessment of the possible formation of key blocks within the repository horizon based on the orientations of discontinuities present in the ESF Main Loop and in the ECRB Cross Drift. Block failure due to seismic and thermal effects have also been analyzed. The corresponding emplacement drift profiles have been developed to depict the drift degradation over time.

6.2 FIELD OBSERVATION OF KEY BLOCKS

Key blocks in the 5-m-diameter Cross Drift are first evident in the crown at about station 10+50 in the Tptpmn unit. Most of the key blocks in this region are of minor size and typically fall immediately after excavation prior to ground support installation. Key blocks are possible in this area because of the increased presence of the plane of weakness (i.e., a vapor phase parting) in the near horizontal orientation that intersects with two opposing near vertical joint planes. Fallout from these key blocks during excavation is typical of the rock in the middle non-lithophysal zone (Tptpmn) of the TSw2 thermal mechanical unit. The largest resultant void is possibly 0.5 cubic meters at approximately station 11+55 as shown in [Figure 2](#). No unstable key blocks were observed in the field.

While ground support monitoring in the ESF Main Loop has provided long-term evidence indicating stable rock support performance, there are several sections in the ESF where excessive raveling and block fall-out have occurred. These typically correspond to the “3.01X” areas, and most often occurred in fault zones and in the TCw and TSw2 thermal mechanical units. The 3.01X areas refer to sections of the ESF Main Loop that were constructed under Section 3.01X of the Subsurface General Construction specification (CRWMS M&O 1997c, p. 15). The specification indicates that special actions may be necessary to continue excavation in the event that adverse ground conditions prevent normal Tunnel Boring Machine operations. A typical opening profiles in a 3.01X area is shown in [Figure 3](#). This profile is indicative of the worst case ground conditions in the Tptpmn lithologic unit of the ESF Main Loop.

6.3 APPROACH

The approach toward this drift degradation analysis involves the following:

- Analyze blocks that have fallen in the field, and their associated joints.
- Collect and assess joint geometrical data and joint frictional properties data from the ESF Main Loop and ECRB Cross Drift to develop the joint modeling inputs for DRKBA.
- Analyze the joint data to assess the potential formation of key blocks using DRKBA, including the maximum block size.
- Analyze the seismic and thermal effects on joint and block movement.

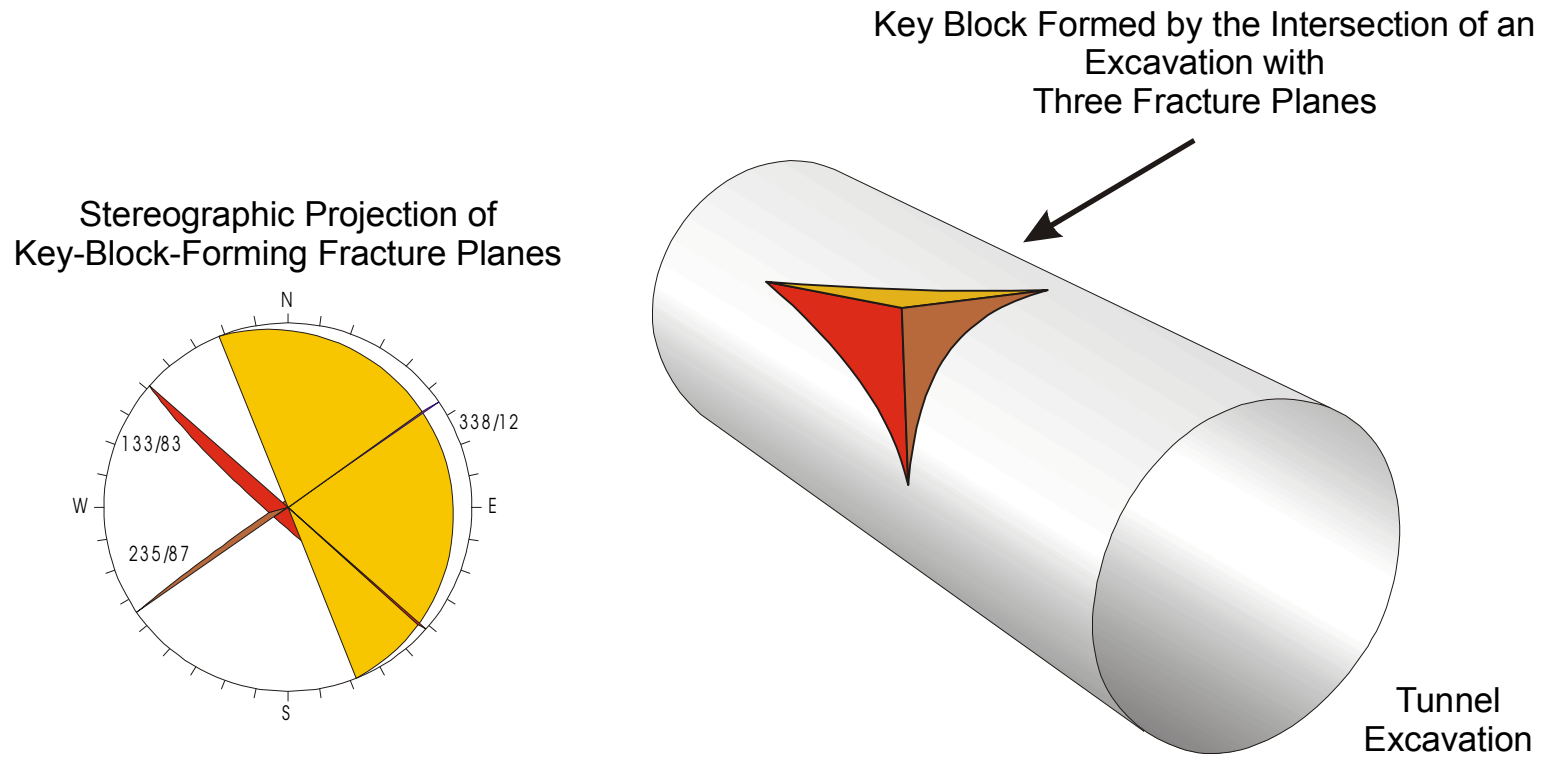


Figure 1. Illustration of a Typical Key Block and Associated Fracture Planes



Figure 2. Evidence of Key Block Occurrence in the ECRB Cross Drift, Station 11+55

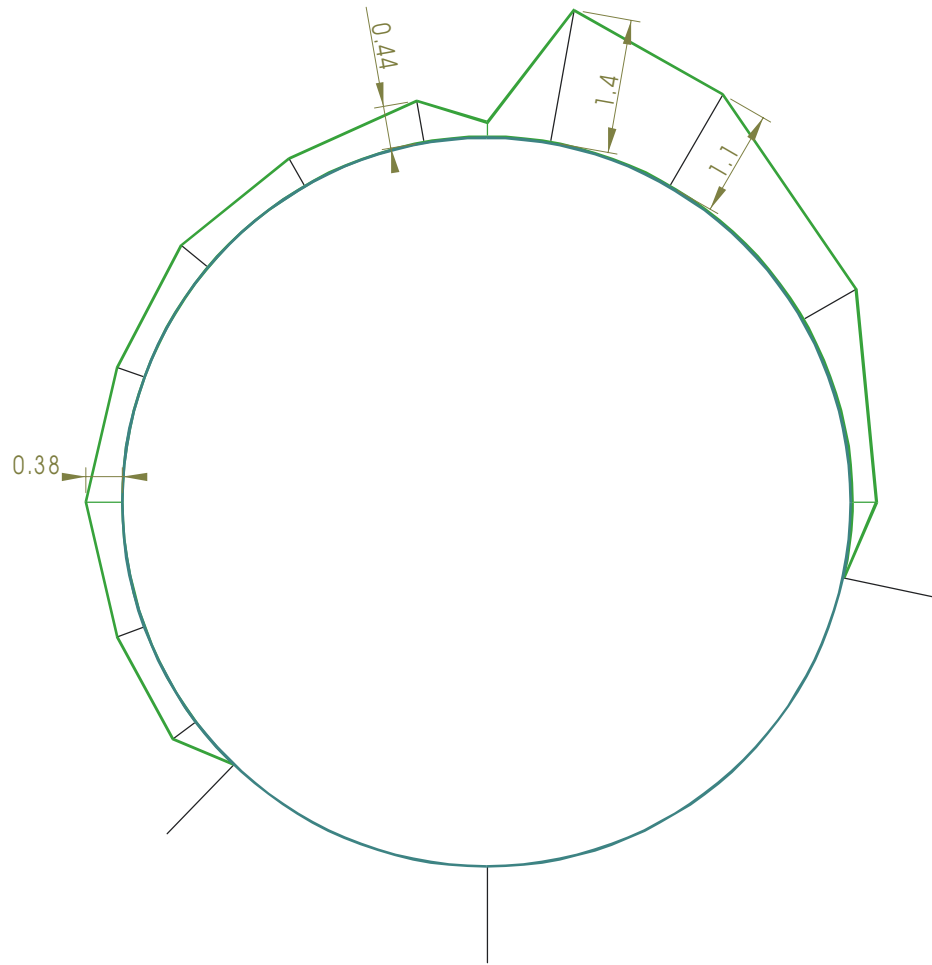


Figure 3. Opening Profile at ESF Station 60+24.70 (Steel Set #1272, Tptpmn Lithostratigraphic Unit)
Based on Field Survey Data (dimensions in meters) (CRWMS M&O 1999c, p. 27)

- Analyze the DRKBA block size distribution data for each lithologic unit within the repository host horizon.
- Determine the number and average volume of rock fall per unit length of drift for various levels of seismic hazard.
- Evaluate post-closure frequency of block failure for 10,000 years.
- Analyze the drift profile showing the progressive movement of joints and blocks with time.

6.3.1 DRKBA Approach

DRKBA is a commercially available acquired software product (as described in Section 3). The software simulates structural discontinuities as circular discs placed in the rock mass according to probabilistic distributions determined from tunnel mapping data. Joint planes are simulated by a Monte Carlo technique from probability distributions representing the orientation, spacing, and trace length of the corresponding joint set. DRKBA then analyzes these blocks to determine whether they are geometrically feasible and to determine whether they are mechanically stable.

A probabilistic key block analysis using DRKBA requires four sets of data. The required data are stored in data files having extensions .mkg, .exc, .den, and .prb, and contain information for the grid, excavation, rock density, and joint sets, respectively. The make grid file (.mkg) includes the information required for building a grid of nodal points for the mesh. The excavation data file (.exc) contains the information for defining an excavation in three dimensional space. The density file (.den) holds the information for the rock density data. The probabilistic joint data file (.prb) includes the required information for generating fracture space from the given fracture probability distributions.

The DRKBA software employs a bipolar Watson distribution for joint orientation data. The principal axis orientation and a concentration factor k are the required inputs for the bipolar Watson distribution. The concentration factor k is an index of the concentration. The larger the value of k , the more the distribution is concentrated towards the principal axis orientation. Joints are represented as circular discs in the DRKBA analysis. Joint radii (see assumption 5.1), spacings, and positioning are simulated with Beta distributions. The Beta distribution is a four-parameter distribution with the parameters a , b , p , and q . The parameters a and b represent the ends of the closed interval upon which the Beta distribution is defined. The parameters p and q determine the shape of the distribution curve, their values were calculated from the mean and standard deviation of the transformed data. The transformed data were obtained by normalizing the data with the maximum value. The cohesion and friction angle of the joints are simulated as a bivariate normal distribution. Inputs for the mean and standard deviation of the joint strength parameters are required.

6.3.2 Statistical Representation of Joint Data

Joint sets were identified based on clustering of the data from joint normal vectors plotted on stereonets as shown in Figures 4 to 7 (see Section 4, Tables 1 and 2 for data sources). The

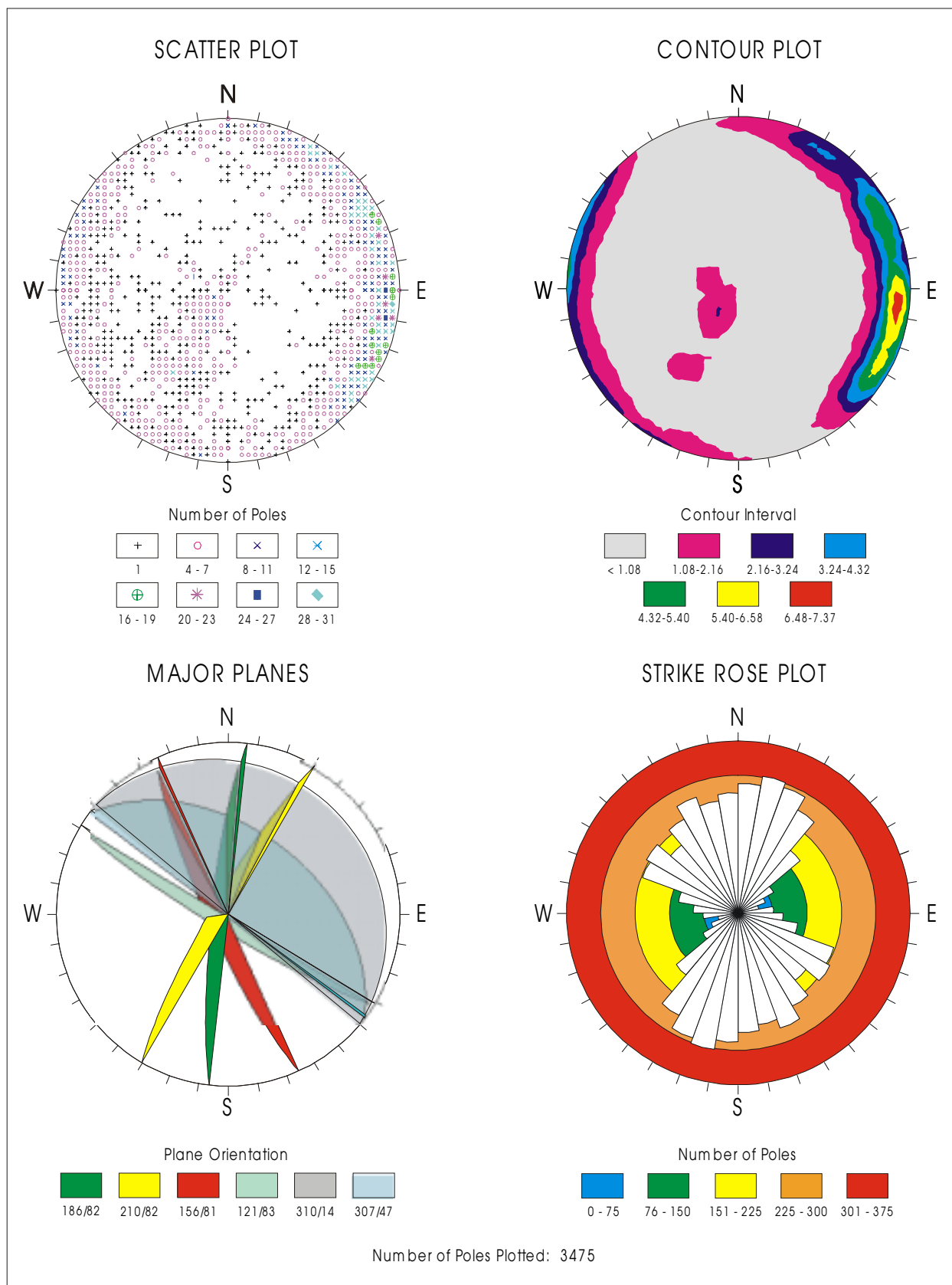


Figure 4. Determination of Primary Joint Sets, Tptpul

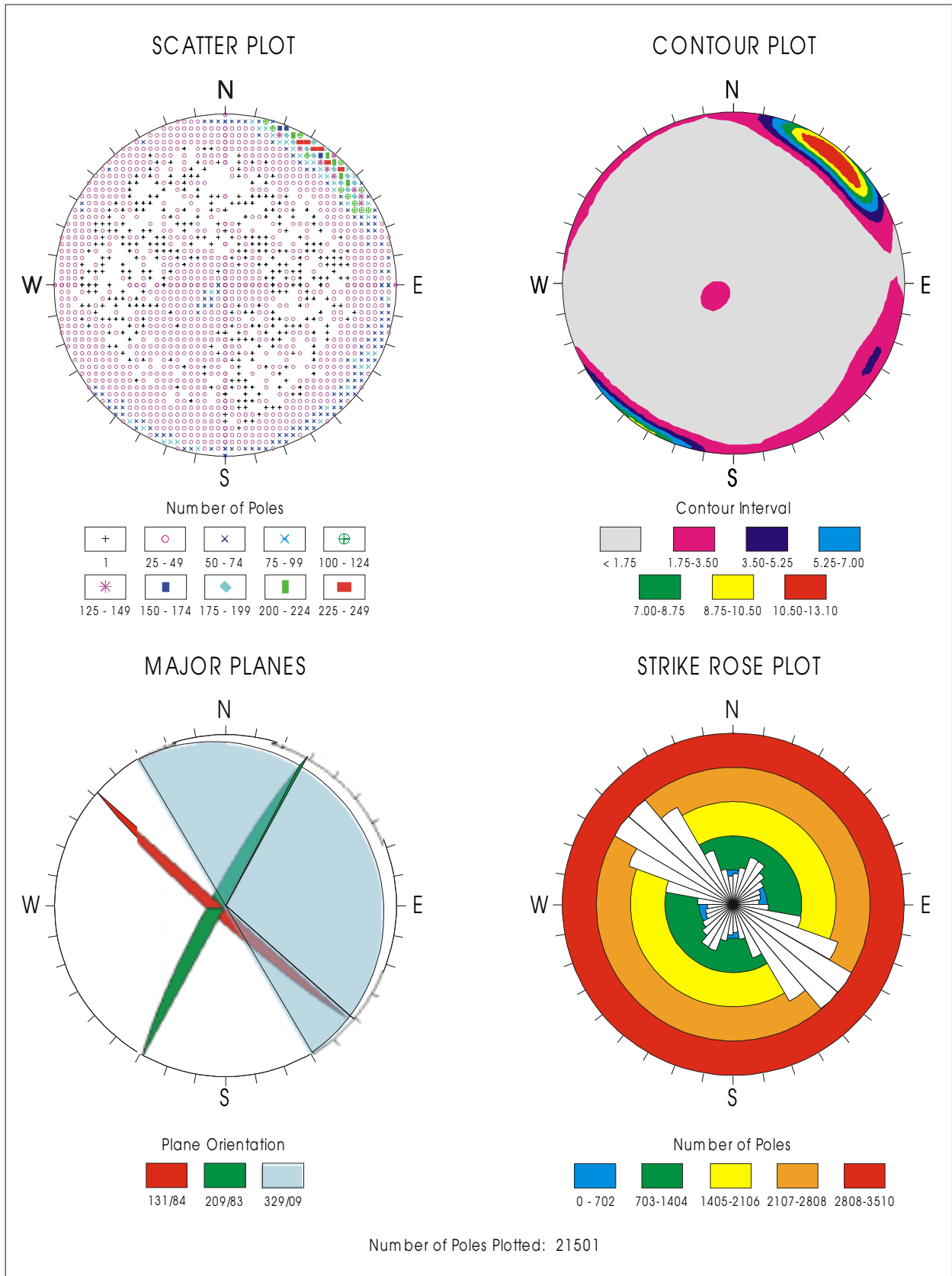


Figure 5. Determination of Primary Joint Sets, Tptpmn

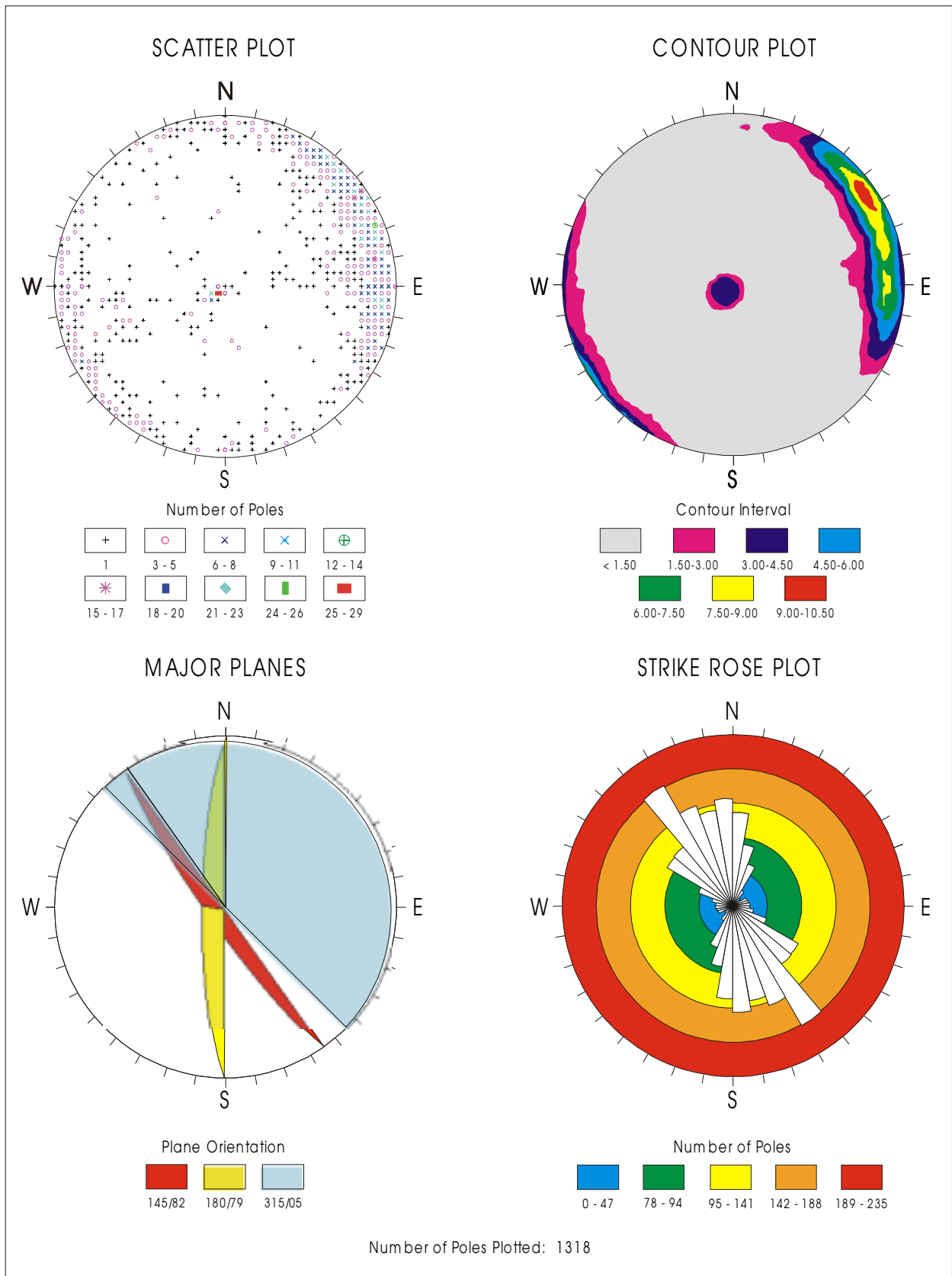


Figure 6. Determination of Primary Joint Sets, Tptpl

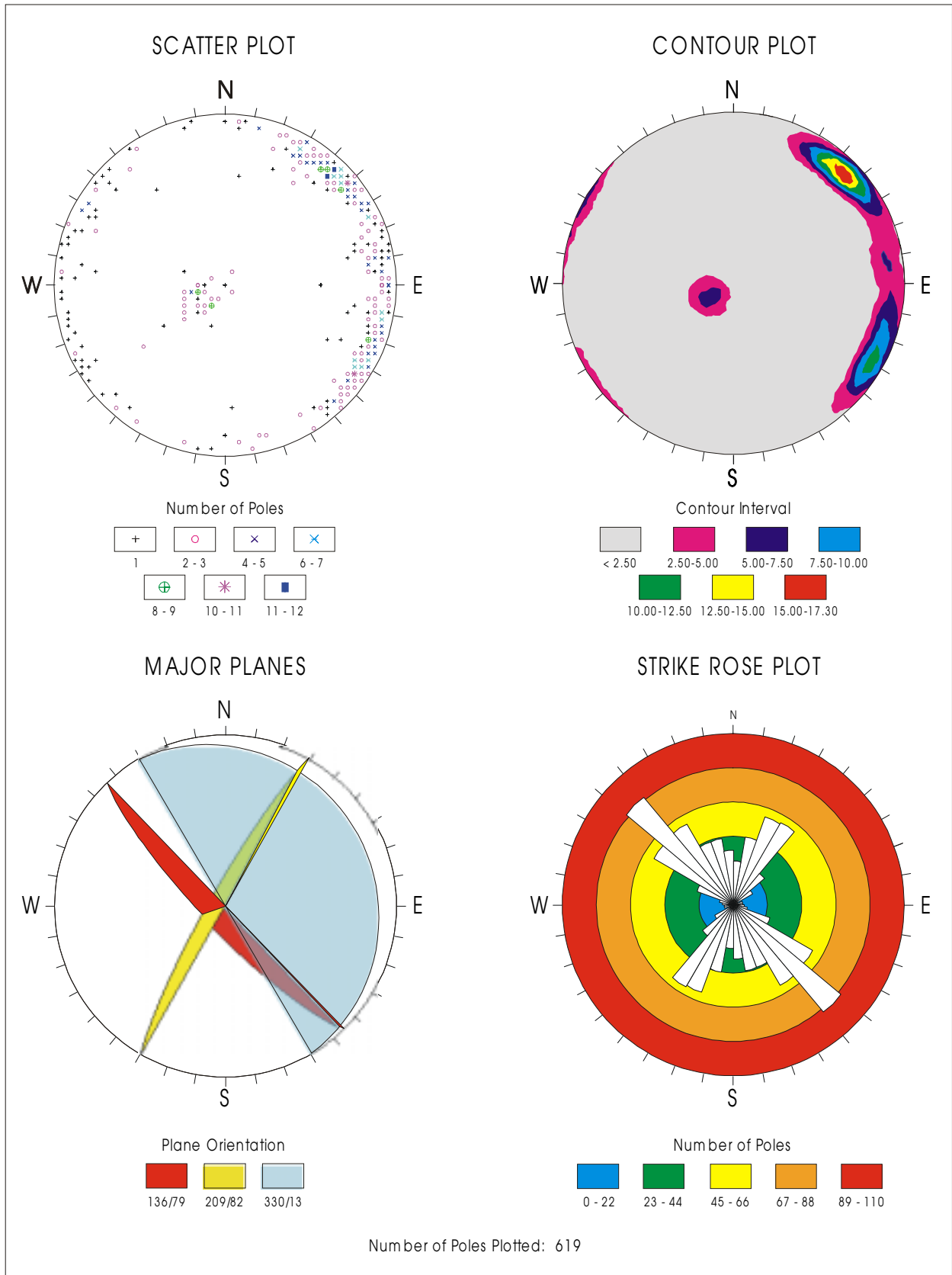


Figure 7. Determination of Primary Joint Sets, Tptpln

scatter plots, contour plots, strike rosettes, and major planes are all included in these figures. The major joint plane is expressed using the strike/dip format in these figures. The joint orientation is expressed in dip direction/dip format in [Table 5](#). In addition to the primary joint sets listed in [Table 5](#), a random joint set has also been simulated to account for any joint that is present in the rock mass but not accounted for in the primary sets. The dispersion of the individual joints about their associated joint set axes was modeled by a Watson bipolar distribution for axial data. This probability distribution is characterized by a unit normal vector representing the mean direction about which the data is clustered and a concentration factor k representing the degree to which the data is clustered about the mean direction. The concentration factors were calculated based on the eigenvalues and eigenvectors of the orientation matrix (Fisher, Lewis, and Embleton 1987). The calculated concentration factors are also listed in [Table 5](#). The process to calculate the concentration factors are included in [Attachment II](#) (see electronic files *New-K-Tptpul.mcd*, *New-K-Tptpmn.mcd*, *New-K-Tptpll.mcd*, and *New-K-Tptpln.mcd*).

Joint radii, spacings, and positioning are simulated with Beta distributions. The offset measured from the center of the trace length to the scan line was used as the positioning parameter. The parameters a , b , p and q for each lithologic unit are listed in [Tables 6 to 9](#), with the details for the calculation of each parameter provided in [Attachment II](#) (see electronic files *New-Beta-Tptpul.xls*, *New-Beta-Tptpmn.xls*, *New-Beta-Tptpll.xls*, and *New-Beta-Tptpln.xls*). [Attachment III](#) provides an example for calculating the distribution parameters with the fracture data of the first joint set for Tptpll unit.

Cohesion and friction angle of the joints are simulated with the bivariate normal distribution. Mean and standard deviation for the cohesion and friction angle are presented in [Section 4](#) (see [Table 3](#)).

6.3.3 Excavation Modeling

The primary excavation in this analysis is a horizontal 5.5-m diameter emplacement drift trending 105° in accordance with the LADS for the repository (CRWMS M&O 1997a, pp. 22 and 33; Wilkins and Heath 1999). Additionally, a range of emplacement drift orientations with the drift azimuth varying every 15° has been analyzed for the static condition only (i.e., with no seismic or thermal loading).

For each Monte Carlo simulation, a 24.4-m-long (80-ft) tunnel has been modeled in three-dimensional space. A circular tunnel opening both with and without backfill was modeled. For the cases with no backfill, 18 plane equations were used to describe the circumference of the circular tunnel, and 2 plane equations were used to describe each end of the tunnel. For the cases with backfill, a simplified tunnel geometry was used to model the opening above the backfill material as described in [Section 6.4.2](#). The backfilled opening was modeled using 15 plane equations to describe the opening perimeter, and 2 plane equations to describe the end of the tunnel. The selection for the length of the tunnel modeled and the number of planes for simulation of the circular opening were based on the computer run time and the accuracy of the simulation. Calculations for the plane equations are included in [Attachment II](#) (electronic files *exca vectors.xls* and *exca vectors-backfill.xls*). The region around the excavation has been

Table 5. Joint Set Orientation Data and Concentration Factors¹

Lithologic Unit	Joint Set Number	Mean Dip Direction ² (degrees)	Mean Dip ² (degrees)	Concentration Factor k
Tptpul	1	276	82	36.648
	2	300	82	20.576
	3	246	81	20.112
	4	211	83	22.425
	5	40	14	16.393
	6	37	14	24.210
	Random	263	70	1.850
Tptpmn	1	221	84	31.586
	2	299	83	26.143
	3	59	9	18.210
	Random	267	79	2.896
Tptpll	1	235	82	27.529
	2	270	79	24.723
	3	45	5	30.375
	Random	230	79	2.497
Tptpln	1	226	79	51.826
	2	299	82	23.304
	3	262	80	36.372
	4	60	13	49.993
	Random	254	79	1.535

¹Calculation details provided in Attachment II, files *New-K-Tptpul.mcd*, *New-K-Tptpmn.mcd*, *New-K-Tptpll.mcd*, and *New-K-Tptpln.mcd*.

²The derivation of the joint set orientation data is shown in Figures 4 through 7.

Table 6. Beta Distribution Parameters for Tptpul Unit¹

Joint Set Number	Parameters	a (m)	b (m)	p	q
1	Spacing	0.0132	16.3307	0.4223	1.5728
	Radius	2.0000	47.1800	0.2137	1.7194
	Positioning	0.0050	9.1500	0.2216	1.9098
2	Spacing	0.0015	16.3325	0.4073	1.3699
	Radius	2.0000	43.8000	0.3937	4.0620
	Positioning	0.0050	6.8500	0.4098	3.8946
3	Spacing	0.0083	16.4285	0.3545	1.1899
	Radius	2.0000	35.6000	0.3844	2.9909
	Positioning	0.0000	6.7500	0.4169	3.3486
4	Spacing	0.0098	16.0907	0.4500	1.3407
	Radius	1.8400	32.9000	0.3264	2.0332
	Positioning	0.0000	7.0000	0.2718	2.1962
5	Spacing	0.0295	14.3903	0.3171	1.1136
	Radius	2.0800	42.2000	0.4845	1.8767
	Positioning	0.0900	7.4500	0.5098	2.0530
6	Spacing	0.0070	16.4655	0.4063	1.0548
	Radius	2.1200	58.4000	0.5676	1.6409
	Positioning	0.0000	9.1500	0.3000	0.8489
Random	Spacing	0.0100	15.8700	0.6101	1.5645
	Radius	1.6400	58.0600	0.2448	2.0376
	Positioning	0.0000	9.1500	0.2186	1.6597

¹Calculation details provided in Attachment II, file *New-Beta-Tptpul.xls*.

Table 7. Beta Distribution Parameters for Tptpmn Unit¹

Joint Set Number	Parameters	a (m)	b (m)	p	q
1	Spacing	0.0008	13.9199	0.2322	5.1372
	Radius	1.8200	108.0000	0.6554	20.7171
	Positioning	0.0000	9.1500	0.7569	10.2825
2	Spacing	0.0033	16.5306	0.4098	3.0879
	Radius	1.6400	141.0600	0.2024	7.2515
	Positioning	0.0000	9.1500	0.3292	4.0327
3	Spacing	0.0018	15.2606	0.2010	5.2988
	Radius	0.3200	101.6000	0.5503	8.5360
	Positioning	0.0150	9.1500	0.6369	4.6763
Random	Spacing	0.0100	15.1900	0.5279	7.6008
	Radius	1.3000	60.6000	0.6333	9.2812
	Positioning	0.0000	9.1500	0.5735	7.6186

¹Calculation details provided in Attachment II, file *New-Beta-Tptpmn.xls*.

Table 8. Beta Distribution Parameters for Tptpll Unit¹

Joint Set Number	Parameters	a (m)	b (m)	p	q
1	Spacing	0.0123	15.7210	0.3070	1.1475
	Radius	1.9000	47.0000	0.3332	1.7478
	Positioning	0.0000	8.2500	0.3443	1.5890
2	Spacing	0.1339	13.6172	0.7050	1.7231
	Radius	2.0400	32.8000	0.1833	0.7549
	Positioning	0.0050	7.2000	0.2507	1.0294
3	Spacing	0.0293	13.7779	0.1385	0.5149
	Radius	3.0800	90.0000	0.1378	0.8908
	Positioning	0.1800	9.1500	0.3089	1.0130
Random	Spacing	0.0500	16.4900	0.5816	1.6822
	Radius	1.7200	53.2400	0.2378	2.3364
	Positioning	0.0000	9.1500	0.2141	2.0886

¹Calculation details provided in Attachment II, file *New-Beta-Tptpll.xls*.

Table 9. Beta Distribution Parameters for Tptpln Unit¹

Joint Set Number	Parameters	a (m)	b (m)	p	q
1	Spacing	0.0094	14.9637	0.1695	1.6013
	Radius	1.9800	29.6000	0.2850	0.9917
	Positioning	0.0150	5.6500	0.2812	1.0604
2	Spacing	0.0417	13.3921	0.2965	1.3043
	Radius	1.8800	51.6000	0.1993	1.1523
	Positioning	0.0600	8.1000	0.1983	0.8379
3	Spacing	0.0271	14.7493	0.5162	1.1849
	Radius	2.0000	29.8000	0.2215	0.4335
	Positioning	0.0500	5.0500	0.1764	0.2919
4	Spacing	0.0230	12.9674	0.2935	1.0515
	Radius	2.0200	10.6000	0.0993	0.6935
	Positioning	0.2150	1.5500	0.9565	2.0600
Random	Spacing	0.1800	14.4900	0.3315	1.0237
	Radius	1.7800	31.7000	0.1334	0.6527
	Positioning	0.0150	7.0750	0.1485	0.8205

¹Calculation details provided in Attachment II, file *New-Beta-Tptpln.xls*.

modeled with a grid consisting of 681,472 nodes. The nodes are spaced 0.3 m (1 ft) apart, with each node representing 0.028 cubic meters (1 cubic foot) of the rock mass.

6.3.4 Seismic Consideration

Underground openings are constrained by the surrounding medium, and it is unlikely that underground openings could move to any significant extent independently of the medium or be subjected to vibration amplification. Two potential causes of block movement during seismic events were observed. The first is related to the differential acceleration in the rock blocks surrounding the tunnel due to seismic excitation (Dowding 1979, p. 19). The second cause is the increase of the tangential force from seismic loading along the sliding surfaces of the rock block (Kaiser, McCreath, and Tannant 1996, p. 8-3).

A high-frequency seismic wave is required for the possibility of block movement due to differential acceleration (Dowding 1979, p. 19). For a case with shear wave velocity of 2000 m/sec intersecting a 5.5-m diameter drift in the repository host rock, the frequency which would produce the differential acceleration was calculated to be approximately 90 Hz. This frequency of concern is very high compared to the principal frequencies (1 to 10 Hz) with major earthquakes. Block movement due to differential acceleration is therefore not considered in this analysis.

With a relatively high ratio of wave length to opening diameter, the surrounding rock mass and the opening itself move nearly as a rigid body with free-field acceleration. A simplified quasi-static approach was used in this analysis to account for the increase of the force along the sliding surfaces. Due to the limitation of DRKBA, seismic loads can not be directly applied to the opening in the numerical simulation. An alternative method with reduction of joint strength parameters was used to account for the seismic effect. The reduced joint strength parameters are listed in [Table 10](#). This method was verified based on the test runs using the distinct element code UDEC (CRWMS M&O 1994). Justification of this method is provided in [Attachment V](#). Notice that joint cohesion is conservatively scaled down to 0.1 MPa from 0.86 MPa listed in [Table 3](#).

Table 10. Reduced Joint Strength Parameters to Account for Seismic Effect

Loading Case	Joint Cohesion (Pa)	Joint Friction Angle (degree)
Static	99,873	41
Seismic level 1	21,282	34
Seismic level 2	10,920	24
Seismic level 3	10,776	18

6.3.5 Thermal and Fracture-Degradation Consideration

The induced thermal stress and the potential degradation of joint mechanical properties are the concerns for the thermal effect to the block movement. Due to the lateral confinement of the rock, the predicted thermal stress is highest in the horizontal direction. The high horizontal thermal stress provides the locking effect for the blocks formed by the predominant vertical joint

sets during the heating period. Due to the limitation of the applying external loads using DRKBA, this locking effect was conservatively ignored in this analysis.

The degradation of joint mechanical properties due to time effect was developed by Kemeny (1991). This approach was used to develop the degradation of joint cohesion based on the site-specific parameters. Figure 8 shows the developed cohesion degradation curve. As shown in this figure, the reduction of joint cohesion is predicted to occur mainly during the first two hundred years. Detail descriptions for this approach is provided in Attachment VI.

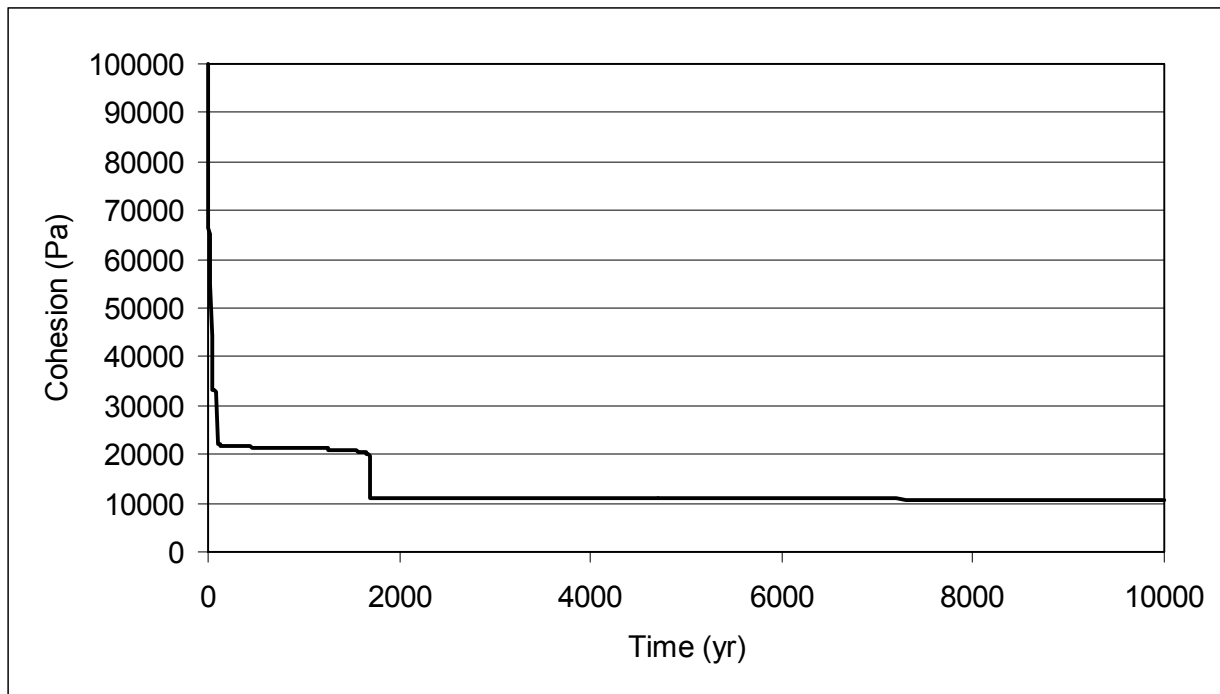


Figure 8. Degradation of Joint Cohesion with Respect to Time

6.4 ANALYSIS RESULTS

The prediction of key blocks forming at the performance confirmation drifts and emplacement drifts located at in the four lithologic units is presented in this section. The results are presented for both a static key block assessment and a quasi-static key block assessment to account for seismic, thermal, and time effects on key blocks.

In the DRKBA analysis, random joint patterns are generated with joint centers positioned in three-dimensional space, considering each joint set in sequence for each Monte Carlo simulation. The forming of key blocks is therefore different in each Monte Carlo simulation. Test runs were conducted to determine an adequate number of Monte Carlo simulations for the analyses as described in Attachment IV. Based on the test run results, 200 Monte Carlo simulations are adequate for the Tptpmn unit and 400 Monte Carlo simulations are adequate for the rest of the units.

6.4.1 Prediction of Key Block Size and Distribution

6.4.1.1 Static Condition

A range of drift orientations with the drift azimuth varied in 15° increments is considered in the static analyses. Figures 9 through 12 present the key block analysis results in the format of cumulative frequency of occurrence for each lithologic unit. The DRKBA input and output files are contained in the compact disc (CD) provided in Attachment II. The cumulative frequencies of occurrence corresponding to 50, 75, 90, 95 and 98 percentile block volume for each unit are listed in Tables 11 to 14. The maximum block sizes predicted from the analyses are also presented in this table. Corresponding graphs are presented in Figures 13 to 16. The predicted block size is generally small. The 95 percentile block ranges from 1.03 to 4.21 m³ for the Tptpul unit, 1.35 to 3.70 m³ for the Tptpmn unit, 0.55 to 8.88 m³ for the Tptpll unit, and 0.61 to 3.50 m³ for the Tptpln unit. For the orientation closest to the LADS layout (i.e., an azimuth of 105°), the 98 percentile block is 2.25 m³ for Tptpul unit, 4.57 m³ for Tptpmn unit, 5.56 m³ for Tptpll unit, and 1.77 m³ for Tptpln unit.

The maximum key block sizes for the range of tunnel orientations evaluated are shown in Figure 17. The orientations predicted for the higher maximum key block sizes are in general parallel to the major high-angle joint sets (major joint set orientations are listed in Table 5). The maximum key block size predicted in this analyses for the emplacement drift is 66 m³ when the drift is oriented at an azimuth of 150° in Tptpll unit. Maximum key block sizes are in general less than 9 m³ when the drift is oriented in between 75° azimuth and 105° azimuth. The lowest maximum block size of 0.75 m³ is found in Tptpll when the drift is oriented at an azimuth of 90°.

The predicted numbers of key blocks per unit length of emplacement drift are listed in Table 15. The number of key blocks formed in the lithophysal rock (i.e., the Tptpul and Tptpll units) and in the Tptpln unit was predicted to be scarce. The number of blocks predicted per 1 km of drift range from 12 to 20 for the Tptpul unit, 1 to 6 for Tptpll unit, 2 to 12 for Tptpln unit. Key blocks are most predominant in the Tptpmn unit, the number of blocks ranging from 26 to 63 per 1 km of drift. The orientations that are predicted to have a higher number of blocks are in general parallel to the major high-angle joint sets. This trend is consistent with that observed for the prediction of the maximum block size.

6.4.1.2 Quasi-Static Seismic Analysis Results

The results for quasi-static analysis with the consideration of seismic effects on rock fall are presented in this section. The method used for the quasi-static analysis to simulate the seismic effect is described in Section 6.3.4. Three levels of earthquake representing 1,000-year event (Level 1), 5,000-year event (Level 2), and 10,000-year event (Level 3) are considered. The LADS drift orientation with an azimuth of 105° is the designated orientation for the quasi-static analysis. The inputs and outputs related to the quasi-static analysis are contained in the CD provided in Attachment II.

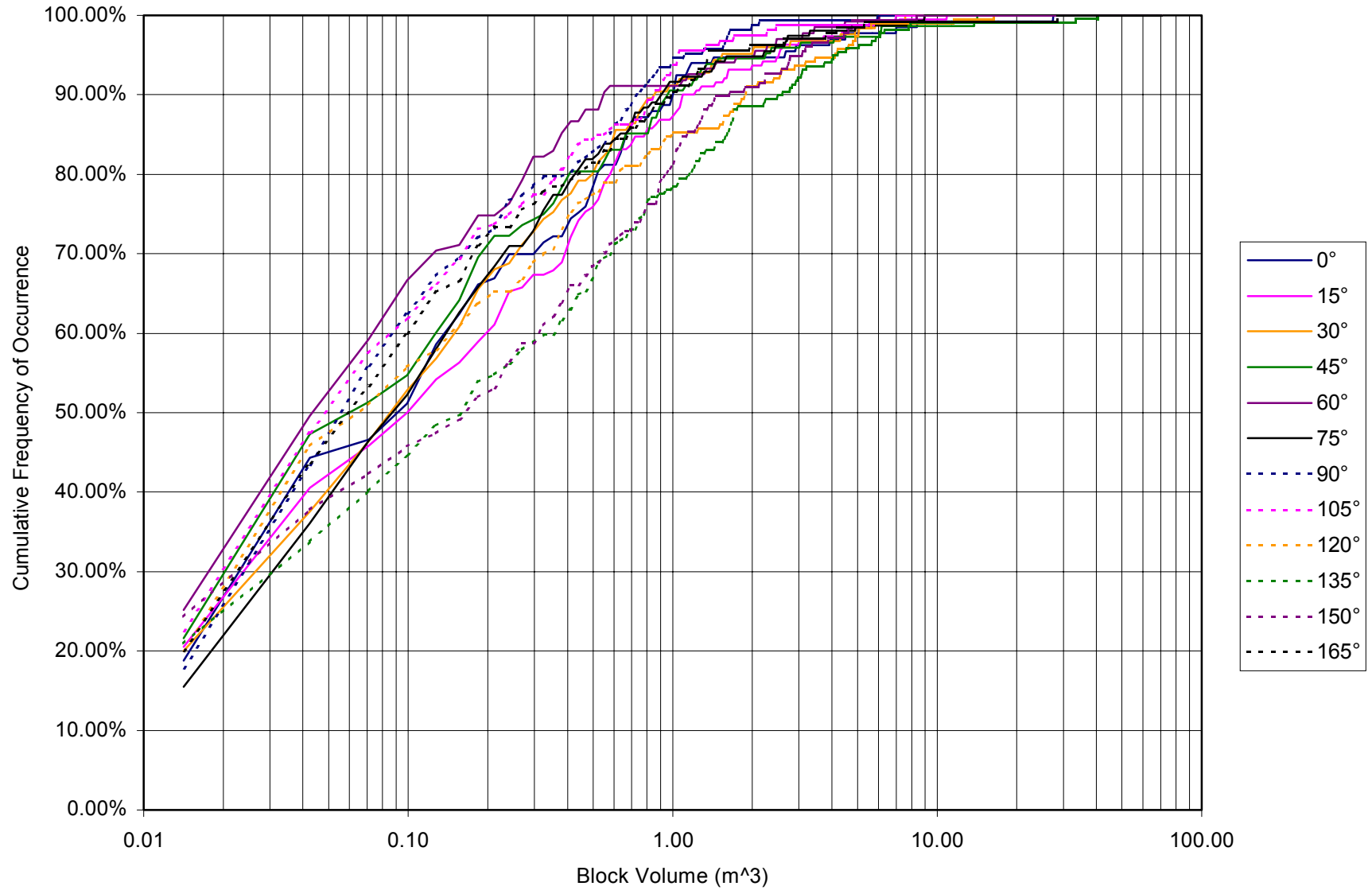


Figure 9. Cumulative Block Size Distribution for Various Drift Orientations in the Tptpul Unit, Static Condition

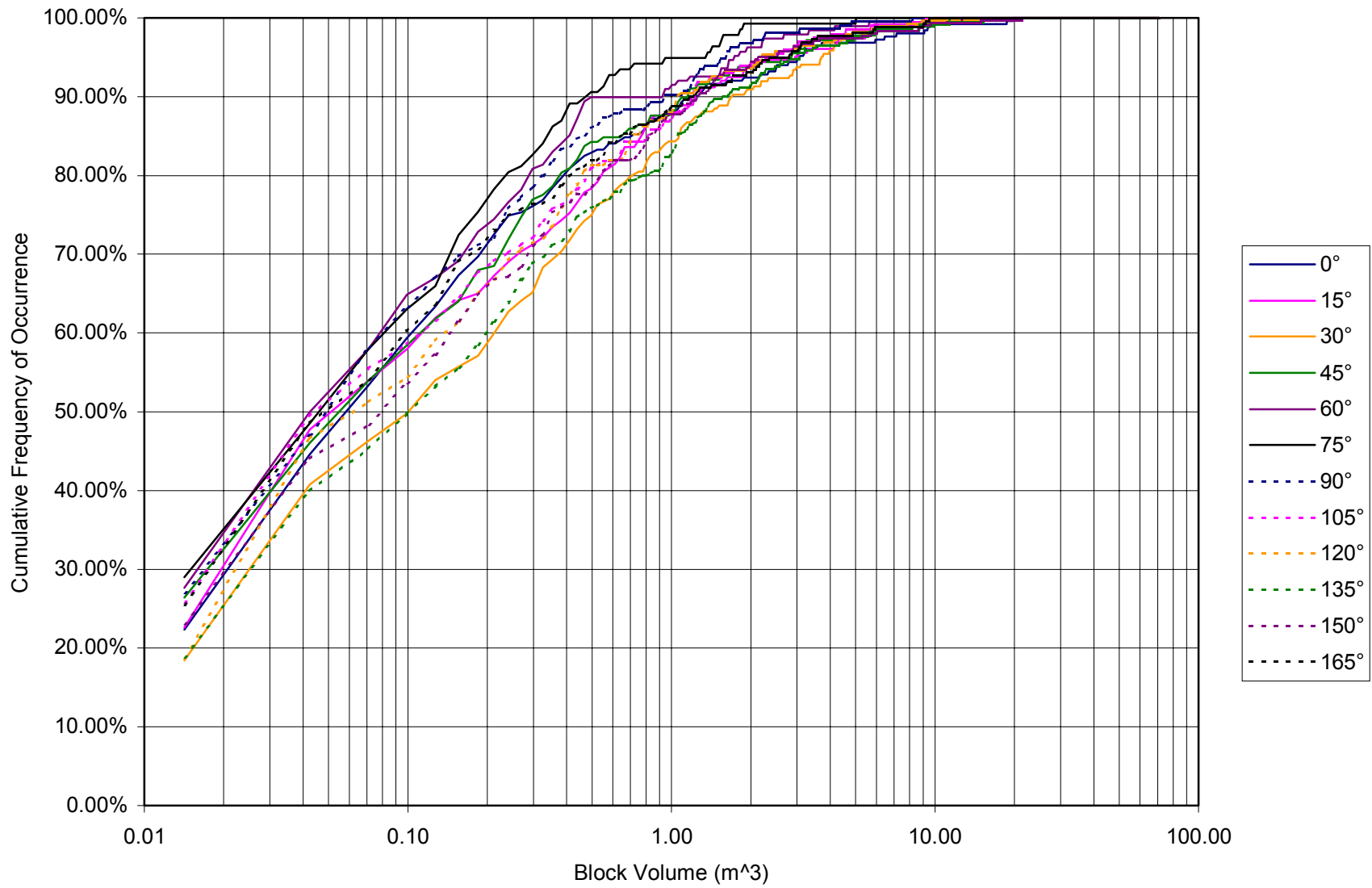


Figure 10. Cumulative Block Size Distribution for Various Drift Orientations in the Ttpmn Unit, Static Condition

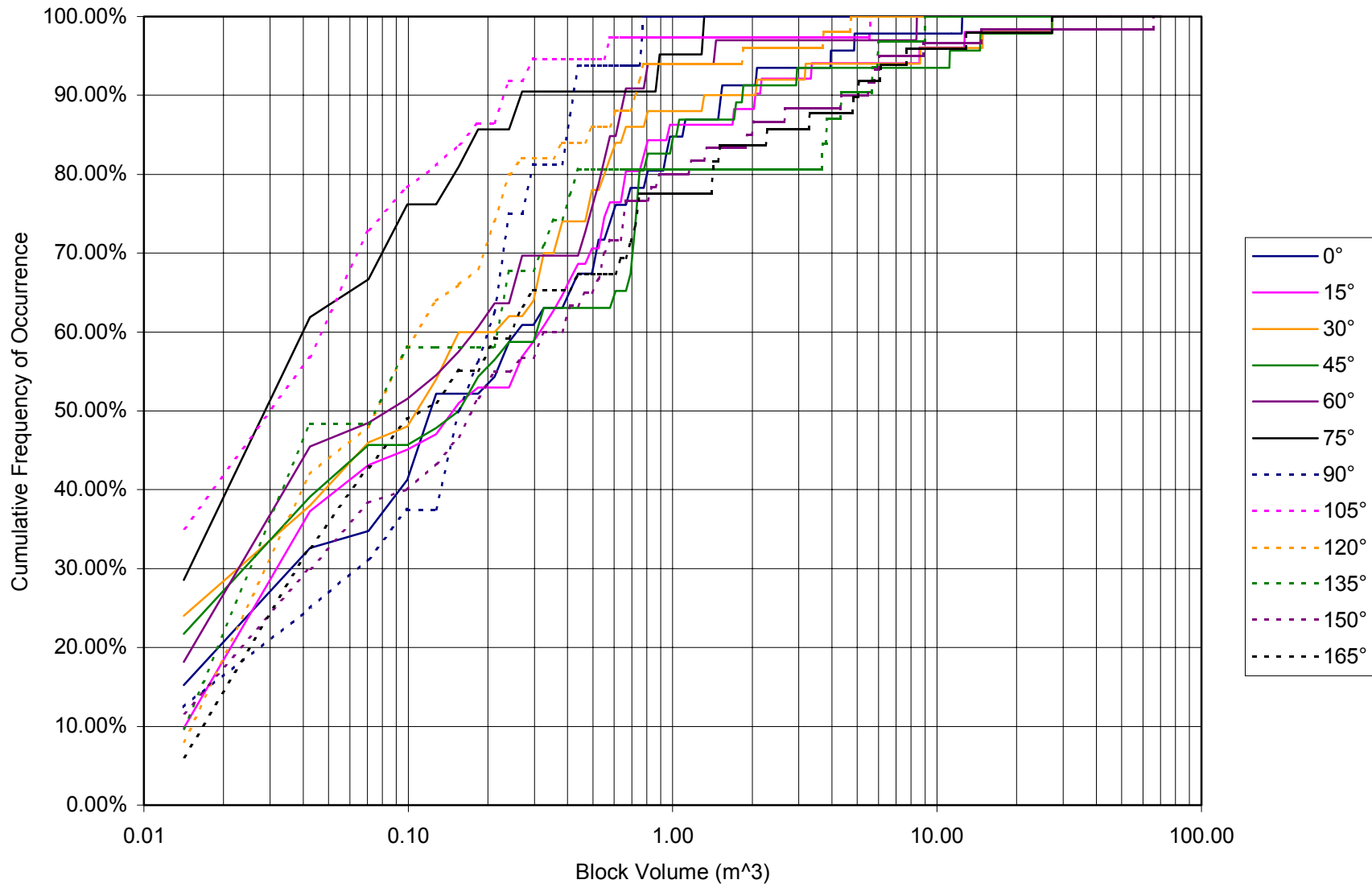


Figure 11. Cumulative Block Size Distribution for Various Drift Orientations in the Tptpl Unit, Static Condition

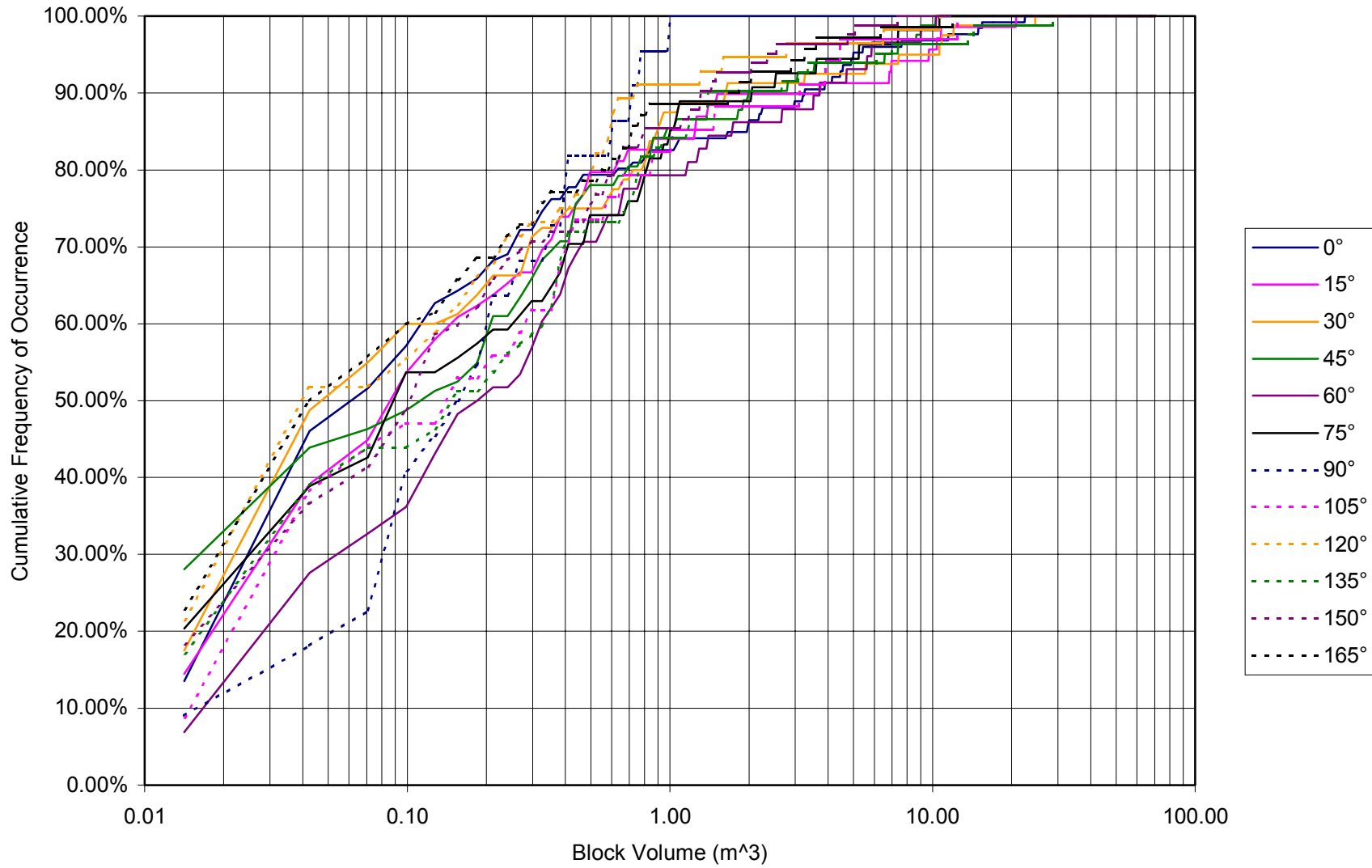


Figure 12. Cumulative Block Size Distribution for Various Drift Orientations in the Tptpln Unit, Static Condition

Table 11. Block Volume (in cubic meter) Corresponding to Various Levels of Predicted Cumulative Frequency of Occurrence, Performance Confirmation Drift in Ttptul Unit

Cumulative Frequency of Occurrence (%)	Drift Orientation (Azimuth in degree)											
	0	15	30	45	60	75	90	105	120	135	150	165
50	0.07	0.10	0.07	0.04	0.04	0.07	0.04	0.04	0.04	0.16	0.16	0.04
75	0.41	0.44	0.33	0.33	0.21	0.30	0.21	0.24	0.38	0.78	0.75	0.24
90	0.98	1.20	0.84	0.95	0.52	0.89	0.72	0.84	1.88	2.59	1.63	0.98
95	2.65	2.51	1.51	2.22	2.02	2.19	1.09	1.03	4.09	4.21	3.07	1.35
98	6.98	4.54	4.88	6.13	3.41	3.27	1.63	2.25	5.05	6.30	4.60	4.15
maximum	27.42	10.86	7.55	14.14	6.02	8.93	5.93	6.95	16.41	40.42	8.37	28.44

Table 12. Block Volume (in cubic meter) Corresponding to Various Levels of Predicted Cumulative Frequency of Occurrence, Emplacement Drift in Ttptmn Unit

Cumulative Frequency of Occurrence (%)	Drift Orientation (Azimuth in degree)											
	0	15	30	45	60	75	90	105	120	135	150	165
50	0.04	0.04	0.10	0.04	0.04	0.04	0.04	0.04	0.04	0.10	0.07	0.04
75	0.24	0.38	0.50	0.27	0.21	0.16	0.21	0.33	0.35	0.44	0.33	0.24
90	1.18	1.20	1.68	1.15	0.92	0.47	0.92	1.18	1.03	1.63	1.23	1.20
95	3.04	2.93	3.70	2.85	1.71	1.35	1.60	2.45	2.17	3.04	2.11	2.79
98	7.12	5.68	5.76	5.90	3.30	1.80	2.25	4.57	4.86	5.65	5.71	4.86
maximum	19.86	9.84	17.34	11.34	12.64	5.00	8.20	9.19	10.89	19.33	21.39	9.47

Table 13. Block Volume (in cubic meter) Corresponding to Various Levels of Predicted Cumulative Frequency of Occurrence, Emplacement Drift in Ttptll Unit

Cumulative Frequency of Occurrence (%)	Drift Orientation (Azimuth in degree)											
	0	15	30	45	60	75	90	105	120	135	150	165
50	0.10	0.13	0.10	0.16	0.07	0.01	0.16	0.01	0.07	0.07	0.16	0.10
75	0.58	0.55	0.47	0.72	0.47	0.07	0.27	0.07	0.21	0.38	0.64	0.72
90	1.51	2.02	2.05	1.83	0.64	0.24	0.41	0.21	0.72	4.32	5.48	5.03
95	3.95	8.57	8.62	11.14	1.43	0.86	0.75	0.55	1.83	5.96	8.88	7.66
98	12.42	12.70	27.34	27.20	8.37	1.29	0.75	5.56	4.71	8.96	14.71	27.17
maximum	12.42	27.31	27.34	27.20	8.37	1.29	0.75	5.56	4.71	8.96	65.99	27.17

Table 14. Block Volume (in cubic meter) Corresponding to Various Levels of Predicted Cumulative Frequency of Occurrence, Emplacement Drift in Tptpln Unit

Cumulative Frequency of Occurrence (%)	Drift Orientation (Azimuth in degree)											
	0	15	30	45	60	75	90	105	120	135	150	165
50	0.01	0.01	0.04	0.04	0.04	0.01	0.01	0.01	0.01	0.01	0.04	0.01
75	0.16	0.24	0.18	0.24	0.21	0.07	0.10	0.21	0.13	0.16	0.24	0.16
90	1.18	0.81	0.50	0.75	0.64	0.38	0.61	0.75	0.52	0.67	0.69	0.55
95	2.87	2.31	1.26	3.50	1.37	0.61	1.03	1.06	1.09	2.02	1.40	1.12
98	5.65	10.55	2.51	5.17	5.17	2.11	3.10	1.77	3.13	6.61	2.51	2.70
maximum	20.66	27.51	17.63	11.77	7.46	7.43	6.84	6.33	4.26	10.97	4.43	12.02

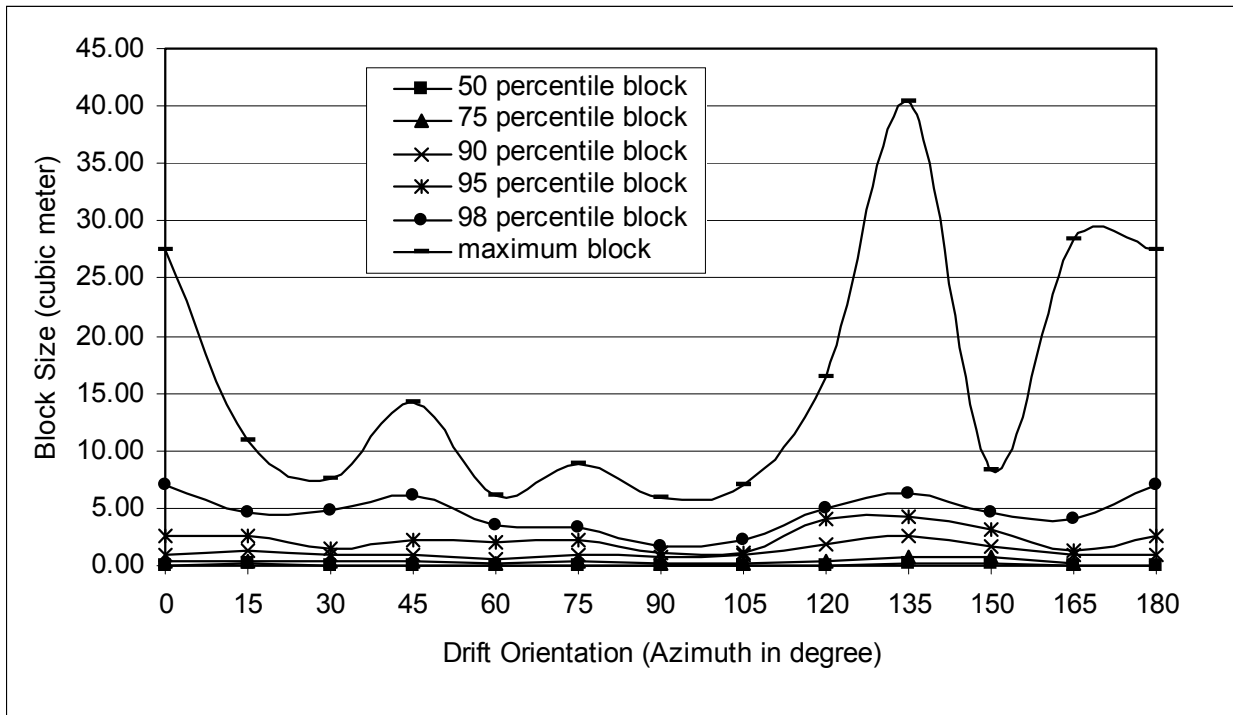


Figure 13. Block Size vs. Drift Orientation, Tptpul Unit

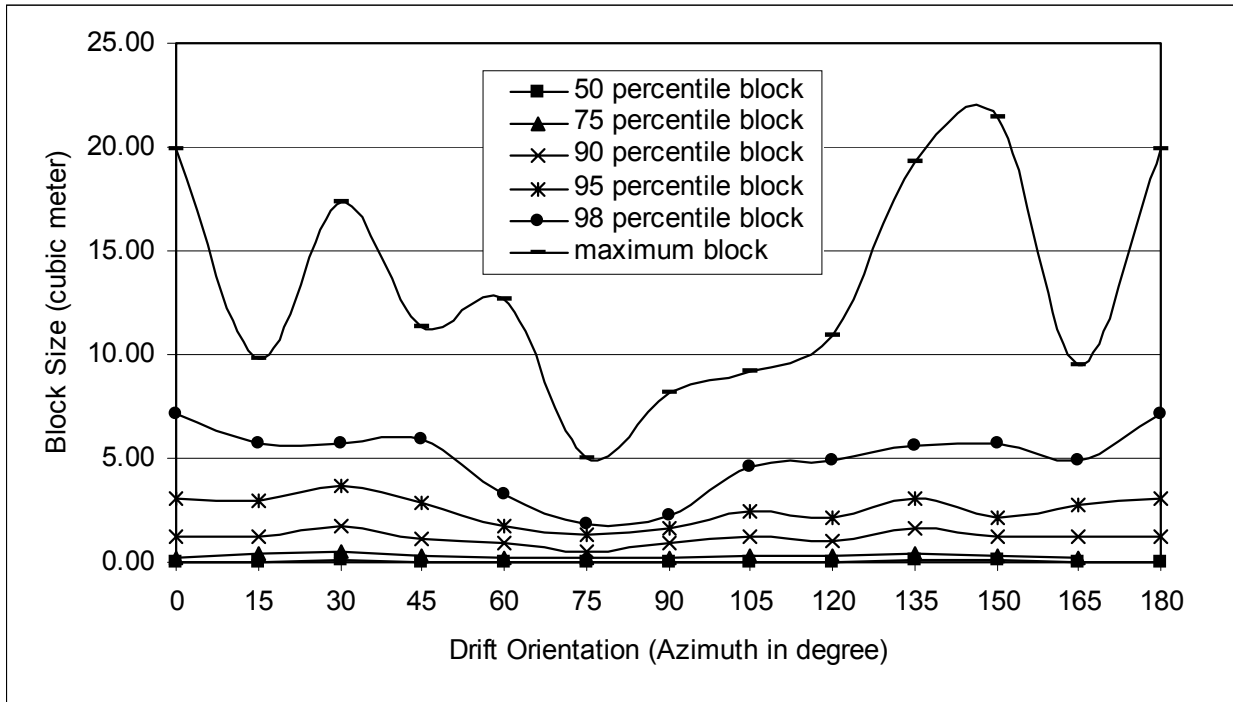


Figure 14. Block Size vs. Drift Orientation, Tptpmn Unit

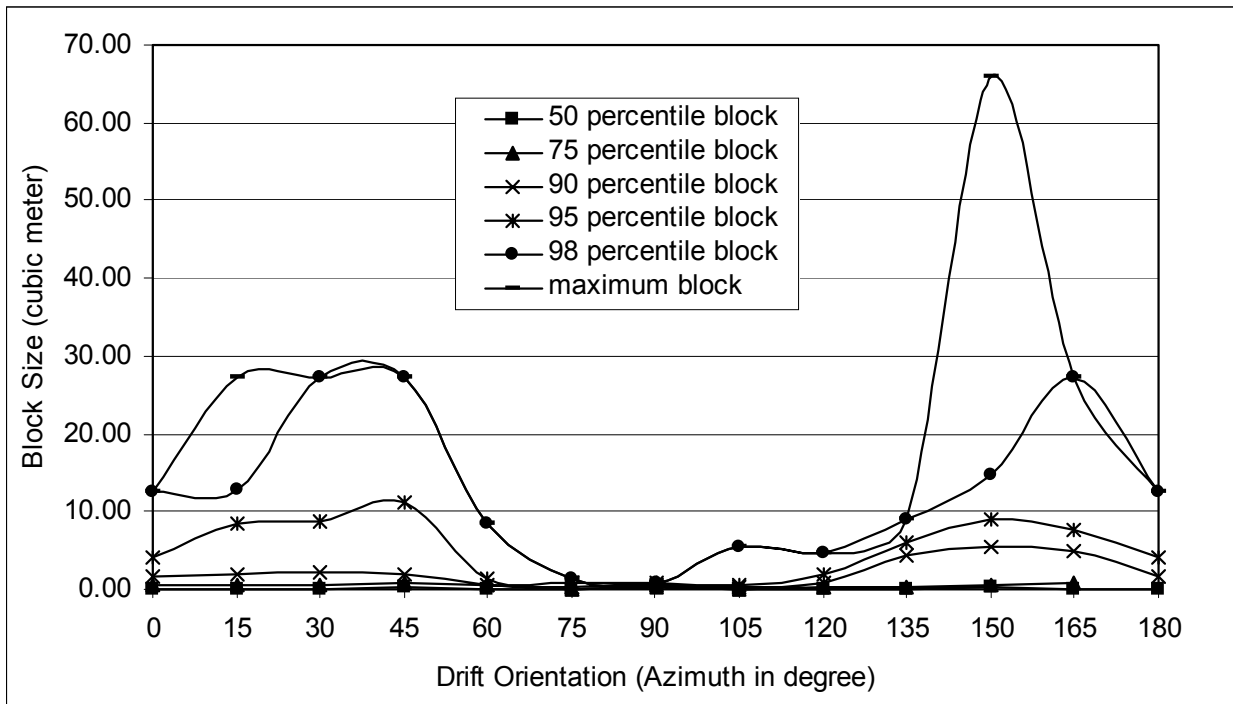


Figure 15. Block Size vs. Drift Orientation, Tptpll Unit

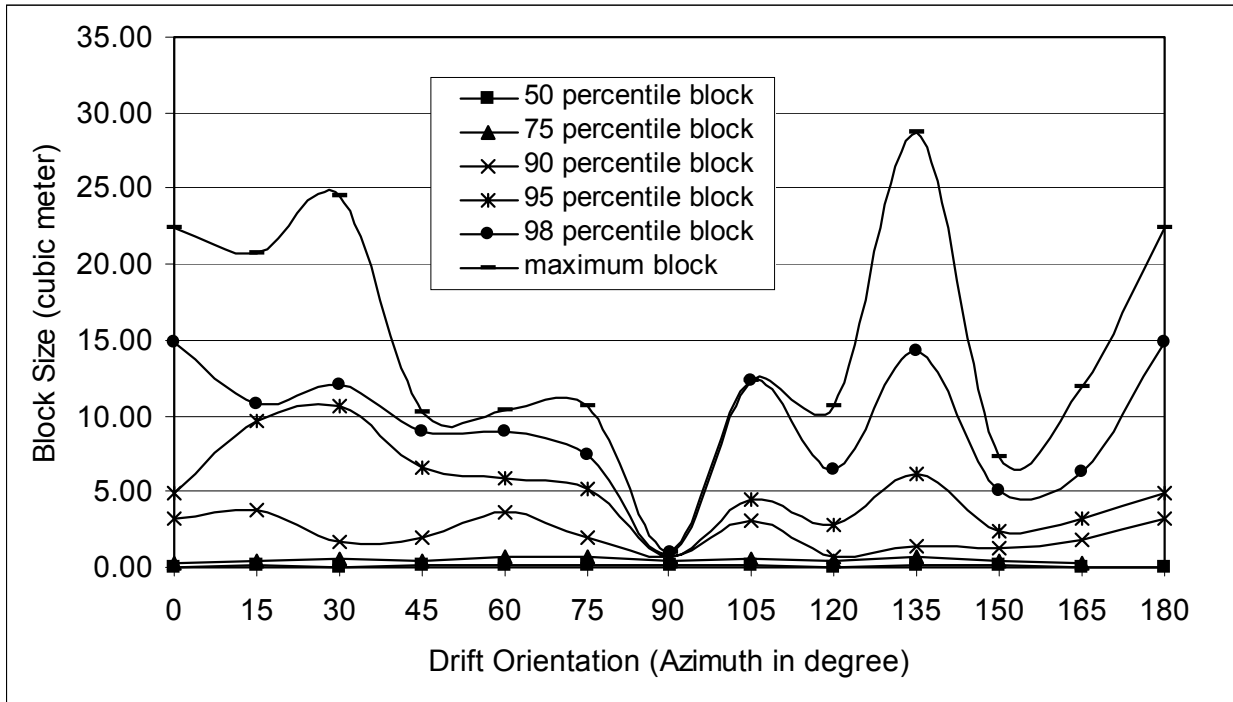


Figure 16. Block Size vs. Drift Orientation, Tptpln Unit

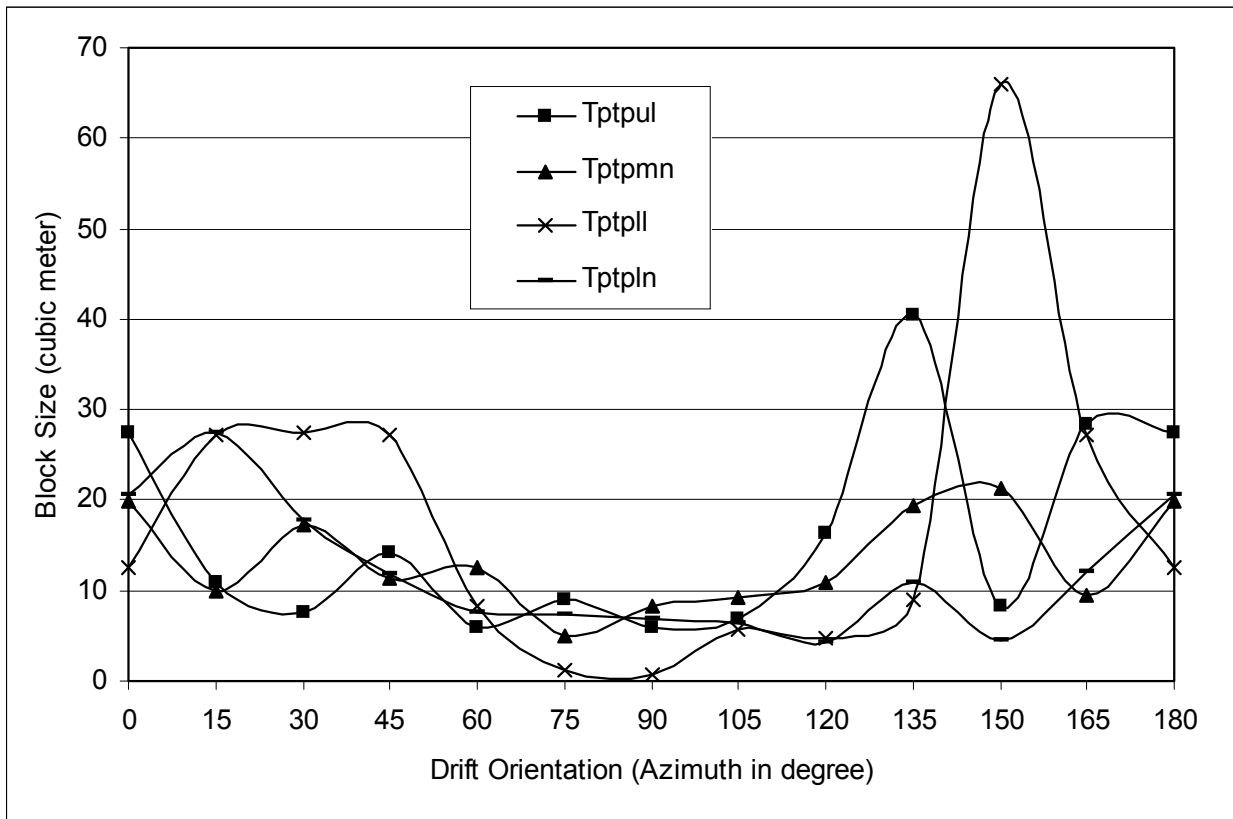


Figure 17. Maximum Block Size vs. Drift Orientation

Table 15. Predicted Number of Key Blocks per Unit Length (km) along Emplacement Drift

Lithologic Unit	Drift Orientation (Azimuth in degree)											
	0	15	30	45	60	75	90	105	120	135	150	165
Tptpul	12	18	12	14	13	14	16	15	18	20	16	13
Ttpmn	47	42	53	33	35	26	40	37	53	63	57	48
Ttpll	4	5	5	4	3	2	1	3	5	3	6	5
Ttpln	12	6	7	8	5	5	2	3	5	8	8	7

Figures 18 through 21 present the key block size distribution for each lithologic unit respectively. In addition to the results from the three levels of earthquake events, static results are also included for comparison. The cumulative frequencies of occurrence corresponding to 50, 75, 90, 95 and 98 percentile block volume for each unit are listed in Tables 16 to 19. The maximum block sizes predicted from the analyses are included in these tables. Corresponding graphs are presented in Figures 22 to 25. The analysis results indicate that the seismic effect on the rock fall size distribution is relatively minor.

The predicted numbers of key blocks per unit length of drift are listed in Table 20. Static results are also included for comparison. The comparison shows that there is an insignificant impact for a 1,000-year event earthquake (Level 1) on the number of rock falls, and only a minor impact for both a 5000-year event earthquake (Level 2) and a 10,000-year event (Level 3). The number of key blocks predicted for Ttpll unit remains scarce, as there was no change in the number of blocks regardless of the level of seismic event.

The predicted average volume of rock fall per unit length of drift is listed in Table 21. The trend for the average volume of rock fall per kilometer is similar to that for the predicted number of key blocks per kilometer.

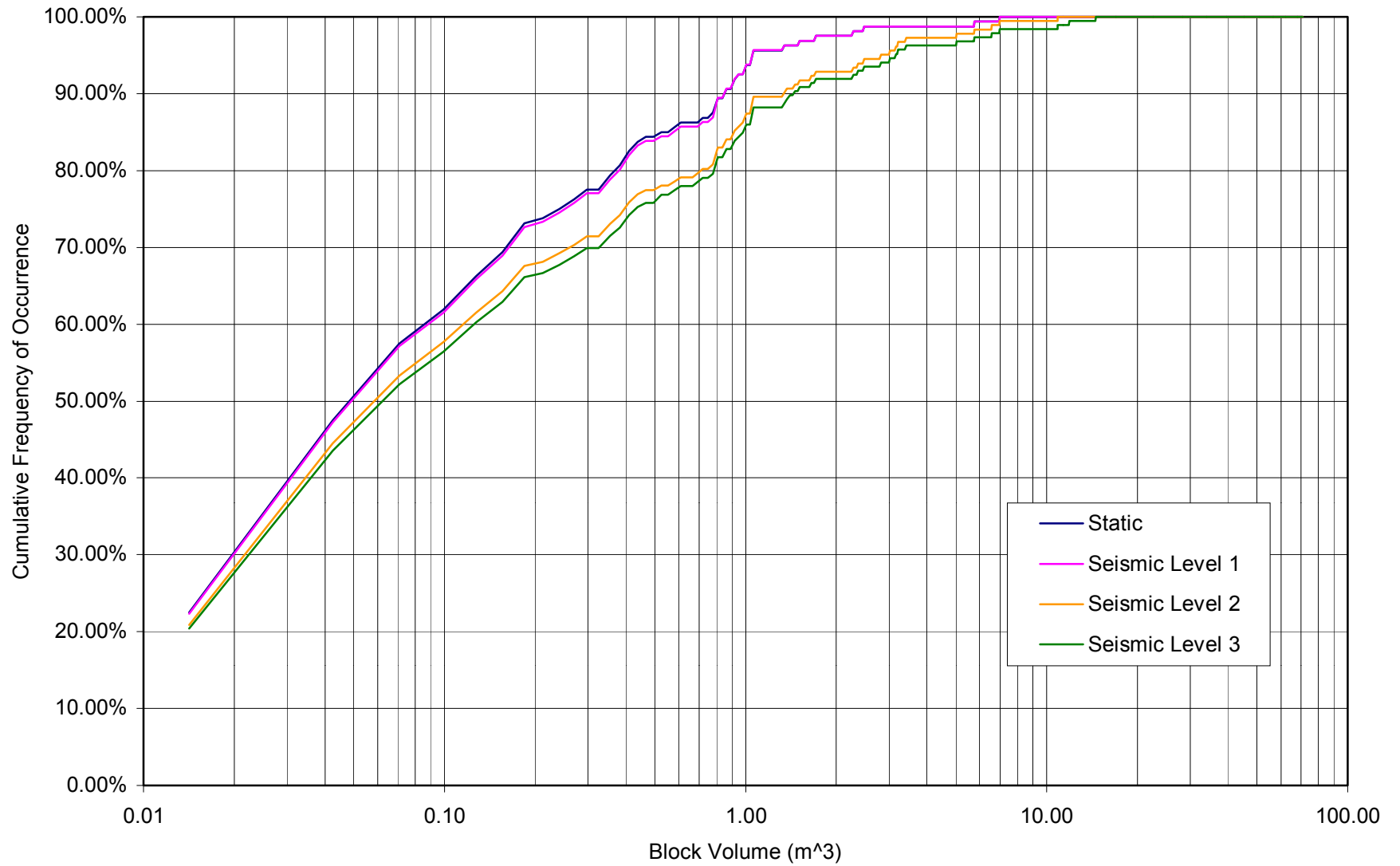
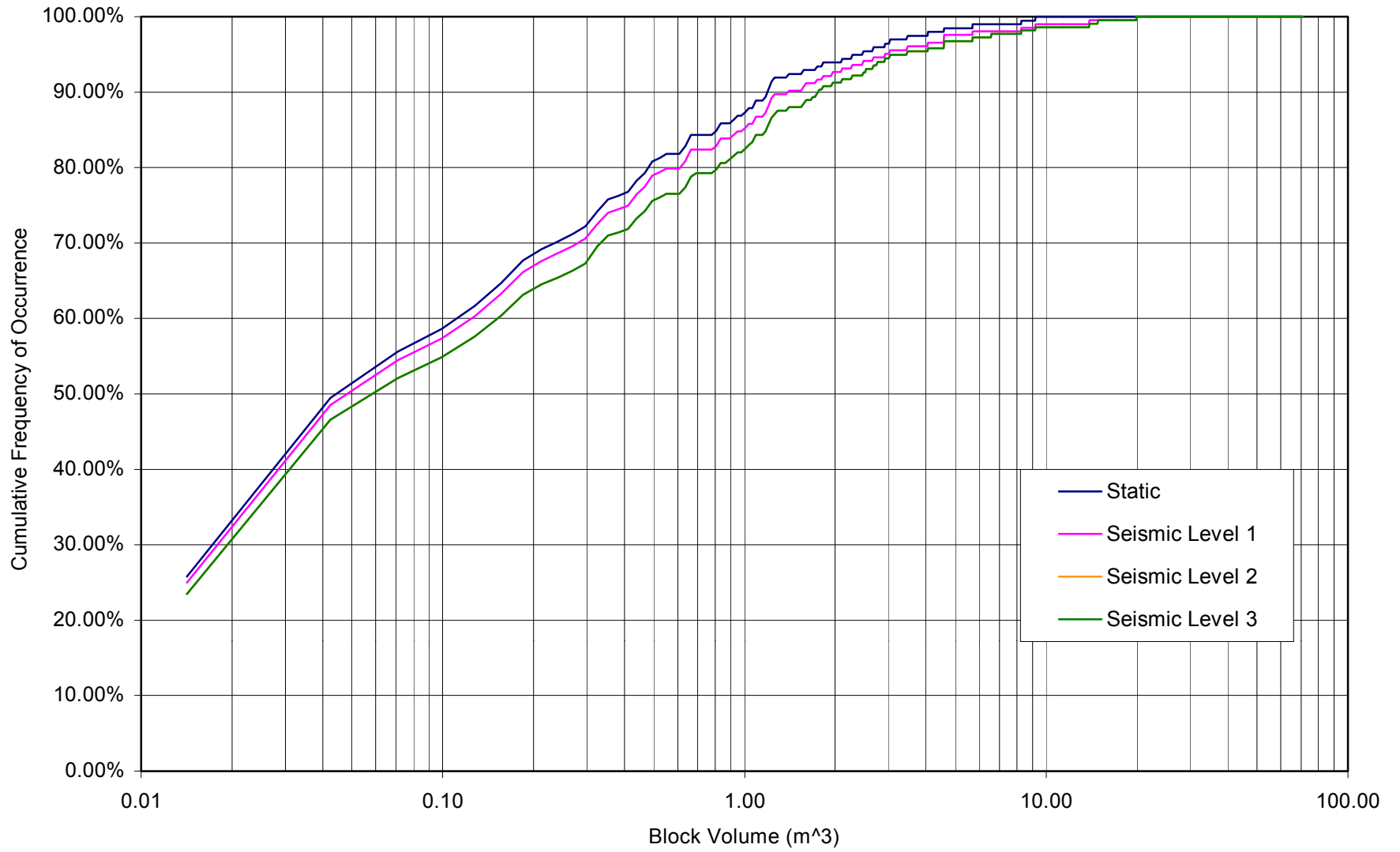
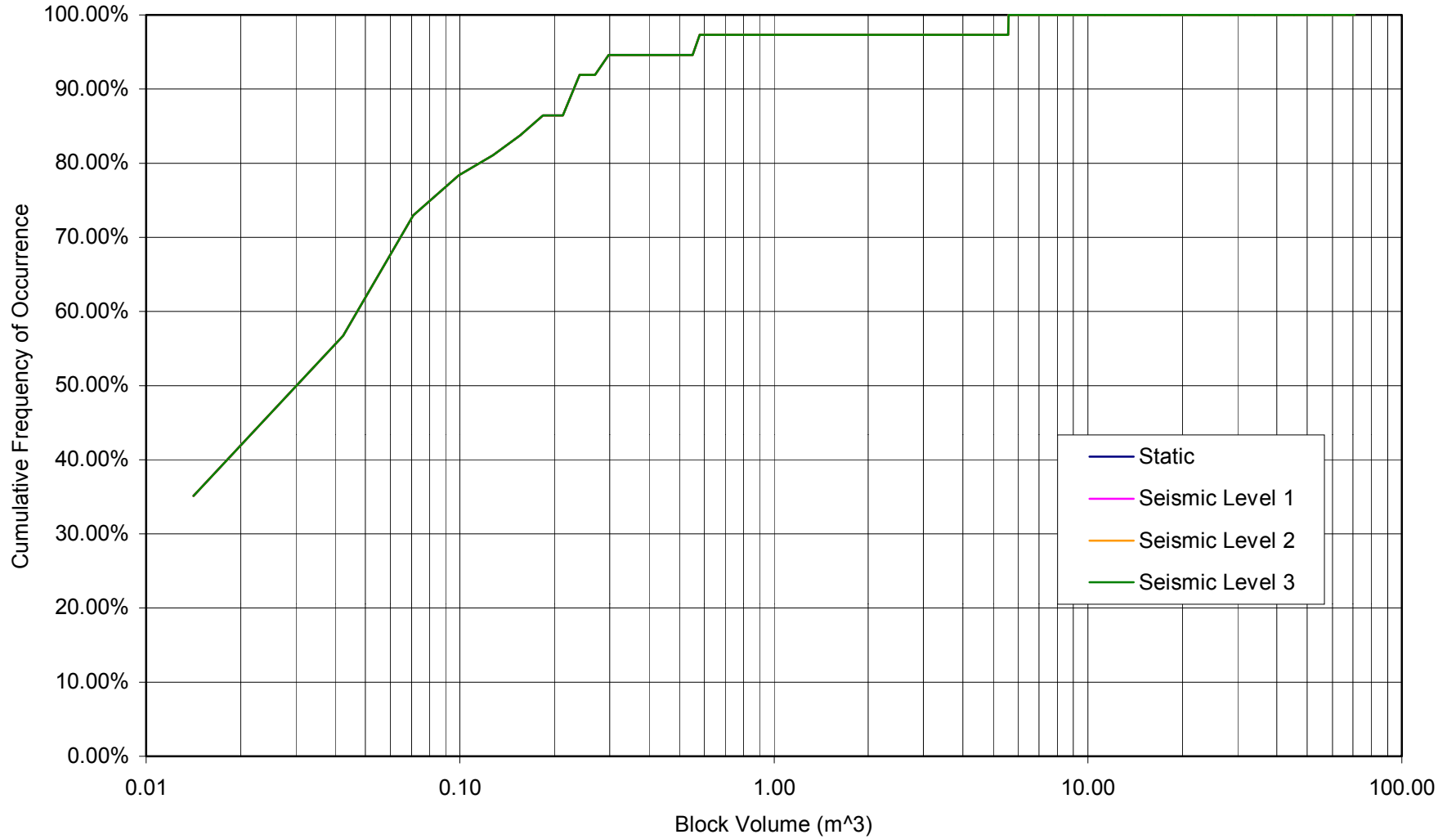


Figure 18. Cumulative Key Block Size Distribution for Seismic Consideration in the Tptpul Unit



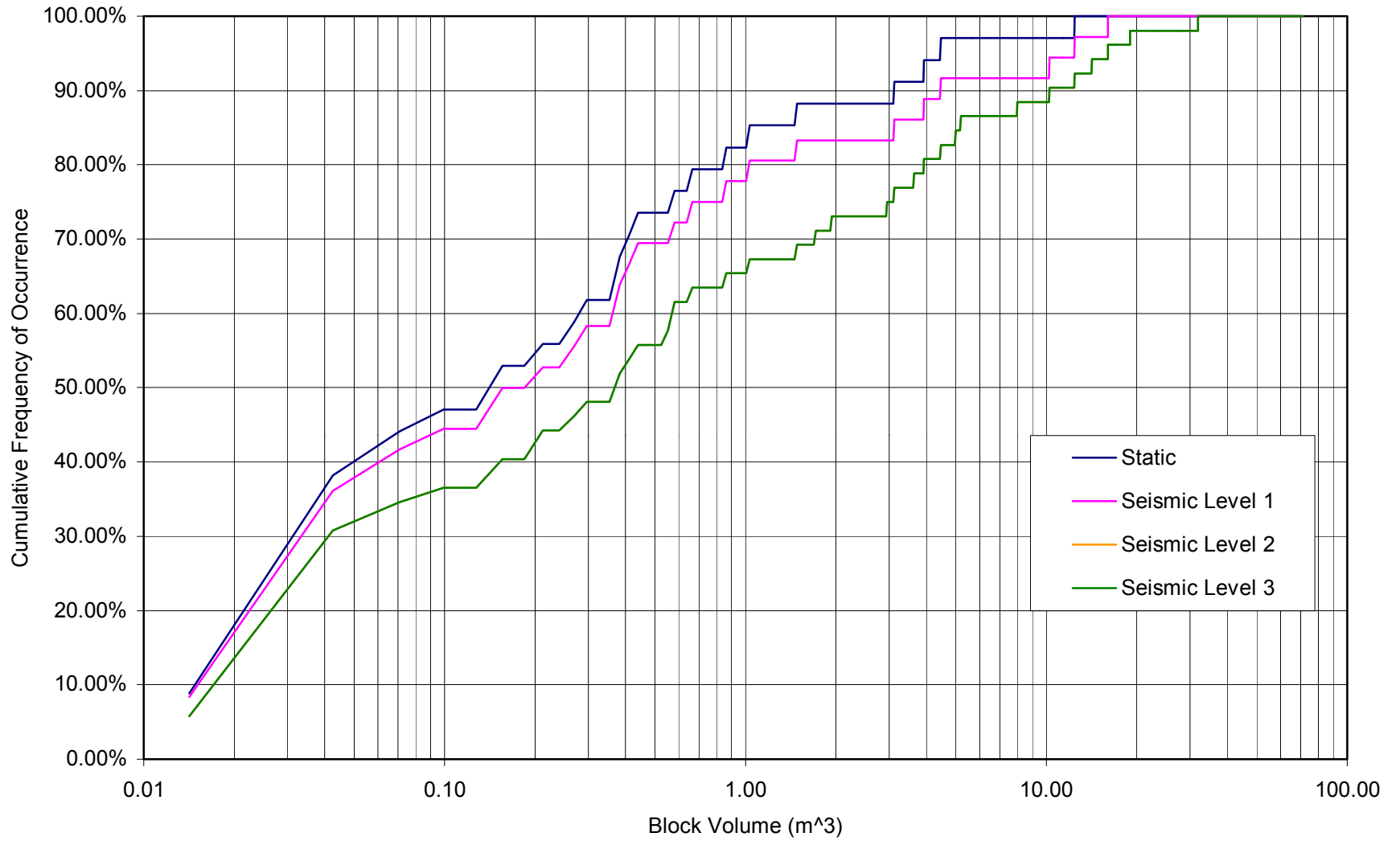
NOTE: The seismic level 2 and seismic level 3 distribution curves are identical.

Figure 19. Cumulative Key Block Size Distribution for Seismic Consideration in the Tptpmn Unit



NOTE: The static, seismic level 1, seismic level 2, and seismic level 3 distribution curves are identical.

Figure 20. Cumulative Key Block Size Distribution for Seismic Consideration in the Tptpl Unit



NOTE: The seismic level 2 and seismic level 3 distribution curves are identical.

Figure 21. Cumulative Key Block Size Distribution for Seismic Consideration in the Tptln Unit

Table 16. Block Volume (in cubic meter) Corresponding to Various Level of Predicted Cumulative Frequency of Occurrence, Performance Confirmation Drift in Ttpul Unit, with Seismic Consideration

Cumulative Frequency of Occurrence (%)	Static	Static Plus Seismic		
		Level 1	Level 2	Level 3
50%	0.04	0.04	0.04	0.04
75%	0.24	0.24	0.38	0.41
90%	0.84	0.84	1.32	1.43
95%	1.03	1.03	2.79	3.13
98%	2.25	2.25	5.73	6.95
maximum	6.95	6.95	10.86	14.54

Table 17. Block Volume (in cubic meter) Corresponding to Various Level of Predicted Cumulative Frequency of Occurrence, Performance Confirmation Drift in Ttpm Unit, with Seismic Consideration

Cumulative Frequency of Occurrence (%)	Static	Static Plus Seismic		
		Level 1	Level 2	Level 3
50%	0.04	0.04	0.04	0.04
75%	0.33	0.41	0.47	0.47
90%	1.18	1.37	1.74	1.74
95%	2.45	2.90	3.44	3.44
98%	4.57	5.68	8.25	8.25
maximum	9.19	19.89	19.89	19.89

Table 18. Block Volume (in cubic meter) Corresponding to Various Level of Predicted Cumulative Frequency of Occurrence, Performance Confirmation Drift in TtpII Unit, with Seismic Consideration

Cumulative Frequency of Occurrence (%)	Static	Static Plus Seismic		
		Level 1	Level 2	Level 3
50%	0.01	0.01	0.01	0.01
75%	0.07	0.07	0.07	0.07
90%	0.21	0.21	0.21	0.21
95%	0.55	0.55	0.55	0.55
98%	5.56	5.56	5.56	5.56
maximum	5.56	5.56	5.56	5.56

Table 19. Block Volume (in cubic meter) Corresponding to Various Level of Predicted Cumulative Frequency of Occurrence, Performance Confirmation Drift in Tptpln Unit, with Seismic Consideration

Cumulative Frequency of Occurrence (%)	Static	Static Plus Seismic		
		Level 1	Level 2	Level 3
50%	0.13	0.18	0.35	0.35
75%	0.55	0.84	3.10	3.10
90%	3.10	4.43	10.21	10.21
95%	4.43	12.39	15.98	15.98
98%	12.39	15.98	18.99	18.99
maximum	12.39	15.98	31.84	31.84

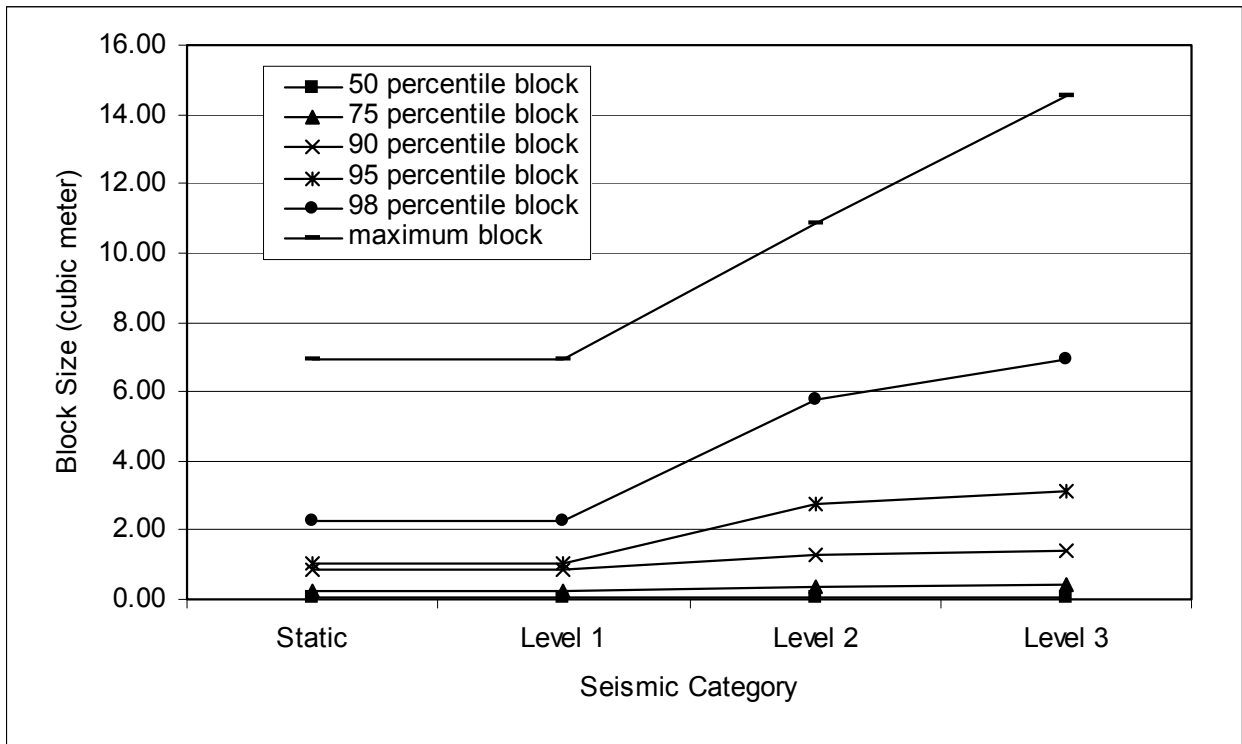


Figure 22. Block Size vs. Seismic Category, Tptpul Unit

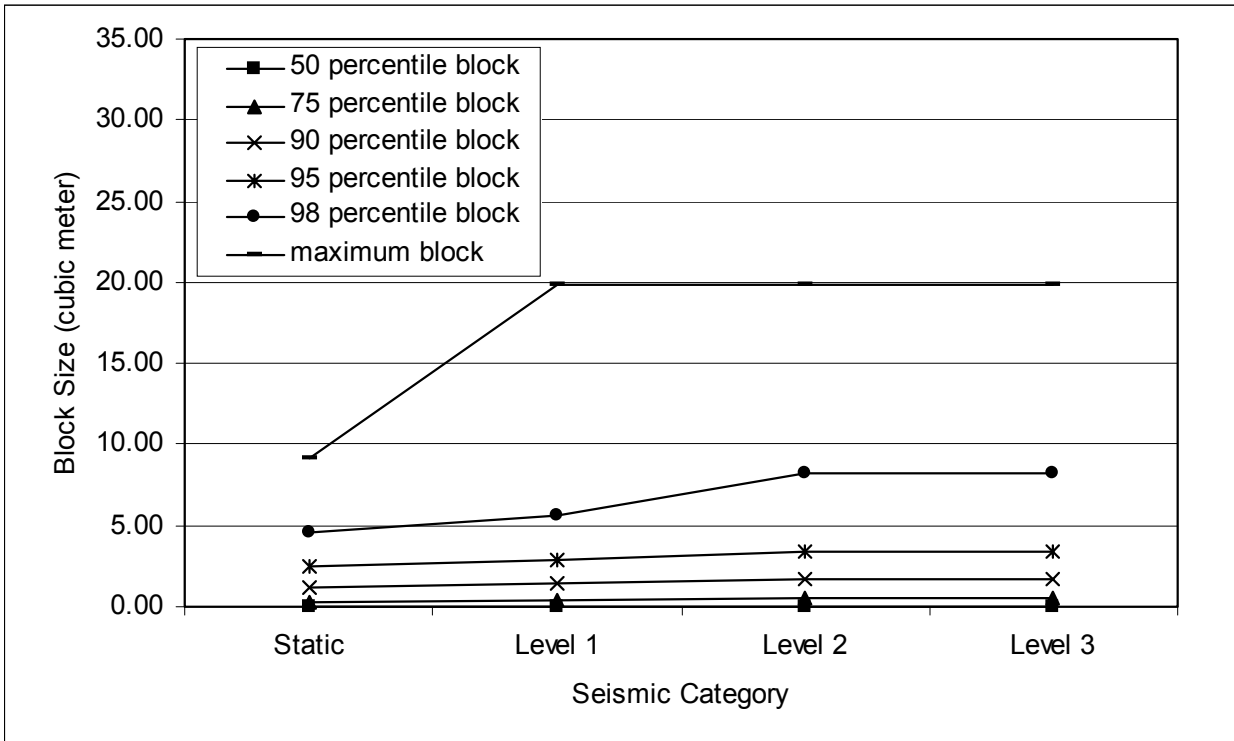


Figure 23. Block Size vs. Seismic Category, Tptpmn Unit

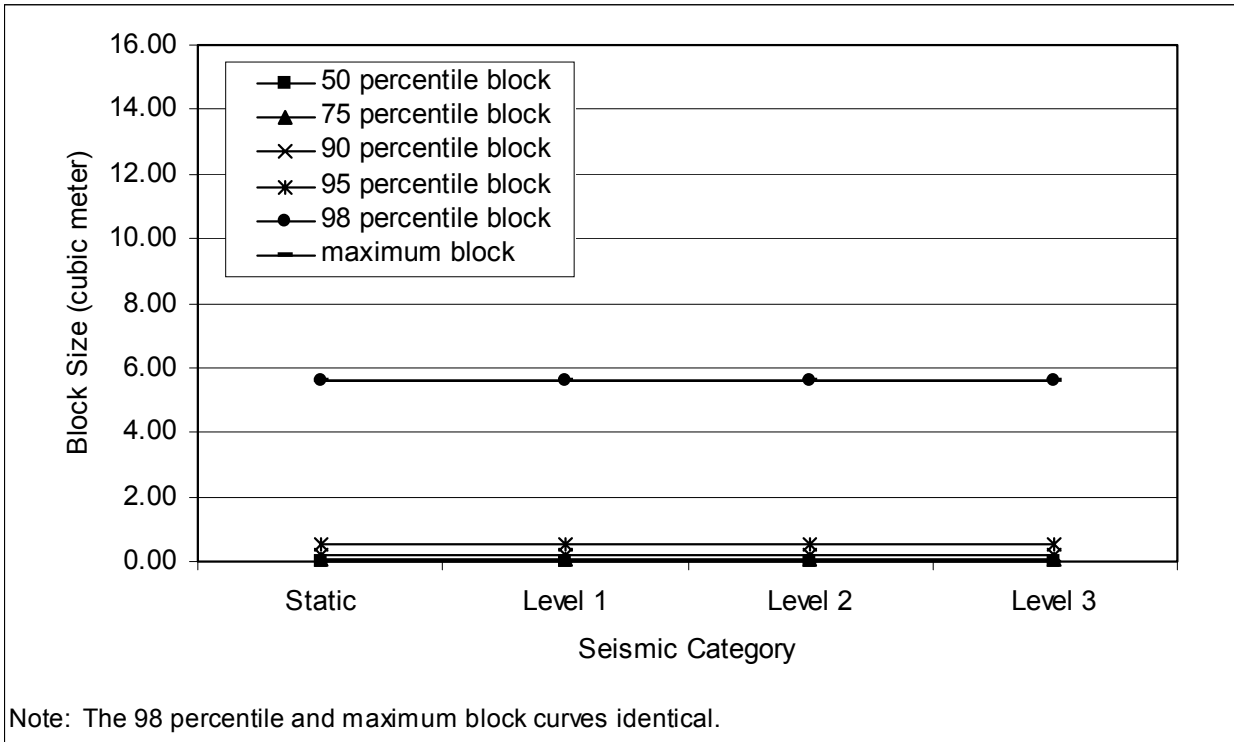


Figure 24. Block Size vs. Seismic Category, Tptpll Unit

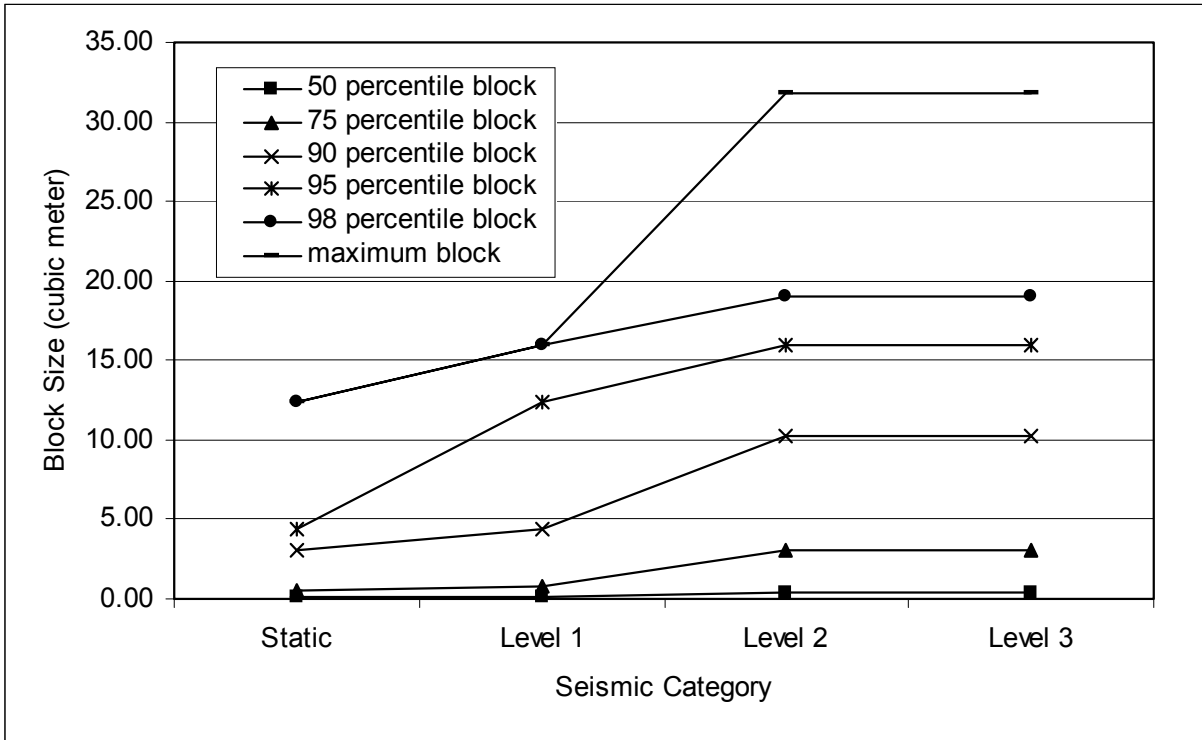


Figure 25. Block Size vs. Seismic Category, Tptpln Unit

Table 20. Predicted Number of Key Blocks per Unit Length (km) along Emplacement Drift, with Seismic Consideration

Lithologic Unit	Static	Static Plus Seismic		
		Level 1	Level 2	Level 3
Tptpul	15	15	17	17
Tptpmn	37	38	40	40
Tptpll	3	3	3	3
Tptpln	3	3	5	5

Table 21. Predicted Average Volume of Key Blocks per Unit Length along Emplacement Drift, with Seismic Consideration

Lithologic Unit	Static (m ³ /km)	Static Plus Seismic (m ³ /km)		
		Level 1	Level 2	Level 3
Tptpul	4.9	5.0	9.5	12.1
Tptpmn	18.2	25.9	32.3	32.3
Tptpll	0.8	0.8	0.8	0.8
Tptplin	3.0	5.5	14.4	14.4

6.4.2 Rock Fall Related to Time-Dependent and Thermal Effects

The results for the analysis with the consideration of time-dependent and thermal effects are presented in this section. The analysis uses an approach that accounts for the time-dependent and thermal effect with joint cohesion degradation. The development and justification of this approach is described in Section 6.3.5 and [Attachment VI](#).

Four different times are selected for the analysis: 0 years (static condition), 200 years, 2,000 years, and 10,000 years. The corresponding joint cohesion for each time is listed in [Table 22](#). The reduction of joint cohesion is predicted to be very small in the period between years 2,000 and 10,000.

Since backfill is part of the engineering barrier system at the post-closure period, backfill is included in the analysis for the consideration of time-dependent and thermal effects. The backfill configuration and the simplified opening geometry used in the analysis are presented in [Figure 26](#). It is apparent that the blocks that form around the springline area will no longer occur in the analysis with backfill.

The predicted number of key blocks per kilometer of drift for the LADS orientation is listed in [Table 23](#). Only minor increases of key blocks are predicted between year 200 and year 2,000. No change is predicted from year 2,000 to year 10,000. The predicted average volume of rock fall per unit length of drift is listed in [Table 24](#). The results indicate that time-dependent and thermal effects have a minor impact on rock fall.

6.4.3 Drift Profile Prediction

The key block approach applied in this analysis has provided an assessment of existing fracture data to determine probable occurrences of rock blocks that would fall into the tunnel opening in the absence of ground support. The DRKBA approach applied considers progressive block failure, such that when an initial key block fails and is removed, then an additional failure surface may open up allowing other blocks to fall. Progressive block failure continues until the crown becomes geometrically and mechanically stable, and no additional blocks can fall. The

Table 22. Reduced Joint Cohesion to Account for Time-Dependent and Thermal Effects

Period (year)	Joint Cohesion (Pa)
0 (Static)	99,873
200	21,674
2,000	10,998
10,000	10,776

Table 23. Predicted Number of Key Blocks per Unit Length (km) along Emplacement Drift, with Time-Dependent and Thermal Consideration

Lithologic Unit	Static	Year 200	Year 2000	Year 10000
Ttpul	15	14	15	15
Ttpmn	37	37	39	39
Ttpll	3	4	4	4
Ttpln	3	4	5	5

Table 24. Predicted Average Volume of Key Blocks per Unit Length (km) along Emplacement Drift, with Time-Dependent and Thermal Consideration

Lithologic Unit	Static	Year 200	Year 2000	Year 10000
Ttpul	4.9	5.1	8.8	8.8
Ttpmn	18.0	15.8	19.0	19.0
Ttpll	0.8	0.8	0.9	0.9
Ttpln	3.0	3.4	8.4	8.4

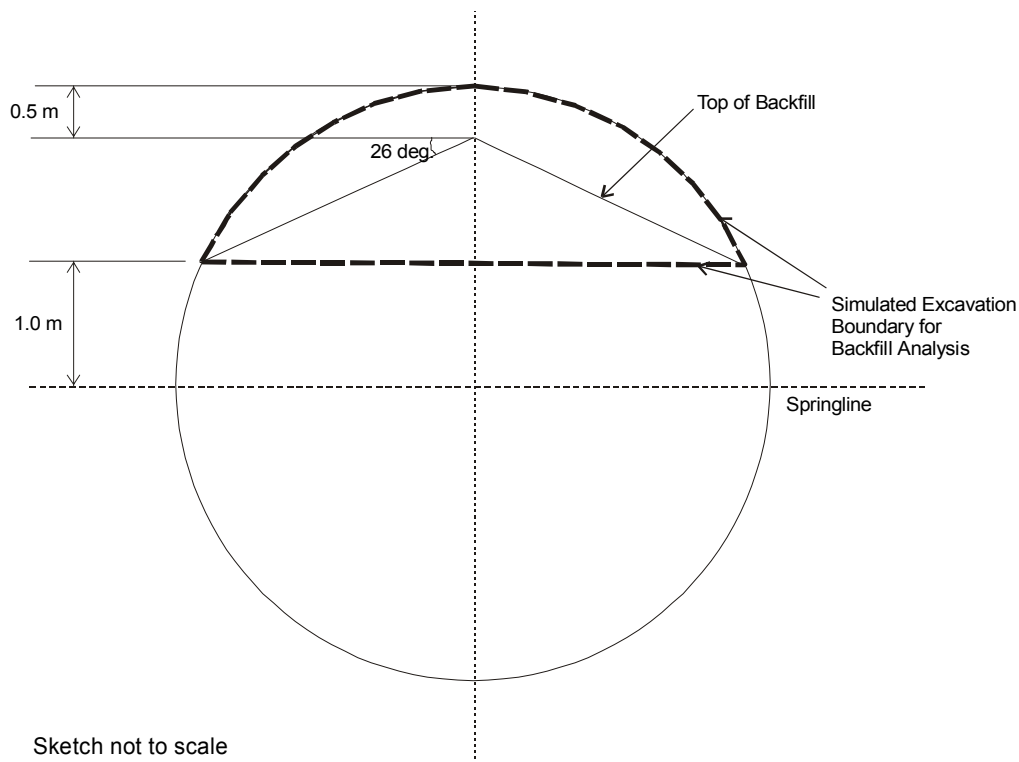
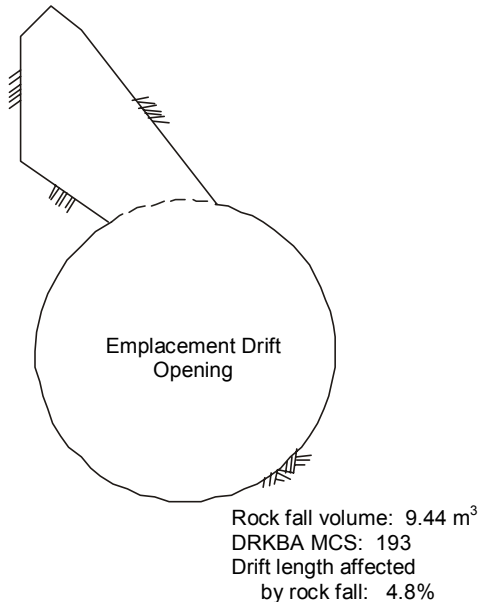


Figure 26. Backfill Configuration and Simplified Opening Geometry
(based on DTN: SN9908T0872799.004)

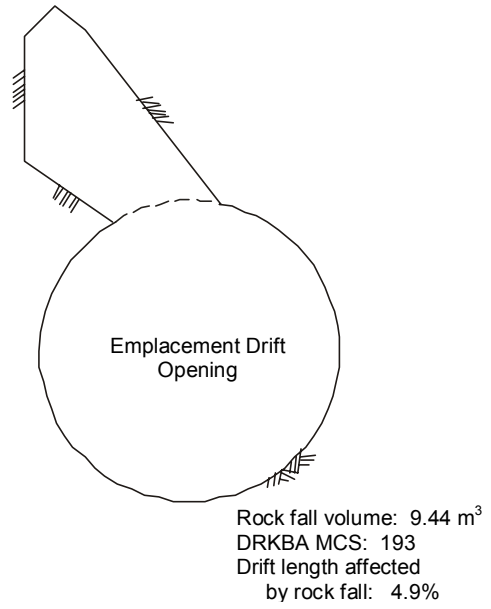
final progressive failure surface provides the basis for the drift profile predictions presented in this section. It should be noted that for a given drift profile, the DRKBA code is indifferent to the volume of the failed blocks relative to the volume of the opening. The effect of rubble (i.e., failed blocks) in the opening and the subsequent bulking of the rubble pile has not been considered in the development of drift profiles.

As described in Section 6.4.1, the emplacement drifts with no backfill in place were simulated for four different cases. The first case considered static loading only. The next three cases considered static plus seismic loading, with each case representing a different level of seismic loading (see Section 6.4.1.2). For the length of drift simulated, a worst-case drift profile (i.e., the area with the greatest volume of failed rock) was selected. These profiles are shown in Figures 27 through 30 for each lithologic unit. It is important to note that most of the emplacement drifts are not affected by rock fall. The percentages of the drifts affected by rock fall are shown in drift profile figure, along with the volume of the failed rock from the profile area and the DRKBA Monte Carlo simulation (MCS) in which the failure occurred.

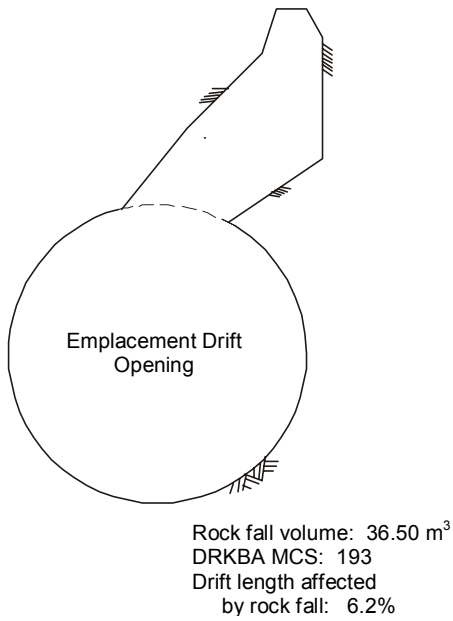
The drift profiles with backfill are shown at four different time intervals, with the progressive drift degradation a function of both thermal loading and the time dependent degradation of joint cohesion. As for the cases with no backfill, the drift profiles (Figures 31 through 34) represent the worst case, or greatest volume of rock fall within the simulated length of tunnel. The percentages of the drifts affected by rock fall considering time-dependent drift degradation are shown in each figure, along with the volume of the failed rock from the profile area and the DRKBA MCS in which the failure occurred.



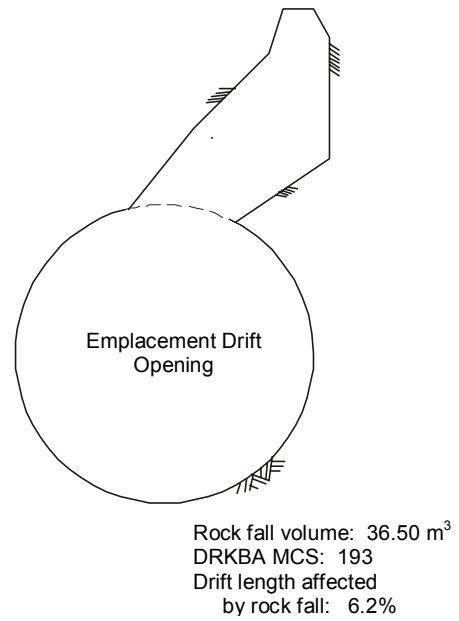
a. Static



b. Seismic Level 1



c. Seismic Level 2



d. Seismic Level 3

Figure 27. Emplacement Drift Profiles Considering Seismic Effects on Rock Fall for the Tptpul Unit

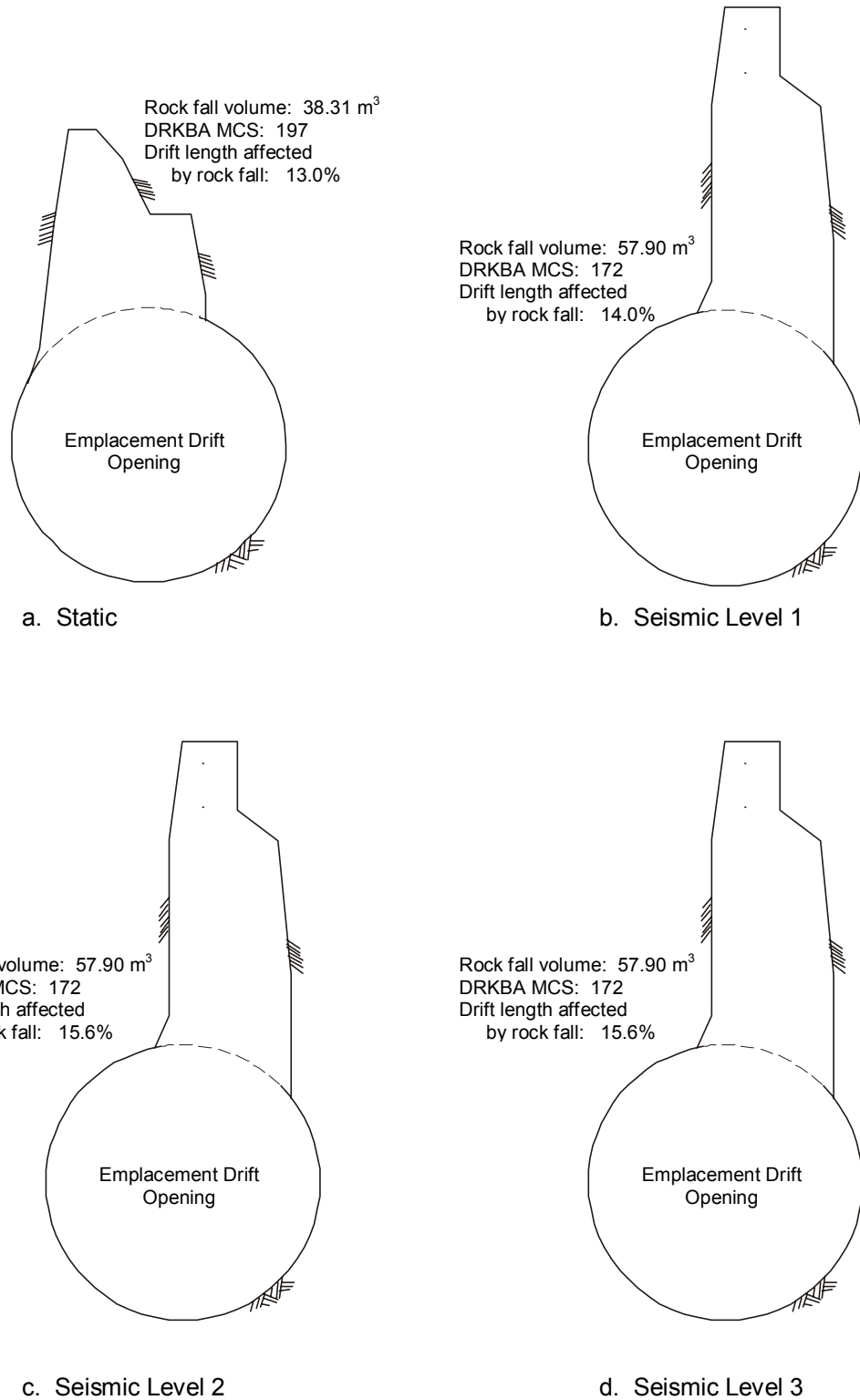
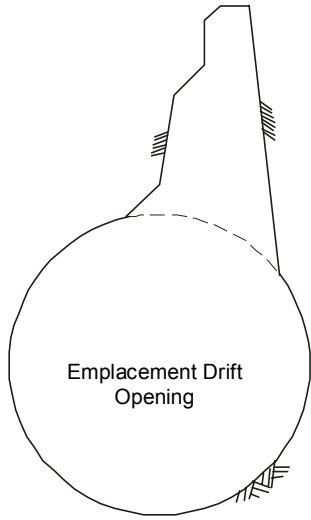
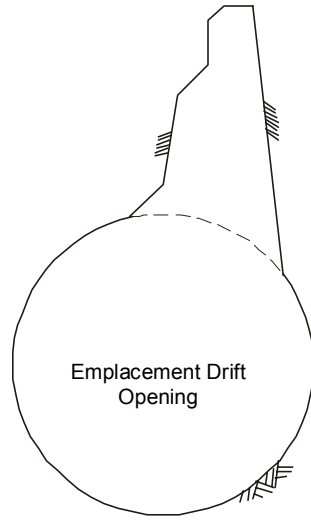


Figure 28. Emplacement Drift Profiles Considering Seismic Effects on Rock Fall for the Tptpmn Unit



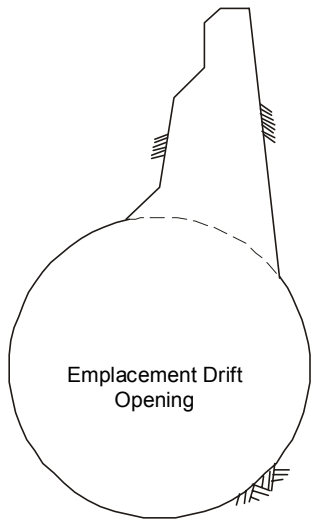
Rock fall volume: 5.67 m³
 DRKBA MCS: 290
 Drift length affected
 by rock fall: 0.9%

a. Static



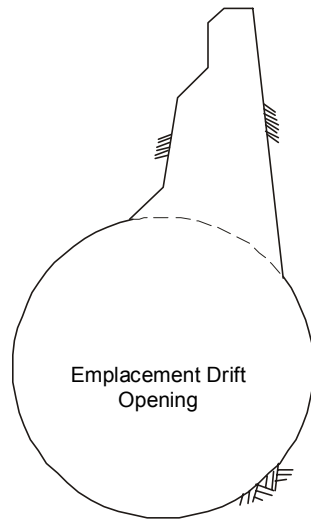
Rock fall volume: 5.67 m³
 DRKBA MCS: 290
 Drift length affected
 by rock fall: 0.9%

b. Seismic Level 1



Rock fall volume: 5.67 m³
 DRKBA MCS: 290
 Drift length affected
 by rock fall: 1.1%

c. Seismic Level 2



Rock fall volume: 5.67 m³
 DRKBA MCS: 290
 Drift length affected
 by rock fall: 1.1%

d. Seismic Level 3

Figure 29. Emplacement Drift Profiles Considering Seismic Effects on Rock Fall for the Tptpl Unit

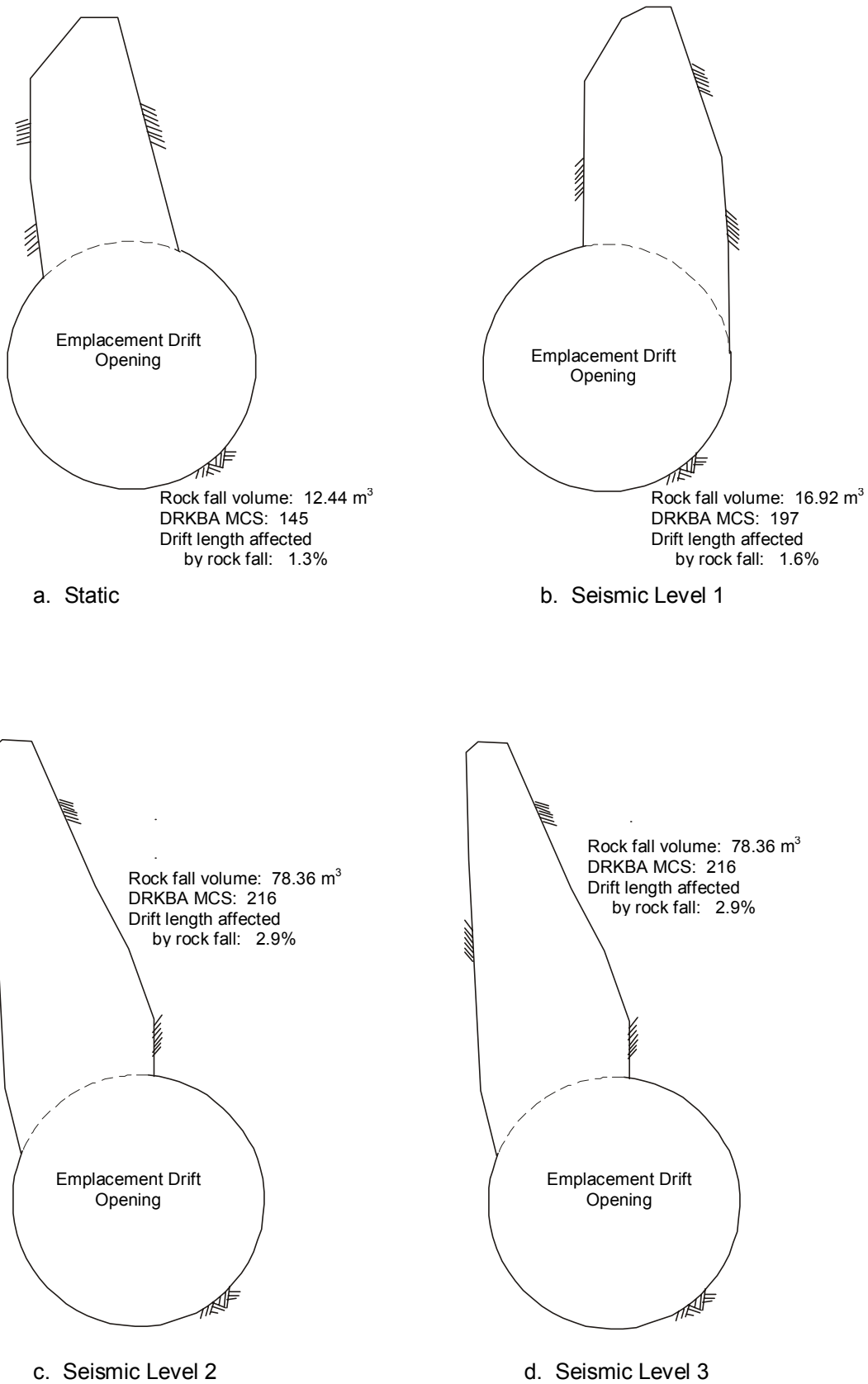
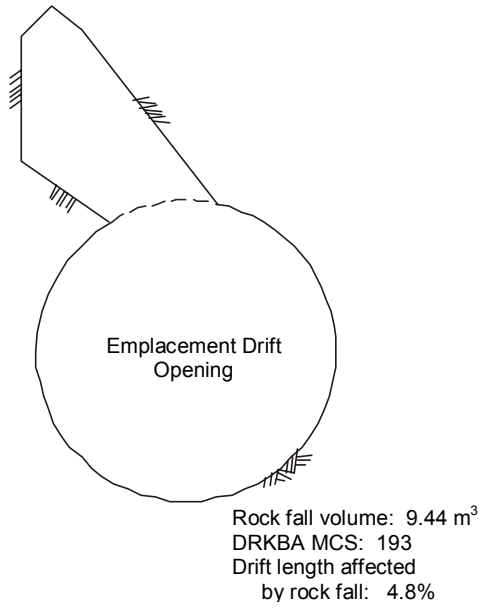
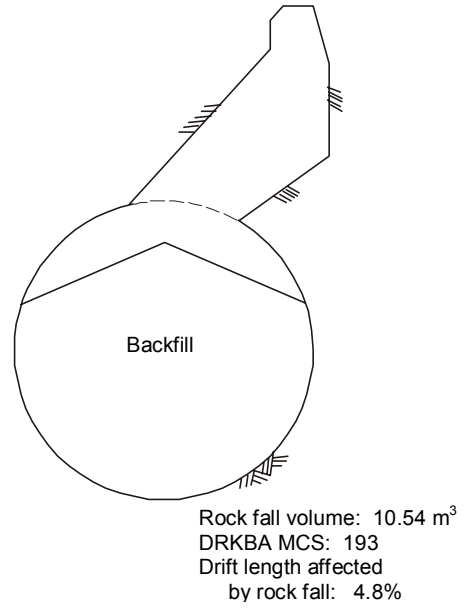


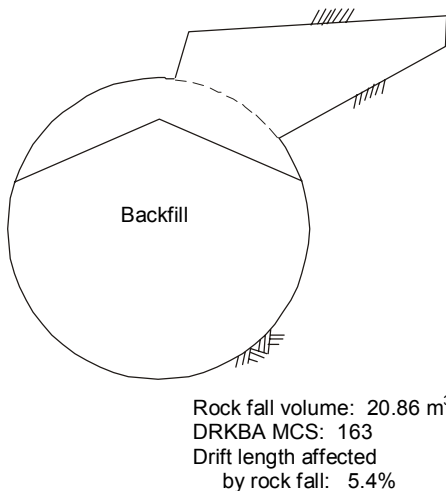
Figure 30. Emplacement Drift Profiles Considering Seismic Effects on Rock Fall for the TptIn Unit



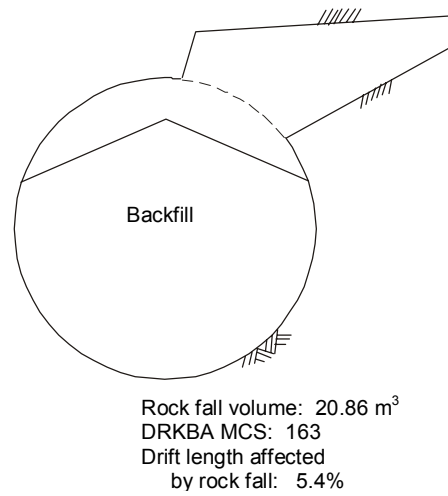
a. 0 Years (Static)



b. 200 Years

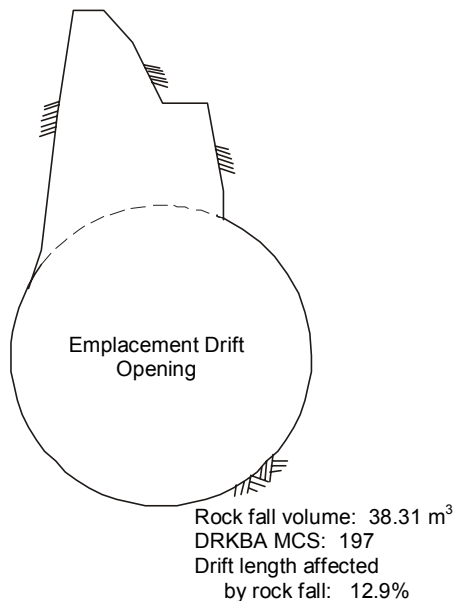


c. 2,000 Years

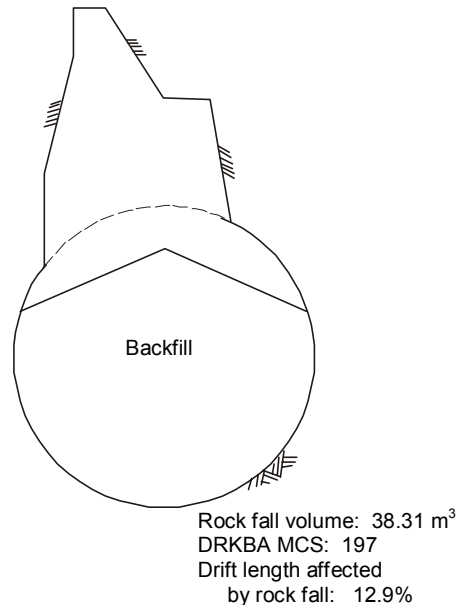


d. 10,000 Years

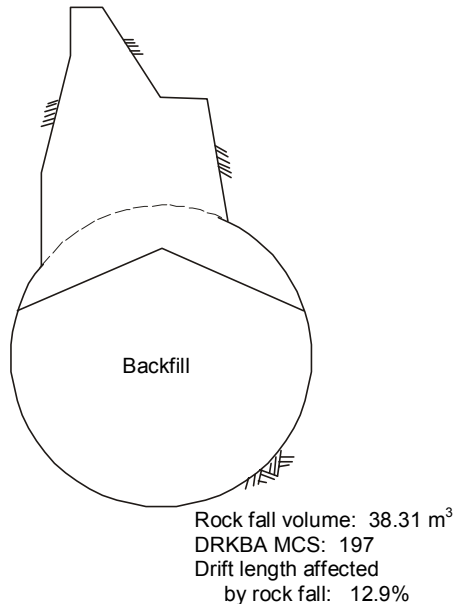
Figure 31. Emplacement Drift Profiles Considering Time-Dependent and Thermal Effects on Rock Fall for the Ttpul Unit



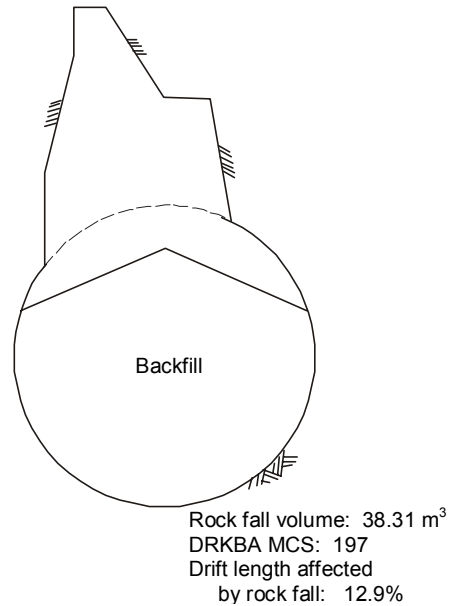
a. 0 Years (Static)



b. 200 Years

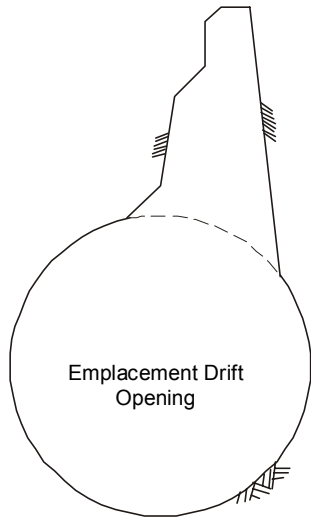


c. 2,000 Years



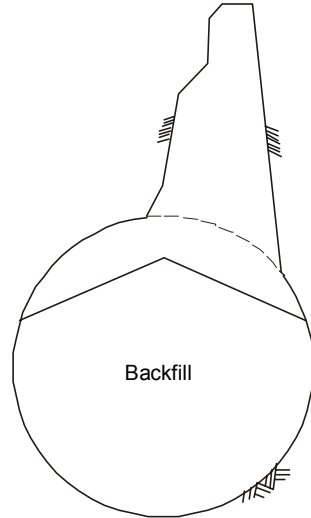
d. 10,000 Years

Figure 32. Emplacement Drift Profiles Considering Time-Dependent and Thermal Effects on Rock Fall for the Ttpmn Unit



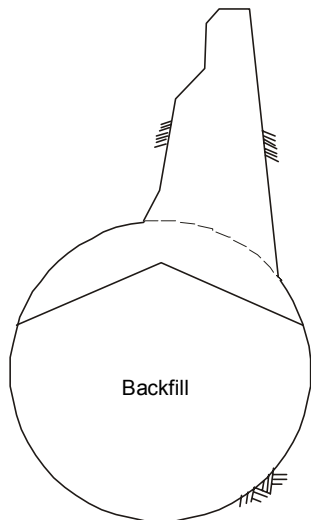
Rock fall volume: 5.67 m³
 DRKBA MCS: 290
 Drift length affected
 by rock fall: 0.9%

a. 0 Years (Static)



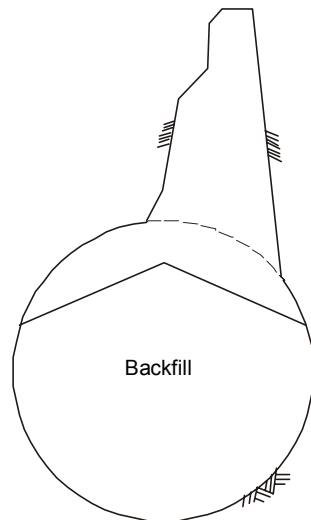
Rock fall volume: 5.67 m³
 DRKBA MCS: 290
 Drift length affected
 by rock fall: 0.9%

b. 200 Years



Rock fall volume: 5.67 m³
 DRKBA MCS: 290
 Drift length affected
 by rock fall: 1.1%

c. 2,000 Years



Rock fall volume: 5.67 m³
 DRKBA MCS: 290
 Drift length affected
 by rock fall: 1.1%

d. 10,000 Years

Figure 33. Emplacement Drift Profiles Considering Time-Dependent and Thermal Effects on Rock Fall for the TptII Unit

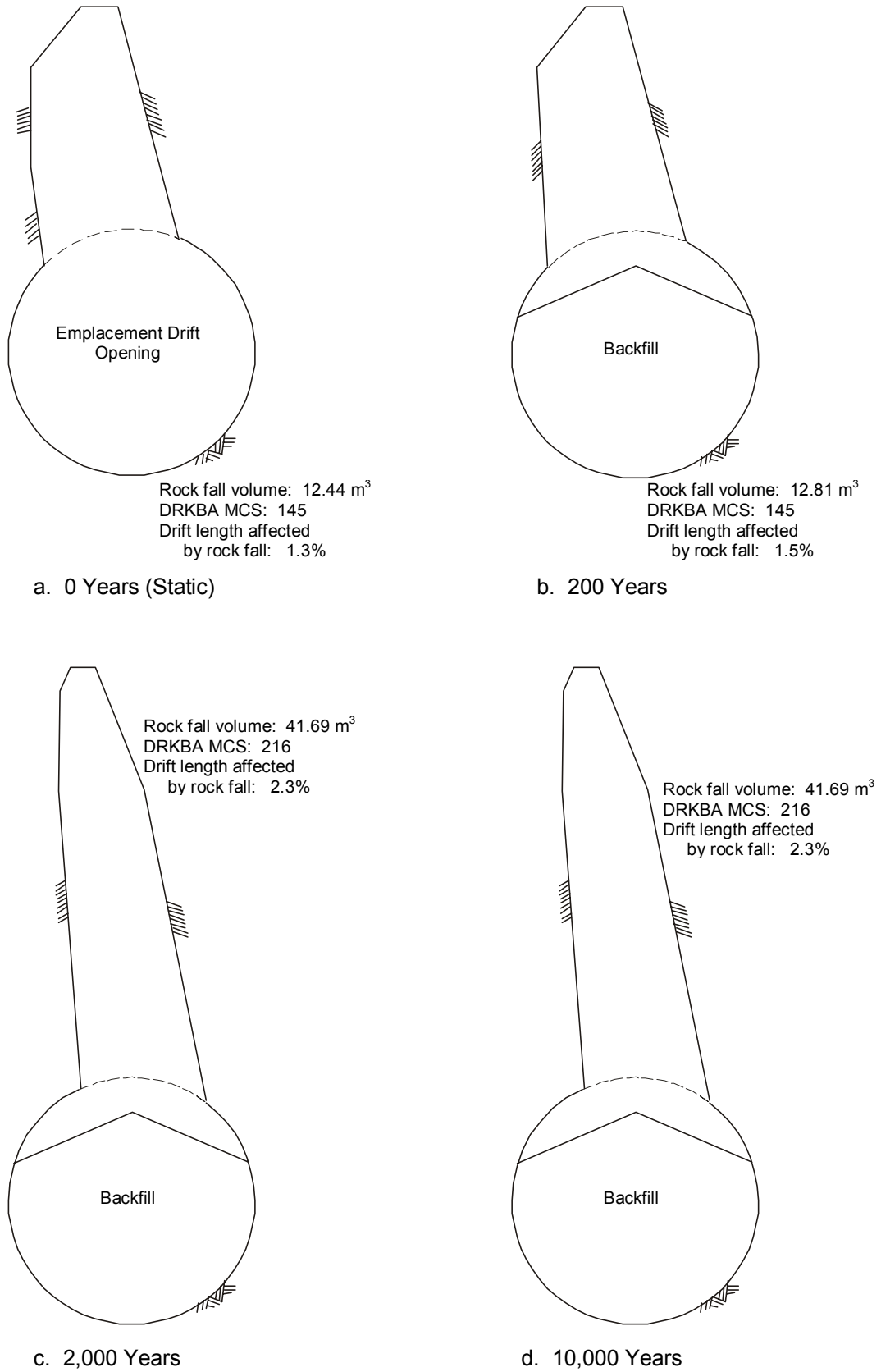


Figure 34. Emplacement Drift Profiles Considering Time-Dependent and Thermal Effects on Rock Fall for the Ttpln Unit

7. CONCLUSIONS

7.1 SUMMARY

A statistical description of the probable block sizes formed by fractures around the emplacement drifts has been developed for each of the lithologic units of the repository host horizon. The change in drift profile resulting from progressive deterioration of the emplacement drifts has been assessed both with and without backfill. Drift profiles have been determined for four different time increments, including static (i.e., upon excavation), 200 years, 2,000 years, and 10,000 years. The effect of seismic events on rock fall has been analyzed. Block size distributions and drift profiles have been determined for three seismic levels, including a 1,000-year event, a 5,000-year event, and a 10,000-year event.

The following conclusions have resulted from this Drift Degradation Analysis:

- The available fracture data are suitable for supporting a detailed key block analysis of the repository host horizon rock mass (TBV-3472). However, the Tptpln fracture data are only available from a relatively small section of the Cross Drift, resulting in a smaller fracture sample size compared to the other lithologic units. This results in a lower degree of confidence that the key block data based on the Tptpln data set is actually representative of the overall Tptpln key block population.
- The seismic effect on the rock fall size distribution for all events analyzed is relatively minor (TBV-3472, TBV-1290).
- The analysis of thermal and time-dependent effects on rock fall in this study is based on a reduction in the joint cohesion. Joint cohesion has been conservatively reduced from a laboratory test value of 0.86 MPa to a value of 0.01 MPa after 10,000 years. The results from this analysis indicate that time-dependent and thermal effects have a minor impact on rock fall (TBV-3472, TBV-1290).
- The worst-case drift degradation profiles have been provided in this analysis. Most of the emplacement drift openings were not affected by rock fall. The highest percentage of drift affected by rock fall was 16% in the Ttpmnm unit. The Ttpmnm unit produced the largest volume of key blocks per kilometer.
- The LADS emplacement drift orientation has an azimuth of 108 degrees. This key block analysis has shown that this drift alignment is relatively favorable in terms of reducing the potential maximum size rock block compared to most drift orientations. However, a re-alignment of the emplacement drifts to an azimuth of approximately 75 degrees could potentially reduce the maximum possible rock block.

7.2 ASSESSMENT

This analysis involved the use of the distinct element code, UDEC, and probabilistic key block theory through the numerical code, DRKBA. These methods are based on industry accepted approaches for analyzing geotechnical problems. In general, the static key block results

presented are representative of the observed key block occurrence in the ESF. The results of this study have shown that key blocks are most predominant in the Tptpmn unit, which agrees with field observations. The size of key blocks observed in the field is generally less than 1 m³, which agrees with the simulated distribution of block sizes presented in this study.

7.3 TBV IMPACT

TBV-3472, which is the result of using unqualified fracture inputs in the DRKBA program, is not expected to impact the results from this analysis. These inputs are based on final, qualified fracture data. The development of the fracture inputs is in the process of being documented according to a qualified procedure, and no significant changes to this data are expected.

TBV-1290, which is the result of using the unqualified code, DRKBA Version 3.3, is the primary TBV item impacting the conclusions of this study. Significant modifications to the code as a result of the qualification process are not anticipated, therefore, the resolution of TBV-1290 is not expected to significantly impact the results presented in this analysis.

The results of this analysis are based on inputs that were initially qualified, but are now subject to verification. These TBVs due to unconfirmed data are listed in [Attachment I](#). Efforts are underway to verify these inputs. Since verification of these inputs is not expected to affect the results of this analysis, a TBV indicator is not required on the analysis outputs as documented herein. The analysis is traceable to the aforementioned inputs, and in the event verification of the input data materially changes the values used herein, an update to this analysis would be required.

7.4 RECOMMENDATIONS

The following recommendations have resulted from this Drift Degradation Analysis:

- Both the DRKBA code and the fracture input data should be qualified, and any resulting impacts to this analysis from the qualification process should be assessed.
- Previous analyses that are based on preliminary key block results should be revised based on the results from this analysis.
- While this analysis has shown that a relatively small percentage of the repository host horizon will be affected by block failure, an extensive field mapping program during repository construction is recommended to help locate potential areas of key block failure.
- The data collected from the small trace length fracture study should be analyzed and their effect on the results from this analysis should be assessed. If the small trace length fracture data have a significant effect on block size distributions, then a revision of this analysis may be necessary.

8. REFERENCES

8.1 DOCUMENTS CITED

CRWMS M&O (Civilian Radioactive Waste Management System Management and Operating Contractor) 1994. *Final V&V Report for Universal Distinct Element Code (UDEC) Version 2.0 Computer Software*. CSCI: B00000000-01717-2006-30004. DI: B00000000-01717-2006-30004 REV 00. Las Vegas, Nevada: CRWMS M&O. ACC: NNA.19940407.0197.

CRWMS M&O 1997a. *Repository Subsurface Layout Configuration Analysis*. BCA000000-01717-0200-00008 REV 00. Las Vegas, Nevada: CRWMS M&O. ACC: MOL.19971201.0879.

CRWMS M&O 1997b. *Yucca Mountain Site Geotechnical Report*. B00000000-01717-5705-00043 REV 01. Las Vegas, Nevada: CRWMS M&O. ACC: MOL.19971017.0736.

CRWMS M&O 1997c. *Subsurface General Construction*. BAB000000-01717-6300-01501 REV 05. Las Vegas, Nevada: CRWMS M&O. ACC: MOL.19980127.0685.

CRWMS M&O 1999a. *Development Plan for Drift Degradation Analysis*. TDP-EBS-MD-000014 REV 01. Las Vegas, Nevada: CRWMS M&O. ACC: MOL.19991005.0221.

CRWMS M&O 1999b. *Engineered Barrier System Performance Modeling (WP#I2012383MX)*. Activity Evaluation. Las Vegas, Nevada: CRWMS M&O. ACC: MOL.19990719.0317.

CRWMS M&O 1999c. *South Ramp 3.01.X Area Ground Support Analysis*. BABEE0000-01717-0200-00023 REV 00. Las Vegas, Nevada: CRWMS M&O. ACC: MOL.19990908.0318.

CRWMS M&O 1999d. *Fracture Data from the Exploratory Studies Facility*. Design Input Transmittal EBS-SSR-99301.T. Las Vegas, Nevada: CRWMS M&O. ACC: MOL.19991011.0070.

CRWMS M&O 1999e. *Natural Environment Data for Engineered Barrier System (EBS) Base Case*. Design Input Transmittal EBS-NEP-99273.T. Las Vegas, Nevada: CRWMS M&O. ACC: MOL.19991005.0146.

Derman, C.; Gleser, L. J.; and Ingram, O. 1973. *A Guide to Probability Theory and Application*. New York, New York: Holt Rhinehart & Winston, Inc. TIC: 242445.

Dowding, C. H. 1979. "Earthquake Stability of Rock Tunnels." *Tunnels and Tunnelling*, June, 15–20. London, Great Britain: Morgan-Grampian Publishing Ltd. TIC: 242115.

Fisher, N.I.; Lewis, T.; and Embleton, B.J.J. 1987. *Statistical Analysis of Spherical Data*. New York, New York: Cambridge University Press. TIC: 208442.

Kaiser, P.K.; McCreath, D.R.; and Tannant, D.D. 1996. *Canadian Rockburst Support Handbook*. Ontario, Canada: Geomechanics Research Centre. TIC: 233844.

Kemeny, J.M. and Cook, N.G.W. 1986. "Effective Moduli, Nonlinear Deformation and Strength of a Cracked Elastic Solid." *International Journal of Rock Mechanics and Mining Sciences & Geomechanics Abstracts*, 23 (2), 107–118. Oxford, United Kingdom: Pergamon Press. TIC: 245751.

Kemeny, J.M. 1991. "A Model for Nonlinear Rock Deformation Under Compression Due to Sub-critical Crack Growth." *International Journal of Rock Mechanics and Mining Sciences & Geomechanics Abstracts*, 28 (6), 459–467. Oxford, United Kingdom: Pergamon Press. TIC: 245750.

Kessler, J. and McGuire, R. 1996. *Yucca Mountain Total System Performance Assessment, Phase 3*. EPRI TR-107191. Palo Alto, California: Electric Power Research Institute. TIC: 238085.

Wilkins, D.R. and Heath, C.A. 1999. "Direction to Transition to Enhanced Design Alternative II." Letter from D.R. Wilkins and C.A. Heath (CRWMS M&O) to Distribution, June 15, 1999, LV.NS.JLY.06/99-026, with enclosures, "Strategy for Baselineing EDA II Requirements" and "Guidelines for Implementation of EDA II." ACC: MOL.19990622.0126; MOL.19990622.0127; MOL.19990622.0128.

8.2 CODES, STANDARDS, REGULATIONS, AND PROCEDURES

AP-2.14Q, Revision 0, ICN 0. *Review of Technical Products*. Washington, D.C.: U.S. Department of Energy, Office of Civilian Radioactive Waste Management. ACC: MOL.19990701.0616.

AP-3.4Q, Revision 0, ICN 0. *Level 3 Change Control*. Washington, D.C.: U.S. Department of Energy, Office of Civilian Radioactive Waste Management. ACC: MOL.19990701.0624.

AP-3.10Q, Revision 1, ICN 0. *Analyses and Models*. Washington, D.C.: U.S. Department of Energy, Office of Civilian Radioactive Waste Management. ACC: MOL.19990702.0314.

AP-3.14Q, Revision 0, ICN 0. *Transmittal of Input*. Washington, D.C.: U.S. Department of Energy, Office of Civilian Radioactive Waste Management. ACC: MOL.19990701.0621.

AP-3.15Q, Revision 0, ICN 1. *Managing Technical Product Inputs*. Washington, D.C.: U.S. Department of Energy, Office of Civilian Radioactive Waste Management. ACC: MOL.19990831.0079.

AP-6.1Q, Revision 3, ICN 0. *Controlled Documents*. Washington, D.C.: U.S. Department of Energy, Office of Civilian Radioactive Waste Management. ACC: MOL.19990702.0309.

AP-17.1Q, Revision 1, ICN 1. *Record Source Responsibilities for Inclusionary Records*. Washington, D.C.: U.S. Department of Energy, Office of Civilian Radioactive Waste Management. ACC: MOL.19990902.0444.

AP-SI.1Q, Revision 1, ICN 0. *Software Management*. Washington, D.C.: U.S. Department of Energy, Office of Civilian Radioactive Waste Management. ACC: MOL.19990502.0164.

AP-SIII.2Q, Revision 0, ICN 0. *Qualification of Unqualified Data and Documentation of the Rationale for Accepted Data*. Washington, D.C.: U.S. Department of Energy, Office of Civilian Radioactive Waste Management. ACC: MOL.19990702.0308.

AP-SIII.3Q, Revision 0, ICN 1. *Submittal and Incorporation of Data to the Technical Data Management System*. Washington, D.C.: U.S. Department of Energy, Office of Civilian Radioactive Waste Management. ACC: MOL.19990831.0078.

NLP-2-0, Revision 5. *Determination of Importance Evaluations*. Las Vegas, Nevada: CRWMS M&O. ACC: MOL.19981116.0120.

QAP-2-0, Revision 5. *Conduct of Activities*. Las Vegas, Nevada: CRWMS M&O. ACC: MOL.19980826.0209.

QAP-2-3, Revision 10. *Classification of Permanent Items*. Las Vegas, Nevada: CRWMS M&O. ACC: MOL.19990316.0006.

YAP-SV.1Q, Revision 0, ICN 0. *Control of the Electronic Management of Data*. Las Vegas, Nevada: U.S. Department of Energy, Yucca Mountain Site Characterization Office. ACC: MOL.19990323.0434.

8.3 SOURCE DATA, LISTED BY DATA TRACKING NUMBER

GS971108314224.024. Revision 1 of Detailed Line Survey Data, Station 18+00 to Station 26+00, North Ramp, Exploratory Studies Facility. Submittal date: 12/03/1997.

GS971108314224.025. Revision 1 of Detailed Line Survey Data, Station 26+00 to Station 30+00, North Ramp and Main Drift, Exploratory Studies Facility. Submittal date: 12/03/1997.

GS960708314224.008. Provisional Results: Geotechnical Data for Station 30+00 to Station 35+00, Main Drift of the ESF. Submittal date: 08/05/1996.

GS960808314224.011. Provisional Results: Geotechnical Data for Station 35+00 to Station 40+00, Main Drift of the ESF. Submittal date: 08/29/1996.

GS960708314224.010. Provisional Results: Geotechnical Data for Station 40+00 to Station 45+00, Main Drift of the ESF. Submittal date: 08/05/1996.

GS971108314224.026. Revision 1 of Detailed Line Survey Data, Station 45+00 to Station 50+00, Main Drift, Exploratory Studies Facility. Submittal date: 12/03/1997.

GS960908314224.014. Provisional Results - ESF Main Drift, Station 50+00 to Station 55+00. Submittal date: 09/09/1996.

GS971108314224.028. Revision 1 of Detailed Line Survey Data, Station 55+00 to Station 60+00, Main Drift and South Ramp, Exploratory Studies Facility. Submittal date: 12/03/1997.

GS970208314224.003. Geotechnical Data for Station 60+00 to Station 65+00, South Ramp of the ESF. Submittal date: 02/12/1997.

GS970808314224.010. Provisional Results: Geotechnical Data for Station 70+00 to Station 75+00, South Ramp of the ESF. Submittal date: 08/25/1997.

GS960908314224.020. Analysis Report: Geology of the North Ramp - Stations 4+00 to 28+00 and Data: Detailed Line Survey and Full Periphery Geotechnical Map - Alcoves 3 (UPCA) and 4 (LPCA), and Comparative Geologic Cross Section - Stations 0+60 to 28+00. Submittal date: 09/09/1996.

GS960808314224.012. Provisional Results: Geotechnical Data for Station 26+00 to 30+00, North Ramp and Main Drift of the ESF, Full Periphery Geotechnical Maps (Drawings OA-46-222 through OA-46-226) and Rock Mass Quality Ratings Report. Submittal date: 08/29/1996.

GS960908314224.015. Provisional Results: Geotechnical Data for Station 30+00 to 40+00, Main Drift of the ESF, Full Periphery Geotechnical Maps and Rock Mass Quality Ratings Report. Submittal date: 09/09/1996.

GS960908314224.016. Provisional Results: Geotechnical Data for Station 40+00 to 50+00, Main Drift of the ESF, Full Periphery Geotechnical Maps and Rock Mass Quality Ratings Report. Submittal date: 09/09/1996.

GS960908314224.017. Provisional Results: Geotechnical Data for Station 50+00 to 55+00, Main Drift of the ESF, Full Periphery Geotechnical Maps and Rock Mass Quality Ratings Report. Submittal date: 09/09/1996.

GS970108314224.002. Provisional Results: Geotechnical Data for Station 55+00 to 60+00, Main Drift of the ESF, Full Periphery Geotechnical Maps (Drawings OA-46-257 through OA-46-262) and Rock Mass Quality Ratings Report. Submittal date: 01/31/1997.

GS970208314224.004. Geotechnical Data for Station 60+00 to 65+00, South Ramp of the ESF. Submittal date: 02/12/1997.

GS970808314224.009. Provisional Results: Geotechnical Data for Station 65+00 to 70+00, South Ramp of the ESF, Full Periphery Geotechnical Maps (Drawings OA-46-269 through OA-46-274) and Rock Mass Quality Ratings Report. Submittal date: 08/18/1997.

GS970808314224.011. Provisional Results: Geotechnical Data for Station 70+00 to 75+00, South Ramp of the ESF. Submittal date: 08/25/1997.

MO9904MWDFPG16.000. Full Periphery Geotechnical Mapping Strike and Dip Data Entry Correction Analysis. Submittal date: 04/06/1999.

GS990408314224.001. Detailed Line Survey Data for Stations 00+00.89 to 14+95.18, ECRB Cross Drift. Submittal date: **in progress**.

GS990408314224.002. Detailed Line Survey Data for Stations 15+00.85 to 26+63.85, ECRB Cross Drift. Submittal date: **in progress**.

GS990408314224.003. Full-periphery Geologic Maps for Station -0+10 to 10+00, ECRB Cross Drift. Submittal date: **in progress**.

GS990408314224.004. Full-periphery Geologic Maps for Station 10+00 to 15+00, ECRB Cross Drift. Submittal date: **in progress**.

GS990408314224.005. Full-periphery Geologic Maps for Station 15+00 to 20+00, ECRB Cross Drift. Submittal date: **in progress**.

GS990408314224.006. Full-periphery Geologic Maps for Station 20+00 to 26+81, ECRB Cross Drift. Submittal date: **in progress**.

SNL02030193001.027. Summary of Bulk Property Measurements Including Saturated Bulk Density for NRG-2, NRG-2A, NRG-2B, NRG-3, NRG-4, NRG-5, NRG-6, NRG-7/7A, SD-9, and SD-12. Submittal date: 08/14/1996.

SNL02112293001.002. Results from Shear Stress Experiments on Natural Fractures from NRG-7. Submittal date: 03/10/1995.

SNL02112293001.003. Results from Shear Stress Experiments on Natural Fractures from NRG-4 and NRG-6. Submittal date: 03/13/1995.

SNL02112293001.005. Mechanical Properties of Fractures in Specimens from Drillhole USW SD-9. Submittal date: 07/15/1996.

SNL02112293001.007. Mechanical Properties of Fractures in Specimens from Drillholes USW-NRG-7/7A and USW SD-12. Submittal date: 08/08/1996.

SNL02030193001.004. Mechanical Properties Data (Ultrasonic Velocities, Static Elastic Properties, Unconfined Strength, and Average Grain Density) for Drillhole USW NRG-6 Samples from Depth 462.3 ft. to 1085.0 ft. Submittal date: 08/05/1993.

SNL02030193001.012. Mechanical Properties Data (Ultrasonic Velocities, Static Elastic Properties, and Unconfined Strength) for Drillhole UE25 NRG-5 Samples from Depth 847.2 ft. to 896.5 ft. Submittal date: 12/02/1993.

SNL02030193001.019. Mechanical Properties Data (Grain Density, Porosity, Unconfined Strength, Confined Strength, Elastic Properties, and Indirect Tensile Strength) for Drillhole USW NRG-7/7A Samples from Depth 507.4 ft. to 881.0 ft. Submittal date: 06/29/1994.

SNL02030193001.020. Mechanical Properties Data (Ultrasonic Velocities, Static Elastic Properties, Unconfined Strength, Triaxial Strength, Dry Bulk Density, and Porosity) for Drillhole USW NRG-7/7A Samples from Depth 554.7 ft. to 1450.1 ft. Submittal date: 07/25/1994.

SNL02030193001.021. Mechanical Properties Data (Ultrasonic Velocities, Static Elastic Properties, Triaxial Strength, Dry Bulk Density, and Porosity) for Drillhole USW NRG-7/7A Samples from Depth 345.0 ft. to 1408.6 ft. Submittal date: 02/16/1995.

SNL02030193001.023. Mechanical Properties Data (Ultrasonic Velocities, Static Elastic Properties, Unconfined Strength, Triaxial Strength, Dry Bulk Density, and Porosity) for Drillhole USW SD-12 Samples from Depth 16.1 ft. to 1300.3 ft. Submittal date: 08/02/1995.

SNL02030193001.026. Mechanical Properties Data (Ultrasonic Velocities, Elastic Moduli and Fracture Strength) for Drillhole USW SD-9. Submittal date: 02/22/1996.

SN9908T0872799.004. Tabulated In-drift Geometric and Thermal Properties used in Drift-scale Models for TSPA-SR (Total System Performance Assessment - Site Recommendation). Submittal date: 08/30/1999.

ATTACHMENT I
DOCUMENT INPUT REFERENCE SHEET

**OFFICE OF CIVILIAN RADIOACTIVE WASTE MANAGEMENT
DOCUMENT INPUT REFERENCE SHEET**

1. Document Identifier No./Rev.:		Change:	Title:							
ANL-EBS-MD-000027 REV 00B		N/A	Drift Degradation Analysis							
Input Document				4. Input Status	5. Section Used in	6. Input Description	7. TBV/TBD Priority	8. TBV Due To		
2. Technical Product Input Source Title and Identifier(s) with Version		3. Section	Unqual.					From Uncontrolled Source	Un-confirmed	
2a	DTN: GS971108314224.024. Revision 1 of Detailed Line Survey Data, Station 18+00 to Station 26+00, North Ramp, Exploratory Studies Facility. Submittal date: 12/03/1997.	Entire	TBV-1278	4, 6	North Ramp Detailed Line Survey fracture data.	1			✓	
1										
2	DTN: GS971108314224.025. Revision 1 of Detailed Line Survey Data, Station 26+00 to Station 30+00, North Ramp and Main Drift, Exploratory Studies Facility. Submittal date: 12/03/1997.	Entire	TBV-1279	4, 6	North Ramp and Main Drift Detailed Line Survey fracture data.	1			✓	
3	DTN: GS960708314224.008. Provisional Results: Geotechnical Data for Station 30+00 to Station 35+00, Main Drift of the ESF. Submittal date: 08/05/1996.	Entire	TBV-1280	4, 6	Main Drift Detailed Line Survey fracture data.	1			✓	
4	DTN: GS960808314224.011. Provisional Results: Geotechnical Data for Station 35+00 to Station 40+00, Main Drift of the ESF. Submittal date: 08/29/1996.	Entire	TBV-1281, TBV-525	4, 6	Main Drift Detailed Line Survey fracture data.	1			✓	
5	DTN: GS960708314224.010. Provisional Results: Geotechnical Data for Station 40+00 to Station 45+00, Main Drift of the ESF. Submittal date: 08/05/1996.	Entire	TBV-1282, TBV-526	4, 6	Main Drift Detailed Line Survey fracture data.	1			✓	
6	DTN: GS971108314224.026. Revision 1 of Detailed Line Survey Data, Station 45+00 to Station 50+00, Main Drift, Exploratory Studies Facility. Submittal date: 12/03/1997.	Entire	TBV-1283	4, 6	Main Drift Detailed Line Survey fracture data.	1			✓	
7	DTN: GS960908314224.014. Provisional Results - ESF Main Drift, Station 50+00 to Station 55+00. Submittal date: 09/09/1996.	Entire	TBV-1284	4, 6	Main Drift Detailed Line Survey fracture data.	1			✓	
8	DTN: GS971108314224.028. Revision 1 of Detailed Line Survey Data, Station 55+00 to Station 60+00, Main Drift and South Ramp, Exploratory Studies Facility. Submittal date: 12/03/1997.	Entire	TBV-1285	4, 6	Main Drift and South Ramp Detailed Line Survey fracture data.	1			✓	

ANL-EBS-MD-000027 REV 00

I-2

November 1999

**OFFICE OF CIVILIAN RADIOACTIVE WASTE MANAGEMENT
DOCUMENT INPUT REFERENCE SHEET**

1. Document Identifier No./Rev.:		Change:	Title:							
ANL-EBS-MD-000027 REV 00B		N/A	Drift Degradation Analysis							
Input Document			4. Input Status	5. Section Used in	6. Input Description	7. TBV/TBD Priority	8. TBV Due To			
2. Technical Product Input Source Title and Identifier(s) with Version		3. Section					Unqual.	From Uncontrolled Source	Un-confirmed	
9	DTN: GS970208314224.003. Geotechnical Data for Station 60+00 to Station 65+00, South Ramp of the ESF. Submittal date: 02/12/1997.		Entire	TBV-1286	4, 6	South Ramp Detailed Line Survey fracture data.	1			✓
10	DTN: GS970808314224.010. Provisional Results: Geotechnical Data for Station 70+00 to Station 75+00, South Ramp of the ESF. Submittal date: 08/25/1997.		Entire	TBV-1288	4, 6	South Ramp Detailed Line Survey fracture data.	1			✓
11	DTN: GS960908314224.020. Analysis Report: Geology of the North Ramp - Stations 4+00 to 28+00 and Data: Detailed Line Survey and Full Periphery Geotechnical Map - Alcoves 3 (UPCA) and 4 (LPCA), and Comparative Geologic Cross Section - Stations 0+60 to 28+00. Submittal date: 09/09/1996.		Entire	TBV-1292	4, 6	North Ramp full periphery geology and geotechnical map data.	1			✓
12	DTN: GS960808314224.012. Provisional Results: Geotechnical Data for Station 26+00 to 30+00, North Ramp and Main Drift of the ESF, Full Periphery Geotechnical Maps (Drawings OA-46-222 through OA-46-226) and Rock Mass Quality Ratings Report. Submittal date: 08/29/1996.		Entire	TBV-1293	4, 6	North Ramp and Main Drift full periphery geology and geotechnical map data.	1			✓
13	DTN: GS960908314224.015. Provisional Results: Geotechnical Data for Station 30+00 to 40+00, Main Drift of the ESF, Full Periphery Geotechnical Maps and Rock Mass Quality Ratings Report. Submittal date: 09/09/1996.		Entire	TBV-1294, TBV-1270	4, 6	Main Drift full periphery geology and geotechnical map data.	1			✓
14	DTN: GS960908314224.016. Provisional Results: Geotechnical Data for Station 40+00 to 50+00, Main Drift of the ESF, Full Periphery Geotechnical Maps and Rock Mass Quality Ratings Report. Submittal date: 09/09/1996.		Entire	TBV-1295, TBV-1271	4, 6	Main Drift full periphery geology and geotechnical map data.	1			✓
15	DTN: GS960908314224.017. Provisional Results: Geotechnical Data for Station 50+00 to 55+00, Main Drift of the ESF, Full Periphery Geotechnical Maps and Rock Mass Quality Ratings Report. Submittal date: 09/09/1996.		Entire	TBV-1296	4, 6	Main Drift full periphery geology and geotechnical map data.	1			✓

ANL-EBS-MD-000027 REV 00

I-3

November 1999

**OFFICE OF CIVILIAN RADIOACTIVE WASTE MANAGEMENT
DOCUMENT INPUT REFERENCE SHEET**

1. Document Identifier No./Rev.:		Change:	Title:							
ANL-EBS-MD-000027 REV 00B		N/A	Drift Degradation Analysis							
Input Document				4. Input Status	5. Section Used in	6. Input Description	7. TBV/TBD Priority	8. TBV Due To		
2. Technical Product Input Source Title and Identifier(s) with Version		3. Section	Unqual.					From Uncontrolled Source	Un-confirmed	
16	DTN: GS970108314224.002. Provisional Results: Geotechnical Data for Station 55+00 to 60+00, Main Drift of the ESF, Full Periphery Geotechnical Maps (Drawings OA-46-257 through OA-46-262) and Rock Mass Quality Ratings Report. Submittal date: 01/31/1997.		Entire	TBV-1297	4, 6	Main Drift full periphery geology and geotechnical map data.	1			✓
17	DTN: GS970208314224.004. Geotechnical Data for Station 60+00 to 65+00, South Ramp of the ESF. Submittal date: 02/12/1997.		Entire	TBV-1298	4, 6	South Ramp full periphery geology and geotechnical map data.	1			✓
18	DTN: GS970808314224.009. Provisional Results: Geotechnical Data for Station 65+00 to 70+00, South Ramp of the ESF, Full Periphery Geotechnical Maps (Drawings OA-46-269 through OA-46-274) and Rock Mass Quality Ratings Report. Submittal date: 08/18/1997.		Entire	TBV-1299	4, 6	South Ramp full periphery geology and geotechnical map data.	1			✓
19	DTN: GS970808314224.011. Provisional Results: Geotechnical Data for Station 70+00 to 75+00, South Ramp of the ESF. Submittal date: 08/25/1997.		Entire	TBV-1300, TBV-1272	4, 6	South Ramp full periphery geology and geotechnical map data.	1			✓
20	DTN: MO9904MWDFFPG16.000. Full Periphery Geotechnical Mapping Strike and Dip Data Entry Correction Analysis. Submittal date: 04/06/1999.		Entire	TBV-3463	4, 6	ESF Main Loop (i.e., North Ramp, Main Drift, and South Ramp) full periphery geotechnical mapping strike and dip correction.	1			✓
21	DTN: GS990408314224.001. Detailed Line Survey Data for Stations 00+00.89 to 14+95.18, ECRB Cross Drift. Submittal date: in progress.		Entire	TBV-3256	4, 6	Cross Drift Detailed Line Survey fracture data.	1			✓

ANL-EBS-MD-000027 REV 00

I-4

November 1999

**OFFICE OF CIVILIAN RADIOACTIVE WASTE MANAGEMENT
DOCUMENT INPUT REFERENCE SHEET**

1. Document Identifier No./Rev.:		Change:	Title:							
ANL-EBS-MD-000027 REV 00B		N/A	Drift Degradation Analysis							
Input Document				4. Input Status	5. Section Used in	6. Input Description	7. TBV/TBD Priority	8. TBV Due To		
2. Technical Product Input Source Title and Identifier(s) with Version			3. Section					Unqual.	From Uncontrolled Source	Un-confirmed
22	DTN: GS990408314224.002. Detailed Line Survey Data for Stations 15+00.85 to 26+63.85, ECRB Cross Drift. Submittal date: in progress.		Entire	TBV-3257	4, 6	Cross Drift Detailed Line Survey fracture data.	1			✓
23	DTN: GS990408314224.003. Full-periphery Geologic Maps for Station -0+10 to 10+00, ECRB Cross Drift. Submittal date: in progress.		Entire	TBV-3466	4, 6	Cross Drift full periphery geology and geotechnical map data.	1			✓
24	DTN: GS990408314224.004. Full-periphery Geologic Maps for Station 10+00 to 15+00, ECRB Cross Drift. Submittal date: in progress.		Entire	TBV-3467	4, 6	Cross Drift full periphery geology and geotechnical map data.	1			✓
25	DTN: GS990408314224.005. Full-periphery Geologic Maps for Station 15+00 to 20+00, ECRB Cross Drift. Submittal date: in progress.		Entire	TBV-3468	4, 6	Cross Drift full periphery geology and geotechnical map data.	1			✓
26	DTN: GS990408314224.006. Full-periphery Geologic Maps for Station 20+00 to 26+81, ECRB Cross Drift. Submittal date: in progress.		Entire	TBV-3469	4, 6	Cross Drift full periphery geology and geotechnical map data.	1			✓
27	DTN: SNL02030193001.027. Summary of Bulk Property Measurements Including Saturated Bulk Density for NRG-2, NRG-2A, NRG-2B, NRG-3, NRG-4, NRG-5, NRG-6, NRG-7/7A, SD-9, and SD-12. Submittal date: 08/14/1996.		Entire	TBV-3470	4, 6	Saturated bulk density borehole data.	1			✓
28	DTN: SNL02112293001.002. Results from Shear Stress Experiments on Natural Fractures from NRG-7. Submittal date: 03/10/1995.		Entire	TBV-1333	4, 6	Fracture shear strength data from boreholes.	1			✓
29	DTN: SNL02112293001.003. Results from Shear Stress Experiments on Natural Fractures from NRG-4 and NRG-6. Submittal date: 03/13/1995.		Entire	TBV-1334	4, 6	Fracture shear strength data from boreholes.	1			✓
30	DTN: SNL02112293001.005. Mechanical Properties of Fractures in Specimens from Drillhole USW SD-9. Submittal date: 07/15/1996.		Entire	TBV-1327	4, 6	Fracture shear strength data from boreholes.	1			✓

ANL-EBS-MD-000027 REV 00

I-5

November 1999

**OFFICE OF CIVILIAN RADIOACTIVE WASTE MANAGEMENT
DOCUMENT INPUT REFERENCE SHEET**

1. Document Identifier No./Rev.:		Change:	Title:							
ANL-EBS-MD-000027 REV 00B		N/A	Drift Degradation Analysis							
Input Document			4. Input Status	5. Section Used in	6. Input Description	7. TBV/TBD Priority	8. TBV Due To			
2. Technical Product Input Source Title and Identifier(s) with Version		3. Section					Unqual.	From Uncontrolled Source	Un-confirmed	
31	DTN: SNL02112293001.007. Mechanical Properties of Fractures in Specimens from Drillholes USW-NRG-7/7A and USW SD-12. Submittal date: 08/08/1996.		Entire	TBV-1328	4, 6	Fracture shear strength data from boreholes.	1			✓
32	DTN: SNL02030193001.004. Mechanical Properties Data (Ultrasonic Velocities, Static Elastic Properties, Unconfined Strength, and Average Grain Density) for Drillhole USW NRG-6 Samples from Depth 462.3 ft. to 1085.0 ft. Submittal date: 08/05/1993.		Table S98485_001	TBV-1305	4, 6	Intact rock elastic properties from the TSw2 unit.	1			✓
33	DTN: SNL02030193001.012. Mechanical Properties Data (Ultrasonic Velocities, Static Elastic Properties, and Unconfined Strength) for Drillhole UE25 NRG-5 Samples from Depth 847.2 ft. to 896.5 ft. Submittal date: 12/02/1993.		Table S99110_003	TBV-1313	4, 6	Intact rock elastic properties from the TSw2 unit.	1			✓
34	DTN: SNL02030193001.019. Mechanical Properties Data (Grain Density, Porosity, Unconfined Strength, Confined Strength, Elastic Properties, and Indirect Tensile Strength) for Drillhole USW NRG-7/7A Samples from Depth 507.4 ft. to 881.0 ft. Submittal date: 06/29/1994.		Table S99115_004	TBV-1320	4, 6	Intact rock elastic properties from the TSw2 unit.	1			✓
35	DTN: SNL02030193001.020. Mechanical Properties Data (Ultrasonic Velocities, Static Elastic Properties, Unconfined Strength, Triaxial Strength, Dry Bulk Density, and Porosity) for Drillhole USW NRG-7/7A Samples from Depth 554.7 ft. to 1450.1 ft. Submittal date: 07/25/1994.		Table S99116_003	TBV-1321	4, 6	Intact rock elastic properties from the TSw2 unit.	1			✓
36	DTN: SNL02030193001.021. Mechanical Properties Data (Ultrasonic Velocities, Static Elastic Properties, Triaxial Strength, Dry Bulk Density, and Porosity) for Drillhole USW NRG-7/7A Samples from Depth 345.0 ft. to 1408.6 ft. Submittal date: 02/16/1995.		Table S99117_003	TBV-1322	4, 6	Intact rock elastic properties from the TSw2 unit.	1			✓
37	DTN: SNL02030193001.023. Mechanical Properties Data (Ultrasonic Velocities, Static Elastic Properties, Unconfined Strength, Triaxial Strength, Dry Bulk Density, and Porosity) for Drillhole USW SD-12 Samples from Depth 16.1 ft. to 1300.3 ft. Submittal date: 08/02/1995.		Table S99120_002	TBV-1324	4, 6	Intact rock elastic properties from the TSw2 unit.	1			✓

ANL-EBS-MD-000027 REV 00

I-6

November 1999

**OFFICE OF CIVILIAN RADIOACTIVE WASTE MANAGEMENT
DOCUMENT INPUT REFERENCE SHEET**

1. Document Identifier No./Rev.:		Change:	Title:							
ANL-EBS-MD-000027 REV 00B		N/A	Drift Degradation Analysis							
Input Document				4. Input Status	5. Section Used in	6. Input Description	7. TBV/TBD Priority	8. TBV Due To		
2. Technical Product Input Source Title and Identifier(s) with Version			3. Section					Unqual.	From Uncontrolled Source	Un-confirmed
38	DTN: SNL02030193001.026. Mechanical Properties Data (Ultrasonic Velocities, Elastic Moduli and Fracture Strength) for Drillhole USW SD-9. Submittal date: 02/22/1996.		Table S99119_002	TBV-1326	4, 6	Intact rock elastic properties from the TSw2 unit.	1			✓
39	DTN: SN9908T0872799.004. Tabulated In-drift Geometric and Thermal Properties used in Drift-scale Models for TSPA-SR (Total System Performance Assessment - Site Recommendation). Submittal date: 08/30/1999.		Entire	TBV-3471	4, 6	Backfill configuration and dimensions.	1	✓		
40	CRWMS M&O (Civilian Radioactive Waste Management System Management and Operating Contractor) 1994. Final V&V Report for Universal Distinct Element Code (UDEEC) Version 2.0 Computer Software. CSCI: B00000000-01717-2006-30004. DI: B00000000-01717-2006-30004 REV 00. Las Vegas, Nevada: CRWMS M&O. ACC: NNA.19940407.0197.		Entire	N/A	3	Software qualification document.	N/A	N/A	N/A	N/A
41	CRWMS M&O 1997a. Repository Subsurface Layout Configuration Analysis. BCA000000-01717-0200-00008 REV 00. Las Vegas, Nevada: CRWMS M&O. ACC: MOL.19971201.0879.		pp. 22 and 23	N/A	1, 6	Source of emplacement drift orientation for the LADS for the repository.	N/A	N/A	N/A	N/A
42	CRWMS M&O 1997b. Yucca Mountain Site Geotechnical Report. B00000000-01717-5705-00043 REV 01. Las Vegas, Nevada: CRWMS M&O. ACC: MOL.19971017.0736.		Section 5	N/A	4	Source of developed intact rock and joint properties	N/A	N/A	N/A	N/A
43	CRWMS M&O 1997c. Subsurface General Construction. BAB000000-01717-6300-01501 REV 05. Las Vegas, Nevada: CRWMS M&O. ACC: MOL.19980127.0685.		p. 15	N/A	6	Definition of 3.01X areas in the ESF.	N/A	N/A	N/A	N/A
44	CRWMS M&O 1999a. Development Plan for Drift Degradation Analysis. TDP-EBS-MD-000014 REV 01. Las Vegas, Nevada: CRWMS M&O. ACC: MOL.19991005.0221.		Entire	N/A	1, 2	Analysis planning document.	N/A	N/A	N/A	N/A

ANL-EBS-MD-000027 REV 00

I-7

November 1999

**OFFICE OF CIVILIAN RADIOACTIVE WASTE MANAGEMENT
DOCUMENT INPUT REFERENCE SHEET**

1. Document Identifier No./Rev.:		Change:	Title:							
ANL-EBS-MD-000027 REV 00B		N/A	Drift Degradation Analysis							
Input Document				4. Input Status	5. Section Used in	6. Input Description	7. TBV/TBD Priority	8. TBV Due To		
2. Technical Product Input Source Title and Identifier(s) with Version			3. Section					Unqual.	From Uncontrolled Source	Un-confirmed
45	CRWMS M&O 1999b. <i>Engineered Barrier System Performance Modeling (WP#12012383MX)</i> . Activity Evaluation. Las Vegas, Nevada: CRWMS M&O. ACC: MOL.19990719.0317.		Entire	N/A	2	QA activity evaluation document.	N/A	N/A	N/A	N/A
46	CRWMS M&O 1999c. <i>South Ramp 3.01.X Area Ground Support Analysis</i> . BABEE0000-01717-0200-00023 REV 00. Las Vegas, Nevada: CRWMS M&O. ACC: MOL.19990908.0318.		p. 27	N/A	6	Description of 3.01X areas in the ESF.	N/A	N/A	N/A	N/A
47	CRWMS M&O 1999d. <i>Fracture Data from the Exploratory Studies Facility</i> . Design Input Transmittal EBS-SSR-99301.T. Las Vegas, Nevada: CRWMS M&O. ACC: MOL.19991011.0070.		Entire	TBV-3472	4, 6	Developed fracture data from the ESF.	1	✓		
48	CRWMS M&O 1999e. <i>Natural Environment Data for Engineered Barrier System (EBS) Base Case</i> . Design Input Transmittal EBS-NEP-99273T. Las Vegas, Nevada: CRWMS M&O. ACC: MOL.19991005.0146.		Entire	TBV-3473	4, 6	Vibratory ground motion parameters: peak ground accelerations, peak ground velocities, and design spectral accelerations.	1			✓
49	Derman, C.; Gleser, L. J.; and Ingram, O. 1973. <i>A Guide to Probability Theory and Application</i> . New York: Holt Rhinehart & Winston, Inc. TIC: 241514.		pp. 398-403	N/A	6	Bases for statistical approach to determine Beta distribution parameters, a, b, p, and q, for joint geometrical data.	N/A	N/A	N/A	N/A
50	Dowding, C. H. 1979. <i>Earthquake Stability of Rock Tunnels. Tunnels and Tunnelling</i> , June, 15-20. London, Great Britain: Morgan-Grampian Publishing Ltd. TIC: 242115.		p. 19	N/A	6	Bases for seismic analyses technical approach.	N/A	N/A	N/A	N/A
51	Fisher, N.I.; Lewis, T.; and Embleton, B.J.J. 1987. <i>Statistical Analysis of Spherical Data</i> . New York, New York: Cambridge University Press. TIC: 208442.		p. 33, pp. 175-776	N/A	6	Bases for approach to determine the concentration factor, k, for joint orientation data.	N/A	N/A	N/A	N/A

ANL-EBS-MD-000027 REV 00

I-8

November 1999

**OFFICE OF CIVILIAN RADIOACTIVE WASTE MANAGEMENT
DOCUMENT INPUT REFERENCE SHEET**

1. Document Identifier No./Rev.:		Change:	Title:							
ANL-EBS-MD-000027 REV 00B		N/A	Drift Degradation Analysis							
Input Document			4. Input Status	5. Section Used in	6. Input Description	7. TBV/TBD Priority	8. TBV Due To			
2. Technical Product Input Source Title and Identifier(s) with Version		3. Section					Unqual.	From Uncontrolled Source	Un-confirmed	
52	Kaiser, P. K.; McCreath, D. R.; and Tannant, D. D. 1996. <i>Canadian Rockburst Support Handbook</i> . Ontario, Canada: Geomechanics Research Centre. TIC: 233844.	p. 8-3	N/A	6	Bases for seismic analyses technical approach.	N/A	N/A	N/A	N/A	
53	Kemeny, J.M. and Cook, N.G.W. 1986. "Effective Moduli, Nonlinear Deformation and Strength of a Cracked Elastic Solid." <i>International Journal of Rock Mechanics and Mining Sciences & Geomechanics Abstracts</i> , 23 (2), 107-118. Oxford, United Kingdom: Pergamon Press. TIC: 245751.	Entire	N/A	6	Bases for time dependent drift degradation approach.	N/A	N/A	N/A	N/A	
54	Kemeny, J.M. 1991. "A Model for Nonlinear Rock Deformation Under Compression Due to Subcritical Crack Growth." <i>International Journal of Rock Mechanics and Mining Sciences & Geomechanics Abstracts</i> , 28 (6), 459-467. Oxford, United Kingdom: Pergamon Press. TIC: 245750.	Entire	N/A	6	Bases for time dependent drift degradation approach.	N/A	N/A	N/A	N/A	
55	Kessler, J. and McGuire, R. 1996. <i>Yucca Mountain Total System Performance Assessment, Phase 3</i> . EPRI TR-107191. Palo Alto, California: Electric Power Research Institute. TIC: 238085.	Section 12	N/A	6	Bases for time dependent drift degradation approach.	N/A	N/A	N/A	N/A	
56	Wilkins, D.R. and Heath, C.A. 1999. "Direction to Transition to Enhanced Design Alternative II." Letter from D.R. Wilkins and C.A. Heath (CRWMS M&O) to Distribution, June 15, 1999, LV.NS.JLY.06/99-026, with enclosures, "Strategy for Baselineing EDA II Requirements" and "Guidelines for Implementation of EDA II." ACC: MOL.19990622.0126; MOL.19990622.0127; MOL.19990622.0128.	Entire	N/A	6	Bases for repository design information.	N/A	N/A	N/A	N/A	

ANL-EBS-MD-000027 REV 00

I-9

November 1999

ATTACHMENT II
DRIFT DEGRADATION ANALYSIS COMPUTER FILES

DRIFT DEGRADATION ANALYSIS COMPUTER FILES

This attachment provides a list of computer files for the drift degradation analysis. The list is separated into two directories on the CD included in this attachment:

- *DRKBA Inputs & Outputs* — includes all the input and output files for the probabilistic key block software, DRKBA
- *Calculation Files* — includes other calculation files.

The input and output files for DRKBA for each case share similar file extensions. [Table II-1](#) explains the type of file and the associated file extension. [Table II-2](#) lists the sub-directories for all the cases run in DRKBA. The subdirectory *Profile* includes all the DXF files for drift profile plots shown in Section 6.4.3. The file name and the associated drift degradation profiles are listed in [Table II-3](#).

Calculation files using the software, EXCEL 97, MathCAD Version 8, and the distinct element program, UDEC, are listed in [Table II-4](#).

Table II-1. File Extension Associated with DRKBA Input and Output Files

File Extension	Description of File
ANA	Input Summary File
MKG	Input Grid File
EXC	Input Excavation File
DEN	Input Density File
PRB	Input Joint Data File
KBO	Output File for Key Block Information
BSD	Output File for Block Size Distribution

Table II-2. List of DRKBA Input and Output Files

Directory	Brief Description
Runpul\k003aa	Ttpul, 0° Azimuth, Static Condition
Runpul\k004aa	Ttpul, 15° Azimuth, Static Condition
Runpul\k005aa	Ttpul, 30° Azimuth, Static Condition
Runpul\k006aa	Ttpul, 45° Azimuth, Static Condition
Runpul\k007aa	Ttpul, 60° Azimuth, Static Condition
Runpul\k008aa	Ttpul, 75° Azimuth, Static Condition
Runpul\k009aa	Ttpul, 90° Azimuth, Static Condition
Runpul\k010aa	Ttpul, 105° Azimuth, Static Condition
Runpul\k011aa	Ttpul, 120° Azimuth, Static Condition
Runpul\k012aa	Ttpul, 135° Azimuth, Static Condition
Runpul\k013aa	Ttpul, 150° Azimuth, Static Condition
Runpul\k014aa	Ttpul, 165° Azimuth, Static Condition
Runpmn\k017aa	Ttpmn, 0° Azimuth, Static Condition
Runpmn\k018aa	Ttpmn, 15° Azimuth, Static Condition
Runpmn\k019aa	Ttpmn, 30° Azimuth, Static Condition

Table II-2. List of DRKBA Input and Output Files (Continued)

Directory	Brief Description
Runpmn\k020aa	Tptpmn, 45° Azimuth, Static Condition
Runpmn\k021aa	Tptpmn, 60° Azimuth, Static Condition
Runpmn\k022aa	Tptpmn, 75° Azimuth, Static Condition
Runpmn\k023aa	Tptpmn, 90° Azimuth, Static Condition
Runpmn\k024aa	Tptpmn, 105° Azimuth, Static Condition
Runpmn\k025aa	Tptpmn, 120° Azimuth, Static Condition
Runpmn\k026aa	Tptpmn, 135° Azimuth, Static Condition
Runpmn\k027aa	Tptpmn 150° Azimuth, Static Condition
Runpmn\k028aa	Tptpmn, 165° Azimuth, Static Condition
Runpll\k031aa	Tptpll, 0° Azimuth, Static Condition
Runpll\k032aa	Tptpll, 15° Azimuth, Static Condition
Runpll\k033aa	Tptpll, 30° Azimuth, Static Condition
Runpll\k034aa	Tptpll, 45° Azimuth, Static Condition
Runpll\k035aa	Tptpll, 60° Azimuth, Static Condition
Runpll\k036aa	Tptpll, 75° Azimuth, Static Condition
Runpll\k037aa	Tptpll, 90° Azimuth, Static Condition
Runpll\k038aa	Tptpll, 105° Azimuth, Static Condition
Runpll\k039aa	Tptpll, 120° Azimuth, Static Condition
Runpll\k040aa	Tptpll, 135° Azimuth, Static Condition
Runpll\k041aa	Tptpll, 150° Azimuth, Static Condition
Runpll\k042aa	Tptpll, 165° Azimuth, Static Condition
Runpln\k045aa	Tptpln, 0° Azimuth, Static Condition
Runpln\k046aa	Tptpln, 15° Azimuth, Static Condition
Runpln\k047aa	Tptpln, 30° Azimuth, Static Condition
Runpln\k048aa	Tptpln, 45° Azimuth, Static Condition
Runpln\k049aa	Tptpln, 60° Azimuth, Static Condition
Runpln\k050aa	Tptpln, 75° Azimuth, Static Condition
Runpln\k051aa	Tptpln, 90° Azimuth, Static Condition
Runpln\k052aa	Tptpln, 105° Azimuth, Static Condition
Runpln\k053aa	Tptpln, 120° Azimuth, Static Condition
Runpln\k054aa	Tptpln, 135° Azimuth, Static Condition
Runpln\k055aa	Tptpln, 150° Azimuth, Static Condition
Runpln\k056aa	Tptpln, 165° Azimuth, Static Condition
seismick010aa\cat1	Tptpul, 105° Azimuth, Seismic, Level 1
seismick010aa\cat2	Tptpul, 105° Azimuth, Seismic, Level 2
seismick010aa\cat3	Tptpul, 105° Azimuth, Seismic, Level 3
seismick024aa\cat1	Tptpmn, 105° Azimuth, Seismic, Level 1
seismick024aa\cat2	Tptpmn, 105° Azimuth, Seismic, Level 2
seismick024aa\cat3	Tptpmn, 105° Azimuth, Seismic, Level 3
seismick038aa\cat1	Tptpll, 105° Azimuth, Seismic, Level 1
seismick038aa\cat2	Tptpll, 105° Azimuth, Seismic, Level 2
seismick038aa\cat3	Tptpln, 105° Azimuth, Seismic, Level 3
seismick052aa\cat1	Tptpln, 105° Azimuth, Seismic, Level 1
seismick052aa\cat2	Tptpln, 105° Azimuth, Seismic, Level 2
seismick052aa\cat3	Tptpln, 105° Azimuth, Seismic, Level 3
Time-dep\k010aalyr200	Tptpul, 105° Azimuth, Time-dependent and Thermal, 200 yr
Time-dep\k010aalyr10k	Tptpul, 105° Azimuth, Time-dependent and Thermal, 10000 yr
Time-dep\k024aalyr200	Tptpmn, 105° Azimuth, Time-dependent and Thermal, 200 yr
Time-dep\k024aalyr10k	Tptpmn, 105° Azimuth, Time-dependent and Thermal, 10000 yr
Time-dep\k038aalyr200	Tptpll, 105° Azimuth, Time-dependent and Thermal, 200 yr
Time-dep\k038aalyr10k	Tptpll, 105° Azimuth, Time-dependent and Thermal, 10000 yr
Time-dep\k052aalyr200	Tptpln, 105° Azimuth, Time-dependent and Thermal, 200 yr
Time-dep\k052aalyr10k	Tptpln, 105° Azimuth, Time-dependent and Thermal, 10000 yr

Table II-3. List of DRKBA Output Files for Degradation Profile

Directory\File Name	Brief Description
Profile\k010c1fs.dxf	Ttpul, Static and Seismic Level 1
Profile\k010n2fs.dxf	Ttpul, Seismic Level 2
Profile\k010n3fs.dxf	Ttpul, Seismic Level 3
Profile\k024stfs.dxf	Ttpmn, Static
Profile\k024n1fs.dxf	Ttpmn, Seismic Level 1, Seismic Level 2, and Seismic Level 3
Profile\k038c2fs.dxf	Ttpll, Static, Seismic Level 1, Seismic Level 2, and Seismic Level 3
Profile\k052c1fs.dxf	Ttpln, Static
Profile\k052n1fs.dxf	Ttpln, Seismic Level 1
Profile\k052n2fs.dxf	Ttpln, Seismic Level 2 and Seismic Level 3
Profile\k010y1fs.dxf	Ttpul, Time-Dependent and Thermal, 200 Yr
Profile\k010y3fs.dxf	Ttpul, Time-Dependent and Thermal, 2000 and 10000 Yr
Profile\k024y3fs.dxf	Ttpmn, Time-Dependent and Thermal, 200, 2000 and 10000 Yr
Profile\k038y3fs.dxf	Ttpll, Time-Dependent and Thermal, 200, 2000 and 10000 Yr
Profile\k052y1fs.dxf	Ttpln, Time-Dependent and Thermal, 200 Yr
Profile\k052y3fs.dxf	Ttpln, Time-Dependent and Thermal, 2000 and 10000 Yr

Table II-4. List of the Calculation Files

File Name	Directory	Software	Brief Description
Cohesion Degradation.xls	Calculation Files	EXCEL 97	Cohesion degradation due to time and thermal effect
Exca vectors.xls	Calculation Files	EXCEL 97	Calculation of the plane equations to describe the 5.5-m-diameter excavation opening
Exca vectors-backfill.xls	Calculation Files	EXCEL 97	Calculation of the plane equations to describe the 5.5-m-diameter excavation opening with backfill
New_Beta_Ttpll.xls	Calculation Files	EXCEL 97	Beta Distribution Parameters (a, b, p, q) for joint spacing, trace length, and location for Ttpll
New_Beta_Ttpln.xls	Calculation Files	EXCEL 97	Beta Distribution Parameters (a, b, p, q) for joint spacing, trace length, and location for Ttpln
New_Beta_Ttpmn.xls	Calculation Files	EXCEL 97	Beta Distribution Parameters (a, b, p, q) for joint spacing, trace length, and location for Ttpmn
New_Beta_Ttpul.xls	Calculation Files	EXCEL 97	Beta Distribution Parameters (a, b, p, q) for joint spacing, trace length, and location for Ttpul
New-K-Ttpll.mcd	Calculation Files	MathCAD 8	Calculation of K factor of joint orientation for Ttpll
New-K-Ttpln.mcd	Calculation Files	MathCAD 8	Calculation of K factor of joint orientation for Ttpln
New-K-Ttpmn.mcd	Calculation Files	MathCAD 8	Calculation of K factor of joint orientation for Ttpmn
New-K-Ttpul.mcd	Calculation Files	MathCAD 8	Calculation of K factor of joint orientation for Ttpul
Orient-Ttpll.xls	Calculation Files	EXCEL 97	Calculation of the components for the Orientation Matrix for Ttpll

Table II-4. List of the Calculation Files (Continued)

File Name	Directory	Software	Brief Description
Orient-Tptpln.xls	Calculation Files	EXCEL 97	Calculation of the components for the Orientation Matrix for Tptpln
Orient-Ttpmnm.xls	Calculation Files	EXCEL 97	Calculation of the components for the Orientation Matrix for Ttpmnm
Orient-Ttpul.xls	Calculation Files	EXCEL 97	Calculation of the components for the Orientation Matrix for Ttpul
Res sum.xls	Calculation Files	EXCEL 97	Summary of maximum key block size results
Thermal curve.xls	Calculation Files	EXCEL 97	Ratio of effective shear stress for thermal effect
Time thermal cohesion degradation.mcd	Calculation Files	MathCAD 8	Cohesion degradation due to time and thermal effect
Total vol seis.xls	Calculation Files	EXCEL 97	Total key block volume calculation, seismic
Total vol time.xls	Calculation Files	EXCEL 97	Total key block volume calculation, time-dependent and thermal
Tpllaa res.xls	Calculation Files	EXCEL 97	Processed key block size distribution output file, Ttpll, Static
Tpllse res.xls	Calculation Files	EXCEL 97	Processed key block size distribution output file, Ttpll, Seismic
Tplltm res.xls	Calculation Files	EXCEL 97	Processed key block size distribution output file, Ttpll, Time-dependent and thermal
Tplnaa res.xls	Calculation Files	EXCEL 97	Processed key block size distribution output file, Ttpln, Static
Tplnse res.xls	Calculation Files	EXCEL 97	Processed key block size distribution output file, Ttpln, Seismic
Tplntm res.xls	Calculation Files	EXCEL 97	Processed key block size distribution output file, Ttpln, Time-dependent and thermal
Tpmnaa res.xls	Calculation Files	EXCEL 97	Processed key block size distribution output file, Ttpmnm, Static
Tpmnse res.xls	Calculation Files	EXCEL 97	Processed key block size distribution output file, Ttpmnm, Seismic
Tpmntm res.xls	Calculation Files	EXCEL 97	Processed key block size distribution output file, Ttpmnm, Time-dependent and thermal
Tpulaa res.xls	Calculation Files	EXCEL 97	Processed key block size distribution output file, Ttpul, Static
Tpulse res.xls	Calculation Files	EXCEL 97	Processed key block size distribution output file, Ttpul, Seismic
Tpultm res.xls	Calculation Files	EXCEL 97	Processed key block size distribution output file, Ttpul, Time-dependent and thermal
N2.dat	Calculation Files\UDEC Analysis	UDEC	Input file for initial consolidation state
N2d2.dat	Calculation Files\UDEC Analysis	UDEC	Input file for dynamic analysis
N2s3.dat	Calculation Files\UDEC Analysis	UDEC	Input file for quasi-static analysis
N2-2.sav	Calculation Files\UDEC Analysis	UDEC	Output file for initial consolidation state
N2-d2.sav	Calculation Files\UDEC Analysis	UDEC	Output file for dynamic analysis
N2-s3.sav	Calculation Files\UDEC Analysis	UDEC	Output file for quasi-static analysis

ATTACHMENT III
CALCULATION EXAMPLE FOR JOINT PARAMETERS
USED IN DRKBA ANALYSIS
(Tptpl, Joint Set 1)

CALCULATION EXAMPLE FOR JOINT PARAMETERS USED IN DRKBA ANALYSIS (Tptpll, Joint Set 1)

An example is provided in this attachment to describe the process of calculating the required joint geometrical parameters. These parameters include the concentration factor k of a bipolar Watson distribution for joint set orientation and a , b , p , and q parameters of the Beta distribution for joint radii, spacings, and positioning. The first joint set identified in the Tptpll unit is used as the example.

The joint spacing, radii (two times the mapped trace lengths), and positioning (offset) were first sorted in the fracture database. The parameters a and b represent the ends of the closed interval upon which the Beta distribution is defined. The smallest and largest joint parameters observed were assigned as a and b parameters. The values of p and q were calculated based on the technique presented by Derman, Gleser, and Ingram (1973, pp. 398-403). In order to determine p and q , the joint data were transformed to the unit interval $[0,1]$ by interpolation between the smallest and largest values encountered. The parameters p and q were then calculated from the mean and standard deviation of the transformed data by means of the following equations:

$$p = \mu [\mu(1-\mu) / \sigma^2 - 1]$$

$$q = (1-\mu) [\mu(1-\mu) / \sigma^2 - 1]$$

where μ is the mean of the transformed data and σ^2 is the variance of the transformed data. The calculations are included in [Table III-1](#).

To calculate the concentration factor, the orientation matrix of the joint data has to be first determined (Fisher, Lewis, and Embleton 1987, pp. 33 and 175-176). The orientation matrix T is defined in the following:

$$T = \begin{bmatrix} \sum x_i^2 & \sum x_i y_i & \sum x_i z_i \\ \sum x_i y_i & \sum y_i^2 & \sum y_i z_i \\ \sum x_i z_i & \sum y_i z_i & \sum z_i^2 \end{bmatrix}$$

where (x_i, y_i, z_i) is the unit normal vector of a joint plane and i ranges from 1 to n (the number of fractures collected in the joint sets). The components of the orientation matrix are calculated in [Table III-2](#).

The solution for the concentration factor k can be approximated based on the largest eigen value (τ_3) of the orientation matrix T (Fisher, Lewis, and Embleton 1987, pp. 175-176). The solution is:

$$k = \begin{array}{ll} 3.75 \times (3\tau_3 - 1) & 0.333 < \tau_3 \leq 0.38 \\ 3.34 \times (3\tau_3 - 1) & 0.38 < \tau_3 \leq 0.65 \\ 0.7 + 1/(1 - \tau_3) & 0.65 < \tau_3 \leq 0.99 \\ 1/(1 - \tau_3) & \tau_3 \geq 0.99 \end{array}$$

Calculations of the eigen values and k factor were conducted using Mathcad and are presented in [Table III-3](#).

Table III-1. Calculation of the a, b, p, and q parameters for Joint Spacing, Radii, and Positioning (Tptpll, Joint Set 1, "New-Beta-Tptpll.xls")

Joint Set #1		Dip= 82		Dip Direction = 235					
Sorted Joint Spacing (m)	Sorted Trace Length (m)	Joint Offset (m)	Joint Offset (all positive, m)	Sorted Joint Offset (m)	Joint Radius (m)	Transformed Spacing	Transformed Radius	Transformed Offset	
15.72	23.50	-0.09	0.09	8.25	47.00	1.0000	1.0000	1.0000	
15.69	18.94	1.70	1.70	7.03	37.88	0.9981	0.7978	0.8521	
15.05	15.01	0.65	0.65	5.35	30.02	0.9573	0.6235	0.6485	
13.52	14.10	-1.21	1.21	5.35	28.20	0.8599	0.5831	0.6485	
13.43	13.50	1.60	1.60	5.30	27.00	0.8540	0.5565	0.6424	
12.99	13.40	-0.80	0.80	5.30	26.80	0.8260	0.5521	0.6424	
12.74	13.40	-0.49	0.49	5.25	26.80	0.8103	0.5521	0.6364	
11.27	13.30	7.03	7.03	5.25	26.60	0.7167	0.5477	0.6364	
11.06	13.30	1.10	1.10	4.80	26.60	0.7035	0.5477	0.5818	
10.62	12.50	-0.38	0.38	4.80	25.00	0.6752	0.5122	0.5818	
10.20	12.40	8.25	8.25	4.78	24.80	0.6488	0.5078	0.5788	
7.83	12.40	-0.80	0.80	4.75	24.80	0.4974	0.5078	0.5758	
7.53	11.20	-0.71	0.71	4.70	22.40	0.4783	0.4545	0.5691	
6.27	10.79	-0.11	0.11	4.40	21.58	0.3981	0.4364	0.5333	
5.80	10.50	0.18	0.18	4.11	21.00	0.3686	0.4235	0.4976	
5.72	10.45	0.51	0.51	4.00	20.90	0.3634	0.4213	0.4848	
5.06	10.40	4.70	4.70	3.95	20.80	0.3215	0.4191	0.4788	
4.94	9.95	1.36	1.36	3.90	19.90	0.3138	0.3991	0.4727	
4.86	9.40	5.25	5.25	3.80	18.80	0.3087	0.3747	0.4606	
4.80	8.60	2.29	2.29	3.21	17.20	0.3048	0.3392	0.3891	
4.60	8.50	1.06	1.06	3.15	17.00	0.2922	0.3348	0.3818	
4.37	8.49	2.03	2.03	2.80	16.98	0.2774	0.3344	0.3394	
4.33	8.40	0.40	0.40	2.70	16.80	0.2750	0.3304	0.3273	
4.32	8.40	-0.33	0.33	2.45	16.80	0.2744	0.3304	0.2970	
4.32	8.40	-0.33	0.33	2.29	16.80	0.2742	0.3304	0.2770	
3.94	8.00	0.10	0.10	2.03	16.00	0.2499	0.3126	0.2455	
3.77	7.30	0.58	0.58	1.80	14.60	0.2392	0.2816	0.2182	
3.75	7.10	-0.03	0.03	1.70	14.20	0.2378	0.2727	0.2061	
3.15	6.98	-0.35	0.35	1.60	13.96	0.1996	0.2674	0.1939	
3.15	5.75	0.85	0.85	1.36	11.50	0.1996	0.2129	0.1642	
3.12	5.67	0.95	0.95	1.30	11.34	0.1978	0.2093	0.1576	
2.61	5.40	2.80	2.80	1.21	10.80	0.1653	0.1973	0.1467	
2.57	4.90	4.00	4.00	1.10	9.80	0.1626	0.1752	0.1327	
2.43	4.50	-0.35	0.35	1.06	9.00	0.1538	0.1574	0.1279	
2.39	3.80	4.75	4.75	1.05	7.60	0.1513	0.1264	0.1273	
2.18	3.78	0.40	0.40	0.95	7.56	0.1381	0.1255	0.1152	
2.13	3.40	4.40	4.40	0.85	6.80	0.1349	0.1086	0.1030	
2.05	3.40	3.80	3.80	0.80	6.80	0.1299	0.1086	0.0970	
1.93	3.40	0.20	0.20	0.80	6.80	0.1218	0.1086	0.0970	
1.88	3.30	3.15	3.15	0.80	6.60	0.1186	0.1042	0.0964	

Table III-1. Calculation of the a, b, p, and q parameters for Joint Spacing, Radii, and Positioning (Tptpll, Joint Set 1, "New-Beta-Tptpll.xls") (Continued)

Sorted Joint Spacing (m)	Sorted Trace Length (m)	Joint Offset (m)	Joint Offset (all positive, m)	Sorted Joint Offset (m)	Joint Radius (m)	Transformed Spacing	Transformed Radius	Transformed Offset
1.74	3.16	3.21	3.21	0.75	6.32	0.1098	0.0980	0.0909
1.68	3.10	0.48	0.48	0.72	6.20	0.1060	0.0953	0.0867
1.65	2.94	0.15	0.15	0.72	5.88	0.1042	0.0882	0.0867
1.64	2.75	0.31	0.31	0.71	5.50	0.1034	0.0798	0.0861
1.51	2.52	-0.02	0.02	0.69	5.04	0.0953	0.0696	0.0830
1.47	2.50	0.57	0.57	0.65	5.00	0.0929	0.0687	0.0788
1.40	2.47	0.47	0.47	0.64	4.94	0.0884	0.0674	0.0770
1.40	2.28	4.78	4.78	0.64	4.56	0.0884	0.0590	0.0770
1.35	2.28	0.50	0.50	0.62	4.56	0.0853	0.0590	0.0752
1.32	2.25	3.95	3.95	0.60	4.50	0.0834	0.0576	0.0727
1.27	2.19	-0.38	0.38	0.60	4.38	0.0803	0.0550	0.0721
1.25	2.15	-0.32	0.32	0.60	4.30	0.0790	0.0532	0.0721
1.22	2.11	-0.16	0.16	0.58	4.22	0.0771	0.0514	0.0697
1.22	2.10	0.00	0.00	0.57	4.20	0.0771	0.0510	0.0691
1.21	2.10	5.30	5.30	0.57	4.20	0.0765	0.0510	0.0685
1.21	1.69	0.62	0.62	0.51	3.38	0.0764	0.0328	0.0618
1.17	1.67	1.30	1.30	0.51	3.34	0.0740	0.0319	0.0612
1.02	1.62	1.80	1.80	0.50	3.24	0.0639	0.0297	0.0606
0.99	1.61	-0.50	0.50	0.50	3.22	0.0620	0.0293	0.0606
0.96	1.60	-0.50	0.50	0.50	3.20	0.0603	0.0288	0.0606
0.94	1.58	0.75	0.75	0.49	3.16	0.0589	0.0279	0.0588
0.83	1.56	-0.15	0.15	0.48	3.12	0.0520	0.0271	0.0576
0.76	1.54	-0.23	0.23	0.48	3.08	0.0476	0.0262	0.0576
0.72	1.51	-0.25	0.25	0.47	3.02	0.0451	0.0248	0.0570
0.71	1.51	0.72	0.72	0.47	3.02	0.0444	0.0248	0.0570
0.69	1.50	0.80	0.80	0.46	3.00	0.0432	0.0244	0.0558
0.64	1.50	2.70	2.70	0.43	3.00	0.0401	0.0244	0.0521
0.60	1.50	2.45	2.45	0.42	3.00	0.0375	0.0244	0.0509
0.60	1.49	5.35	5.35	0.40	2.98	0.0375	0.0239	0.0485
0.51	1.48	0.26	0.26	0.40	2.96	0.0319	0.0235	0.0479
0.49	1.48	-0.51	0.51	0.38	2.96	0.0306	0.0235	0.0455
0.46	1.48	-0.37	0.37	0.38	2.96	0.0287	0.0235	0.0455
0.38	1.46	4.11	4.11	0.37	2.92	0.0231	0.0226	0.0448
0.36	1.45	-0.60	0.60	0.35	2.90	0.0223	0.0222	0.0418
0.33	1.45	-0.43	0.43	0.35	2.90	0.0200	0.0222	0.0418
0.32	1.43	-0.69	0.69	0.33	2.86	0.0196	0.0213	0.0400
0.28	1.43	0.13	0.13	0.33	2.86	0.0168	0.0213	0.0400
0.25	1.39	-0.32	0.32	0.33	2.78	0.0149	0.0195	0.0394
0.25	1.37	0.64	0.64	0.33	2.74	0.0149	0.0186	0.0394
0.24	1.32	-0.57	0.57	0.32	2.64	0.0143	0.0164	0.0388
0.22	1.30	0.48	0.48	0.32	2.60	0.0130	0.0155	0.0388
0.20	1.30	-0.60	0.60	0.31	2.60	0.0118	0.0155	0.0376

Table III-1. Calculation of the a, b, p, and q parameters for Joint Spacing, Radii, and Positioning (Tptpll, Joint Set 1, "New-Beta-Tptpll.xls") (Continued)

	Sorted Joint Spacing (m)	Sorted Trace Length (m)	Joint Offset (m)	Joint Offset (all positive, m)	Sorted Joint Offset (m)	Joint Radius (m)	Transformed Spacing	Transformed Radius	Transformed Offset
	0.18	1.29	-0.145	0.145	0.295	2.58	0.0105	0.0151	0.0358
	0.14	1.27	-0.47	0.47	0.295	2.54	0.0078	0.0142	0.0358
	0.10	1.27	-0.235	0.235	0.26	2.54	0.0055	0.0142	0.0315
	0.10	1.27	-0.6	0.6	0.25	2.54	0.0055	0.0142	0.0303
	0.07	1.25	-0.295	0.295	0.25	2.5	0.0036	0.0133	0.0303
	0.06	1.24	-0.635	0.635	0.235	2.48	0.0030	0.0129	0.0285
	0.01	1.24	-0.05	0.05	0.225	2.48	0.0000	0.0129	0.0273
		1.19	0.05	0.05	0.2	2.38		0.0106	0.0242
		1.16	0.2	0.2	0.2	2.32		0.0093	0.0242
		1.15	0.46	0.46	0.175	2.3		0.0089	0.0212
		1.14	0.33	0.33	0.16	2.28		0.0084	0.0194
		1.09	0.295	0.295	0.15	2.18		0.0062	0.0182
		1.08	1.05	1.05	0.15	2.16		0.0058	0.0182
		1.08	3.9	3.9	0.145	2.16		0.0058	0.0176
		1.07	5.25	5.25	0.125	2.14		0.0053	0.0152
		1.04	5.3	5.3	0.11	2.08		0.0040	0.0133
		1.03	4.8	4.8	0.1	2.06		0.0035	0.0121
		1.03	4.8	4.8	0.085	2.06		0.0035	0.0103
		1.01	5.35	5.35	0.05	2.02		0.0027	0.0061
		1.01	0.715	0.715	0.05	2.02		0.0027	0.0061
		1	0.25	0.25	0.025	2		0.0022	0.0030
		0.98	-0.325	0.325	0.025	1.96		0.0013	0.0030
		0.95	-0.42	0.42	0	1.9		0.0000	0.0000
Mean	3.33	4.56	—	—	1.47	9.12	0.2111	0.1601	0.1781
Std. Dev.	4.09	4.71	—	—	1.84	9.42	0.2605	0.2089	0.2234
Min.	0.01	0.95	—	—	0.00	1.90	—	—	—
Max.	15.72	23.50	—	—	8.25	47.00	—	—	—
p				—			0.3070	0.3332	0.3443
q				—			1.1475	1.7478	1.5890

Table III-2. Calculation of the Components for the Orientation Matrix ("Orient-Tptll.xls")

Station (m)	Azimuth	Dip	Dip Vector Component			Strike Vector Component			Pole Vector Component			xi*xi	xi*yi	xi*zi	yi*yi	yi*zi	zi*zi
			xd	yd	zd	xs	ys	zs	xi	yi	zi						
5751.02	139	75	-0.195	-0.170	-0.966	-0.656	0.755	0.000	0.729	0.634	-0.259	0.5314	0.4620	-0.1887	0.4016	-0.1640	0.0670
5753.70	136	84	-0.075	-0.073	-0.995	-0.695	0.719	0.000	0.715	0.691	-0.105	0.5118	0.4942	-0.0748	0.4773	-0.0722	0.0109
5761.50	137	72	-0.226	-0.211	-0.951	-0.682	0.731	0.000	0.696	0.649	-0.309	0.4838	0.4512	-0.2149	0.4207	-0.2004	0.0955
5761.72	145	72	-0.253	-0.177	-0.951	-0.574	0.819	0.000	0.779	0.546	-0.309	0.6069	0.4250	-0.2407	0.2976	-0.1686	0.0955
5791.33	148	90	0.000	0.000	-1.000	-0.530	0.848	0.000	0.848	0.530	0.000	0.7192	0.4494	0.0000	0.2808	0.0000	0.0000
5791.92	151	84	-0.091	-0.051	-0.995	-0.485	0.875	0.000	0.870	0.482	-0.105	0.7566	0.4194	-0.0909	0.2325	-0.0504	0.0109
5798.94	133	77	-0.153	-0.165	-0.974	-0.731	0.682	0.000	0.665	0.713	-0.225	0.4416	0.4735	-0.1495	0.5078	-0.1603	0.0506
5800.50	144	85	-0.071	-0.051	-0.996	-0.588	0.809	0.000	0.806	0.586	-0.087	0.6495	0.4719	-0.0702	0.3429	-0.0510	0.0076
5805.57	152	76	-0.214	-0.114	-0.970	-0.469	0.883	0.000	0.857	0.456	-0.242	0.7340	0.3903	-0.2073	0.2075	-0.1102	0.0585
5813.05	155	76	-0.219	-0.102	-0.970	-0.423	0.906	0.000	0.879	0.410	-0.242	0.7733	0.3606	-0.2127	0.1682	-0.0992	0.0585
5820.95	159	81	-0.146	-0.056	-0.988	-0.358	0.934	0.000	0.922	0.354	-0.156	0.8502	0.3264	-0.1442	0.1253	-0.0554	0.0245
5828.98	144	84	-0.085	-0.061	-0.995	-0.588	0.809	0.000	0.805	0.585	-0.105	0.6474	0.4703	-0.0841	0.3417	-0.0611	0.0109
5829.00	156	79	-0.174	-0.078	-0.982	-0.407	0.914	0.000	0.897	0.399	-0.191	0.8042	0.3580	-0.1711	0.1594	-0.0762	0.0364
5841.23	149	85	-0.075	-0.045	-0.996	-0.515	0.857	0.000	0.854	0.513	-0.087	0.7292	0.4381	-0.0744	0.2632	-0.0447	0.0076
5845.47	143	81	-0.125	-0.094	-0.988	-0.602	0.799	0.000	0.789	0.594	-0.156	0.6222	0.4689	-0.1234	0.3533	-0.0930	0.0245
5846.00	151	83	-0.107	-0.059	-0.993	-0.485	0.875	0.000	0.868	0.481	-0.122	0.7536	0.4177	-0.1058	0.2315	-0.0586	0.0149
5846.52	135	77	-0.159	-0.159	-0.974	-0.707	0.707	0.000	0.689	0.689	-0.225	0.4747	0.4747	-0.1550	0.4747	-0.1550	0.0506
5848.49	132	88	-0.023	-0.026	-0.999	-0.743	0.669	0.000	0.669	0.743	-0.035	0.4472	0.4967	-0.0233	0.5516	-0.0259	0.0012
5848.89	140	75	-0.198	-0.166	-0.966	-0.643	0.766	0.000	0.740	0.621	-0.259	0.5475	0.4594	-0.1915	0.3855	-0.1607	0.0670
5851.55	144	74	-0.223	-0.162	-0.961	-0.588	0.809	0.000	0.778	0.565	-0.276	0.6048	0.4394	-0.2144	0.3192	-0.1557	0.0760
5858.65	133	77	-0.153	-0.165	-0.974	-0.731	0.682	0.000	0.665	0.713	-0.225	0.4416	0.4735	-0.1495	0.5078	-0.1603	0.0506
5864.74	326	85	0.072	0.049	-0.996	0.559	-0.829	0.000	-0.826	-0.557	-0.087	0.6821	0.4601	0.0720	0.3103	0.0486	0.0076
1445.49	330	80	0.150	0.087	-0.985	0.500	-0.866	0.000	-0.853	-0.492	-0.174	0.7274	0.4200	0.1481	0.2425	0.0855	0.0302
1506.35	132	80	-0.116	-0.129	-0.985	-0.743	0.669	0.000	0.659	0.732	-0.174	0.4342	0.4823	-0.1144	0.5356	-0.1271	0.0302
1512.14	132	87	-0.035	-0.039	-0.999	-0.743	0.669	0.000	0.668	0.742	-0.052	0.4465	0.4959	-0.0350	0.5508	-0.0388	0.0027
1652.91	152	76	-0.214	-0.114	-0.970	-0.469	0.883	0.000	0.857	0.456	-0.242	0.7340	0.3903	-0.2073	0.2075	-0.1102	0.0585
1803.20	161	72	-0.292	-0.101	-0.951	-0.326	0.946	0.000	0.899	0.310	-0.309	0.8086	0.2784	-0.2779	0.0959	-0.0957	0.0955
1818.45	129	71	-0.205	-0.253	-0.946	-0.777	0.629	0.000	0.595	0.735	-0.326	0.3541	0.4372	-0.1937	0.5399	-0.2392	0.1060
1823.58	133	89	-0.012	-0.013	-1.000	-0.731	0.682	0.000	0.682	0.731	-0.017	0.4650	0.4986	-0.0119	0.5347	-0.0128	0.0003
1825.00	137	84	-0.076	-0.071	-0.995	-0.682	0.731	0.000	0.727	0.678	-0.105	0.5290	0.4933	-0.0760	0.4600	-0.0709	0.0109
1851.69	338	87	0.049	0.020	-0.999	0.375	-0.927	0.000	-0.926	-0.374	-0.052	0.8573	0.3464	0.0485	0.1399	0.0196	0.0027
1867.62	136	84	-0.075	-0.073	-0.995	-0.695	0.719	0.000	0.715	0.691	-0.105	0.5118	0.4942	-0.0748	0.4773	-0.0722	0.0109
1870.81	325	82	0.114	0.080	-0.990	0.574	-0.819	0.000	-0.811	-0.568	-0.139	0.6580	0.4607	0.1129	0.3226	0.0790	0.0194
1883.72	145	78	-0.170	-0.119	-0.978	-0.574	0.819	0.000	0.801	0.561	-0.208	0.6420	0.4495	-0.1666	0.3148	-0.1166	0.0432
1900.24	158	88	-0.032	-0.013	-0.999	-0.375	0.927	0.000	0.927	0.374	-0.035	0.8586	0.3469	-0.0323	0.1402	-0.0131	0.0012
1917.12	148	77	-0.191	-0.119	-0.974	-0.530	0.848	0.000	0.826	0.516	-0.225	0.6828	0.4267	-0.1859	0.2666	-0.1162	0.0506
1928.54	155	83	-0.110	-0.052	-0.993	-0.423	0.906	0.000	0.900	0.419	-0.122	0.8092	0.3773	-0.1096	0.1760	-0.0511	0.0149
1941.70	147	80	-0.146	-0.095	-0.985	-0.545	0.839	0.000	0.826	0.536	-0.174	0.6822	0.4430	-0.1434	0.2877	-0.0931	0.0302
1941.98	159	82	-0.130	-0.050	-0.990	-0.358	0.934	0.000	0.924	0.355	-0.139	0.8547	0.3281	-0.1287	0.1259	-0.0494	0.0194
1975.74	129	84	-0.066	-0.081	-0.995	-0.777	0.629	0.000	0.626	0.773	-0.105	0.3917	0.4837	-0.0654	0.5974	-0.0808	0.0109

Table III-2. Calculation of the Components for the Orientation Matrix ("Orient-Tptll.xls") (Continued)

Station (m)	Azimuth	Dip	Dip Vector Component			Strike Vector Component			Pole Vector Component			xi*xi	xi*yi	xi*zi	yi*yi	yi*zi	zi*zi
			xd	yd	zd	xs	ys	zs	xi	yi	zi						
1978.20	147	88	-0.029	-0.019	-0.999	-0.545	0.839	0.000	0.838	0.544	-0.035	0.7025	0.4562	-0.0293	0.2963	-0.0190	0.0012
2038.81	140	84	-0.080	-0.067	-0.995	-0.643	0.766	0.000	0.762	0.639	-0.105	0.5804	0.4870	-0.0796	0.4087	-0.0668	0.0109
2062.13	140	82	-0.107	-0.089	-0.990	-0.643	0.766	0.000	0.759	0.637	-0.139	0.5755	0.4829	-0.1056	0.4052	-0.0886	0.0194
2062.35	142	80	-0.137	-0.107	-0.985	-0.616	0.788	0.000	0.776	0.606	-0.174	0.6022	0.4705	-0.1348	0.3676	-0.1053	0.0302
2100.12	323	82	0.111	0.084	-0.990	0.602	-0.799	0.000	-0.791	-0.596	-0.139	0.6255	0.4713	0.1101	0.3552	0.0829	0.0194
2119.70	330	77	0.195	0.112	-0.974	0.500	-0.866	0.000	-0.844	-0.487	-0.225	0.7120	0.4111	0.1898	0.2373	0.1096	0.0506
2141.65	148	88	-0.030	-0.018	-0.999	-0.530	0.848	0.000	0.848	0.530	-0.035	0.7183	0.4488	-0.0296	0.2805	-0.0185	0.0012
2142.92	152	87	-0.046	-0.025	-0.999	-0.469	0.883	0.000	0.882	0.469	-0.052	0.7775	0.4134	-0.0461	0.2198	-0.0245	0.0027
2145.08	138	82	-0.103	-0.093	-0.990	-0.669	0.743	0.000	0.736	0.663	-0.139	0.5416	0.4876	-0.1024	0.4391	-0.0922	0.0194
2153.01	157	87	-0.048	-0.020	-0.999	-0.391	0.921	0.000	0.919	0.390	-0.052	0.8450	0.3587	-0.0481	0.1523	-0.0204	0.0027
2156.20	136	81	-0.113	-0.109	-0.988	-0.695	0.719	0.000	0.710	0.686	-0.156	0.5048	0.4875	-0.1111	0.4707	-0.1073	0.0245
2158.80	148	78	-0.176	-0.110	-0.978	-0.530	0.848	0.000	0.830	0.518	-0.208	0.6881	0.4300	-0.1725	0.2687	-0.1078	0.0432
2159.05	152	75	-0.229	-0.122	-0.966	-0.469	0.883	0.000	0.853	0.453	-0.259	0.7274	0.3868	-0.2207	0.2056	-0.1174	0.0670
2160.29	149	74	-0.236	-0.142	-0.961	-0.515	0.857	0.000	0.824	0.495	-0.276	0.6789	0.4079	-0.2271	0.2451	-0.1365	0.0760
2161.48	153	85	-0.078	-0.040	-0.996	-0.454	0.891	0.000	0.888	0.452	-0.087	0.7879	0.4014	-0.0774	0.2045	-0.0394	0.0076
2162.18	146	88	-0.029	-0.020	-0.999	-0.559	0.829	0.000	0.829	0.559	-0.035	0.6865	0.4630	-0.0289	0.3123	-0.0195	0.0012
2163.60	140	88	-0.027	-0.022	-0.999	-0.643	0.766	0.000	0.766	0.642	-0.035	0.5861	0.4918	-0.0267	0.4127	-0.0224	0.0012
2177.30	140	83	-0.093	-0.078	-0.993	-0.643	0.766	0.000	0.760	0.638	-0.122	0.5781	0.4851	-0.0927	0.4070	-0.0778	0.0149
2179.00	140	79	-0.146	-0.123	-0.982	-0.643	0.766	0.000	0.752	0.631	-0.191	0.5655	0.4745	-0.1435	0.3981	-0.1204	0.0364
2180.00	137	79	-0.140	-0.130	-0.982	-0.682	0.731	0.000	0.718	0.669	-0.191	0.5154	0.4806	-0.1370	0.4482	-0.1277	0.0364
2197.90	138	74	-0.205	-0.184	-0.961	-0.669	0.743	0.000	0.714	0.643	-0.276	0.5103	0.4595	-0.1969	0.4137	-0.1773	0.0760
2198.85	130	73	-0.188	-0.224	-0.956	-0.766	0.643	0.000	0.615	0.733	-0.292	0.3779	0.4503	-0.1797	0.5367	-0.2142	0.0855
2198.95	145	78	-0.170	-0.119	-0.978	-0.574	0.819	0.000	0.801	0.561	-0.208	0.6420	0.4495	-0.1666	0.3148	-0.1166	0.0432
2199.56	160	80	-0.163	-0.059	-0.985	-0.342	0.940	0.000	0.925	0.337	-0.174	0.8564	0.3117	-0.1607	0.1135	-0.0585	0.0302
2200.85	135	78	-0.147	-0.147	-0.978	-0.707	0.707	0.000	0.692	0.692	-0.208	0.4784	0.4784	-0.1438	0.4784	-0.1438	0.0432
2211.19	150	84	-0.091	-0.052	-0.995	-0.500	0.866	0.000	0.861	0.497	-0.105	0.7418	0.4283	-0.0900	0.2473	-0.0520	0.0109
2212.03	140	87	-0.040	-0.034	-0.999	-0.643	0.766	0.000	0.765	0.642	-0.052	0.5852	0.4911	-0.0400	0.4120	-0.0336	0.0027
2223.24	145	74	-0.226	-0.158	-0.961	-0.574	0.819	0.000	0.787	0.551	-0.276	0.6200	0.4341	-0.2170	0.3040	-0.1520	0.0760
2223.31	135	80	-0.123	-0.123	-0.985	-0.707	0.707	0.000	0.696	0.696	-0.174	0.4849	0.4849	-0.1209	0.4849	-0.1209	0.0302
2223.83	150	72	-0.268	-0.155	-0.951	-0.500	0.866	0.000	0.824	0.476	-0.309	0.6784	0.3917	-0.2545	0.2261	-0.1469	0.0955
2225.20	154	82	-0.125	-0.061	-0.990	-0.438	0.899	0.000	0.890	0.434	-0.139	0.7922	0.3864	-0.1239	0.1884	-0.0604	0.0194
2225.30	157	80	-0.160	-0.068	-0.985	-0.391	0.921	0.000	0.907	0.385	-0.174	0.8218	0.3488	-0.1574	0.1481	-0.0668	0.0302
2227.06	142	84	-0.082	-0.064	-0.995	-0.616	0.788	0.000	0.784	0.612	-0.105	0.6142	0.4798	-0.0819	0.3749	-0.0640	0.0109
2231.44	155	74	-0.250	-0.116	-0.961	-0.423	0.906	0.000	0.871	0.406	-0.276	0.7590	0.3539	-0.2401	0.1650	-0.1120	0.0760
2231.94	135	86	-0.049	-0.049	-0.998	-0.707	0.707	0.000	0.705	0.705	-0.070	0.4976	0.4976	-0.0492	0.4976	-0.0492	0.0049
2233.17	326	85	0.072	0.049	-0.996	0.559	-0.829	0.000	-0.826	-0.557	-0.087	0.6821	0.4601	0.0720	0.3103	0.0486	0.0076
2234.51	335	86	0.063	0.029	-0.998	0.423	-0.906	0.000	-0.904	-0.422	-0.070	0.8174	0.3812	0.0631	0.1777	0.0294	0.0049
2234.57	331	87	0.046	0.025	-0.999	0.485	-0.875	0.000	-0.873	-0.484	-0.052	0.7629	0.4229	0.0457	0.2344	0.0253	0.0027
2235.60	158	88	-0.032	-0.013	-0.999	-0.375	0.927	0.000	0.927	0.374	-0.035	0.8586	0.3469	-0.0323	0.1402	-0.0131	0.0012
2236.07	159	83	-0.114	-0.044	-0.993	-0.358	0.934	0.000	0.927	0.356	-0.122	0.8586	0.3296	-0.1129	0.1265	-0.0433	0.0149

Table III-2. Calculation of the Components for the Orientation Matrix ("Orient-Tptpl.xls") (Continued)

Station (m)	Azimuth	Dip	Dip Vector Component			Strike Vector Component			Pole Vector Component			24.43 89xi* xi	xi*yi	xi*zi	yi*yi	yi*zi	zi*zi
			xd	yd	zd	xs	ys	zs	xi	yi	zi						
2237.60	143	72	-0.247	-0.186	-0.951	-0.602	0.799	0.000	0.760	0.572	-0.309	0.5769	0.4347	-0.2347	0.3276	-0.1769	0.0955
2238.32	130	74	-0.177	-0.211	-0.961	-0.766	0.643	0.000	0.618	0.736	-0.276	0.3818	0.4550	-0.1703	0.5422	-0.2030	0.0760
2238.93	160	80	-0.163	-0.059	-0.985	-0.342	0.940	0.000	0.925	0.337	-0.174	0.8564	0.3117	-0.1607	0.1135	-0.0585	0.0302
2239.66	135	86	-0.049	-0.049	-0.998	-0.707	0.707	0.000	0.705	0.705	-0.070	0.4976	0.4976	-0.0492	0.4976	-0.0492	0.0049
2239.84	137	88	-0.026	-0.024	-0.999	-0.682	0.731	0.000	0.731	0.682	-0.035	0.5342	0.4982	-0.0255	0.4646	-0.0238	0.0012
2241.74	146	82	-0.115	-0.078	-0.990	-0.559	0.829	0.000	0.821	0.554	-0.139	0.6740	0.4546	-0.1143	0.3066	-0.0771	0.0194
2242.39	148	88	-0.030	-0.018	-0.999	-0.530	0.848	0.000	0.848	0.530	-0.035	0.7183	0.4488	-0.0296	0.2805	-0.0185	0.0012
2244.81	134	87	-0.036	-0.038	-0.999	-0.719	0.695	0.000	0.694	0.718	-0.052	0.4812	0.4983	-0.0363	0.5160	-0.0376	0.0027
2245.19	318	72	0.230	0.207	-0.951	0.669	-0.743	0.000	-0.707	-0.636	-0.309	0.4995	0.4498	0.2184	0.4050	0.1967	0.0955
2247.40	138	84	-0.078	-0.070	-0.995	-0.669	0.743	0.000	0.739	0.665	-0.105	0.5462	0.4918	-0.0773	0.4428	-0.0696	0.0109
2247.64	158	81	-0.145	-0.059	-0.988	-0.375	0.927	0.000	0.916	0.370	-0.156	0.8386	0.3388	-0.1433	0.1369	-0.0579	0.0245
2253.99	322	76	0.191	0.149	-0.970	0.616	-0.788	0.000	-0.765	-0.597	-0.242	0.5846	0.4568	0.1850	0.3569	0.1445	0.0585
2255.23	137	89	-0.013	-0.012	-1.000	-0.682	0.731	0.000	0.731	0.682	-0.017	0.5347	0.4986	-0.0128	0.4650	-0.0119	0.0003
2259.62	148	72	-0.262	-0.164	-0.951	-0.530	0.848	0.000	0.807	0.504	-0.309	0.6505	0.4065	-0.2492	0.2540	-0.1557	0.0955
2265.50	151	75	-0.226	-0.125	-0.966	-0.485	0.875	0.000	0.845	0.468	-0.259	0.7137	0.3956	-0.2187	0.2193	-0.1212	0.0670
2265.70	157	78	-0.191	-0.081	-0.978	-0.391	0.921	0.000	0.900	0.382	-0.208	0.8107	0.3441	-0.1872	0.1461	-0.0795	0.0432
2267.78	133	78	-0.142	-0.152	-0.978	-0.731	0.682	0.000	0.667	0.715	-0.208	0.4450	0.4772	-0.1387	0.5118	-0.1487	0.0432
2278.54	134	85	-0.061	-0.063	-0.996	-0.719	0.695	0.000	0.692	0.717	-0.087	0.4789	0.4959	-0.0603	0.5135	-0.0625	0.0076
2279.31	138	84	-0.078	-0.070	-0.995	-0.669	0.743	0.000	0.739	0.665	-0.105	0.5462	0.4918	-0.0773	0.4428	-0.0696	0.0109
2295.21	140	78	-0.159	-0.134	-0.978	-0.643	0.766	0.000	0.749	0.629	-0.208	0.5615	0.4711	-0.1558	0.3953	-0.1307	0.0432
2299.20	150	83	-0.106	-0.061	-0.993	-0.500	0.866	0.000	0.860	0.496	-0.122	0.7389	0.4266	-0.1048	0.2463	-0.0605	0.0149
2316.88	138	81	-0.116	-0.105	-0.988	-0.669	0.743	0.000	0.734	0.661	-0.156	0.5387	0.4851	-0.1148	0.4368	-0.1034	0.0245
2320.70	147	82	-0.117	-0.076	-0.990	-0.545	0.839	0.000	0.831	0.539	-0.139	0.6897	0.4479	-0.1156	0.2909	-0.0751	0.0194
2322.65	138	80	-0.129	-0.116	-0.985	-0.669	0.743	0.000	0.732	0.659	-0.174	0.5356	0.4823	-0.1271	0.4342	-0.1144	0.0302
SUM												66.132	45.475	-10.228	34.551	-7.382	3.317

Table III-3. Calculation of the Concentration Factor k for Joint Orientation ("New-Tptpl.mcd")

K Factor Calculation for Watson Bipolar Distribution:
 (xx, xy,xz,yy,yz,zz calculated in EXCEL workseet
Orient-Tptpl.xls)

Tptpl, Joint Set 1

$$xx := 66.1322$$

$$xy := 45.4751$$

$$xz := -10.2284$$

$$yy := 34.5513$$

$$yz := -7.3818$$

$$zz := 3.3167$$

$$T := \begin{bmatrix} xx & xy & xz \\ xy & yy & yz \\ xz & yz & zz \end{bmatrix}$$

$$c := \text{eigenvals}(T) \quad c = \begin{bmatrix} 2.217 \\ 1.66 \\ 100.124 \end{bmatrix}$$

$$n := c_0 + c_1 + c_2$$

$$cn := \frac{c}{n} \quad cn = \begin{bmatrix} 0.021 \\ 0.016 \\ 0.963 \end{bmatrix} \quad \tau_3 := \max(cn)$$

$$K1 := 3.75 \cdot (3 \tau_3 - 1) \quad K2 := 3.34 \cdot (3 \tau_3 - 1)$$

$$K3 := 0.7 + \frac{1}{(1 - \tau_3)} \quad K4 := \frac{1}{(1 - \tau_3)}$$

$$K := \begin{cases} K1 & \text{if } 0.333 < \tau_3 \leq 0.36 \\ K2 & \text{if } 0.38 < \tau_3 \leq 0.65 \\ K3 & \text{if } 0.65 < \tau_3 \leq 0.99 \\ K4 & \text{if } \tau_3 \geq 0.99 \end{cases} \quad K = 27.529$$

ATTACHMENT IV

DETERMINATION OF THE NUMBER OF DRKBA MONTE CARLO SIMULATIONS

DETERMINATION OF THE NUMBER OF DRKBA MONTE CARLO SIMULATIONS

In the DRKBA analysis, random joint patterns are generated with joint centers positioned in three-dimensional space, considering each joint set in sequence for each Monte Carlo simulation. The forming of key blocks is therefore different in each Monte Carlo simulation. To determine the adequate number of Monte Carlo simulations for the analyses, test runs were first conducted. The criteria used to determine the adequate number of Monte Carlo simulations include (1) consistent prediction of the block size distribution and (2) consistent prediction of the maximum block size.

Test runs were first conducted for the Tptpln unit with 200, 400, and 600 Monte Carlo simulations. [Figure IV-1](#) shows the block size distribution curves in the form of cumulative frequency of occurrence. The prediction of block size distribution for 400 simulations is similar to the results from 600 simulations as indicated in [Figure IV-1](#). However, for the case of 200 simulations, a larger block size was predicted for the same level of cumulative frequency of occurrence compared to the cases with 400 and 600 simulations. The predicted numbers of blocks per 10 simulations for the three cases are presented in [Figures IV-2](#). The results are in good agreement for all three cases. The maximum block sizes predicted for the three cases are identical as shown in [Figure IV-3](#). It was determined that 400 simulations are adequate for the DRKBA analyses in Tptpln unit based on the results of these three test runs.

For the Tptpmn unit, tests runs with 100, 200, and 400 Monte Carlo simulations were conducted. [Figure IV-4](#) shows the block size distribution curves for the three cases. The prediction of block size distribution for 200 simulations is similar to the results from 400 simulations. The predicted numbers of blocks per 10 simulations for the three cases are presented in [Figures IV-5](#). The results show an increasing number of blocks for higher number of simulations. The maximum block sizes predicted for the three cases are shown in [Figure IV-6](#). The maximum blocks predicted for 200 and 400 simulations are identical, while the maximum block size for the 100 simulation is significantly smaller. It was determined that 200 simulations are adequate for the DRKBA analyses for Tptpmn unit.

The predicted number of key block per simulation for Tptpul and Tptpll are in general similar to that of the Tptpln unit. Therefore, 400 simulations are also used for the analyses conducted in Tptpul and Tptpll units.

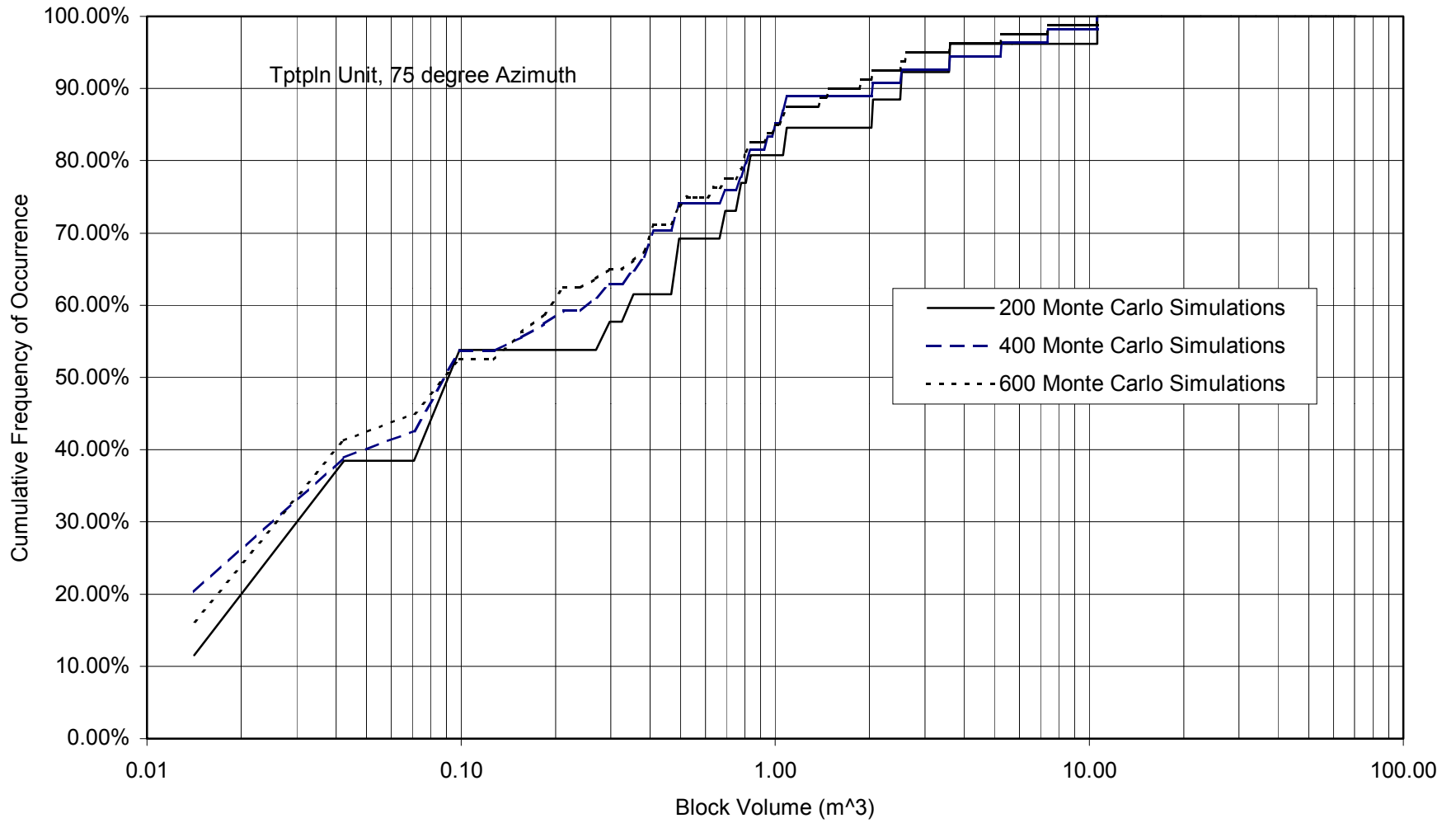


Figure IV-1. Block Size Distributions for the Test Runs, TptIn Unit

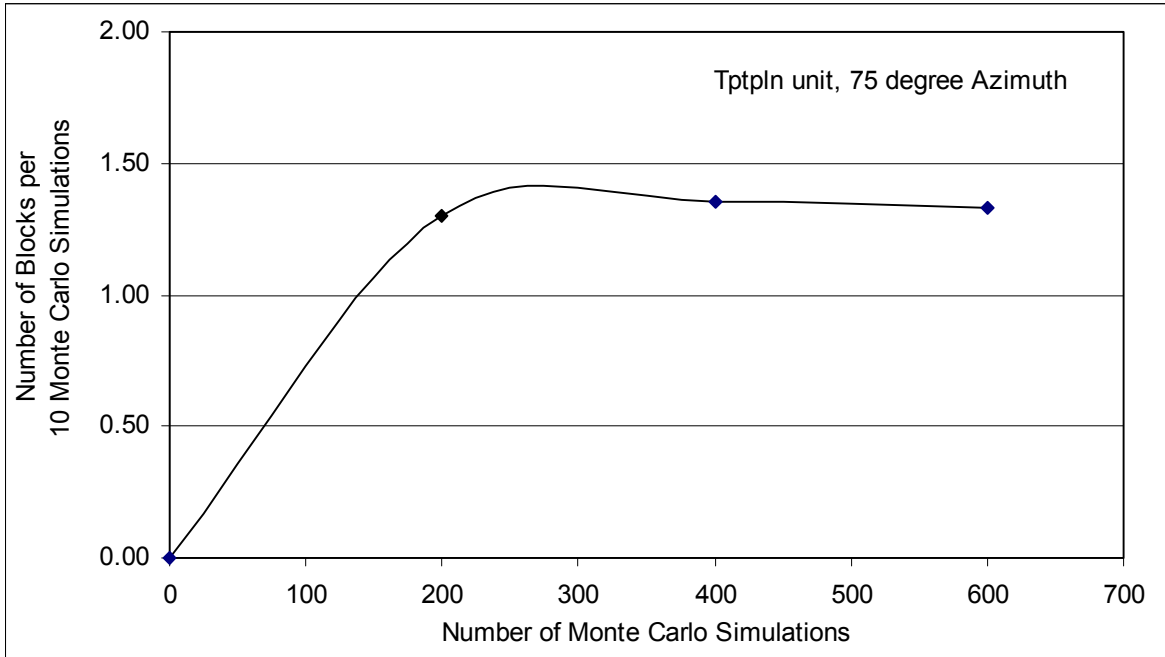


Figure IV-2. Predicted Number of Key Blocks Per 10 Monte Carlo Simulations, Tptpln Unit

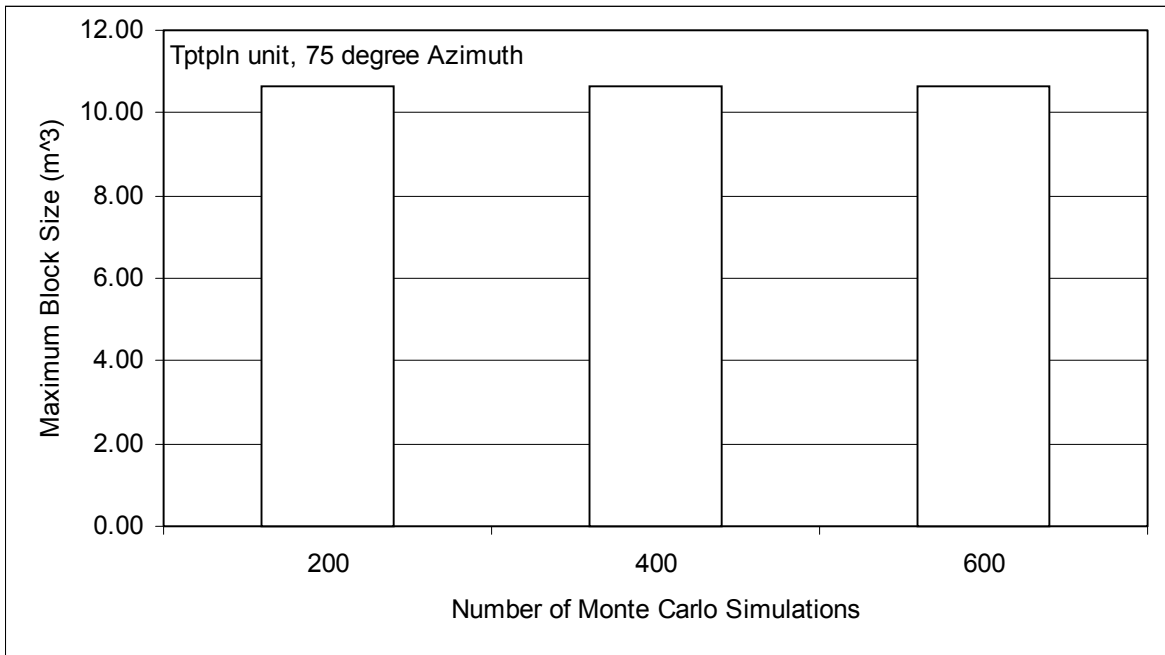


Figure IV-3. Predicted Number of Maximum Block Size, Tptpln Unit

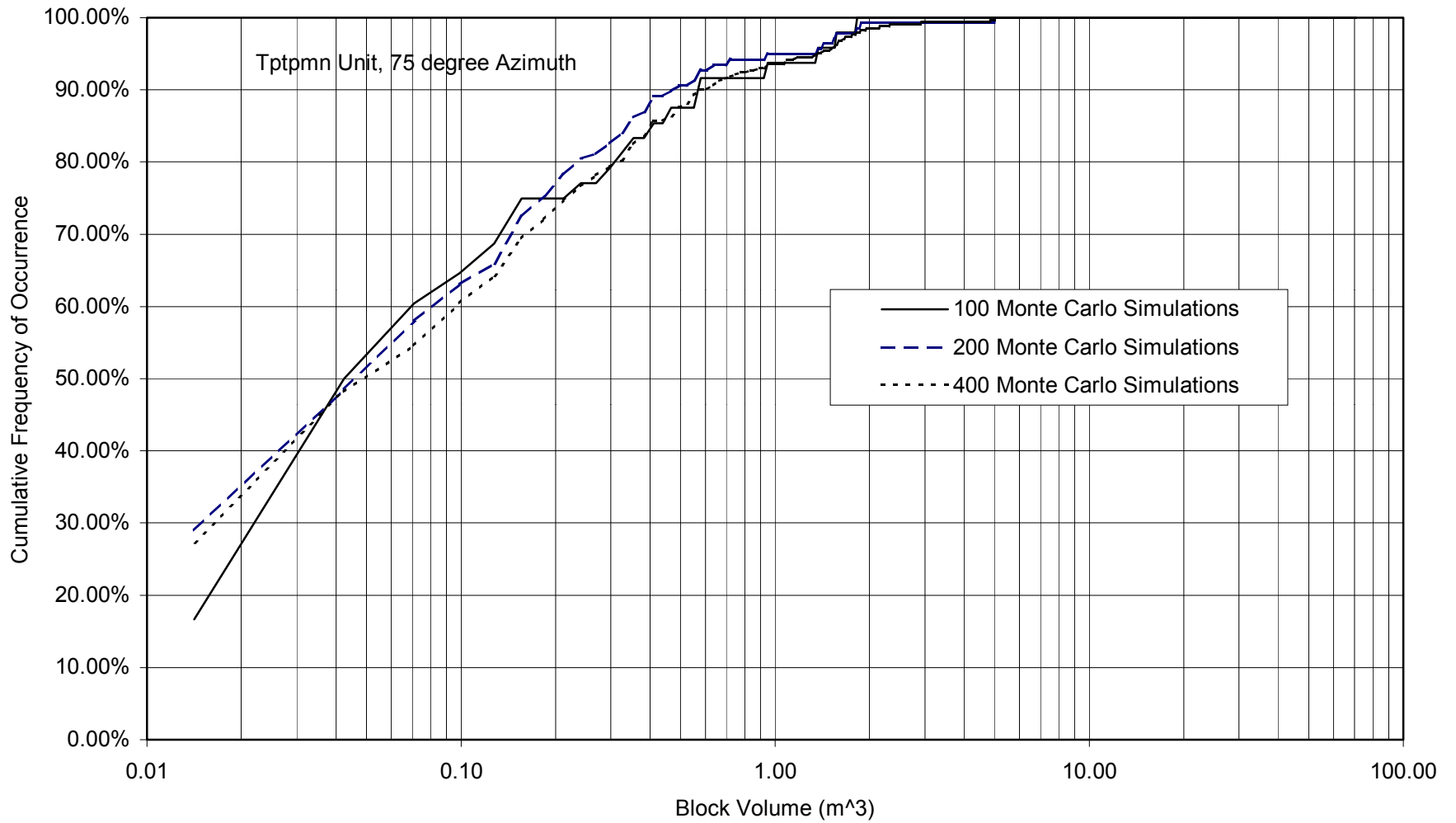


Figure IV-4. Block Size Distributions for the Test Runs, Tptpmn Unit

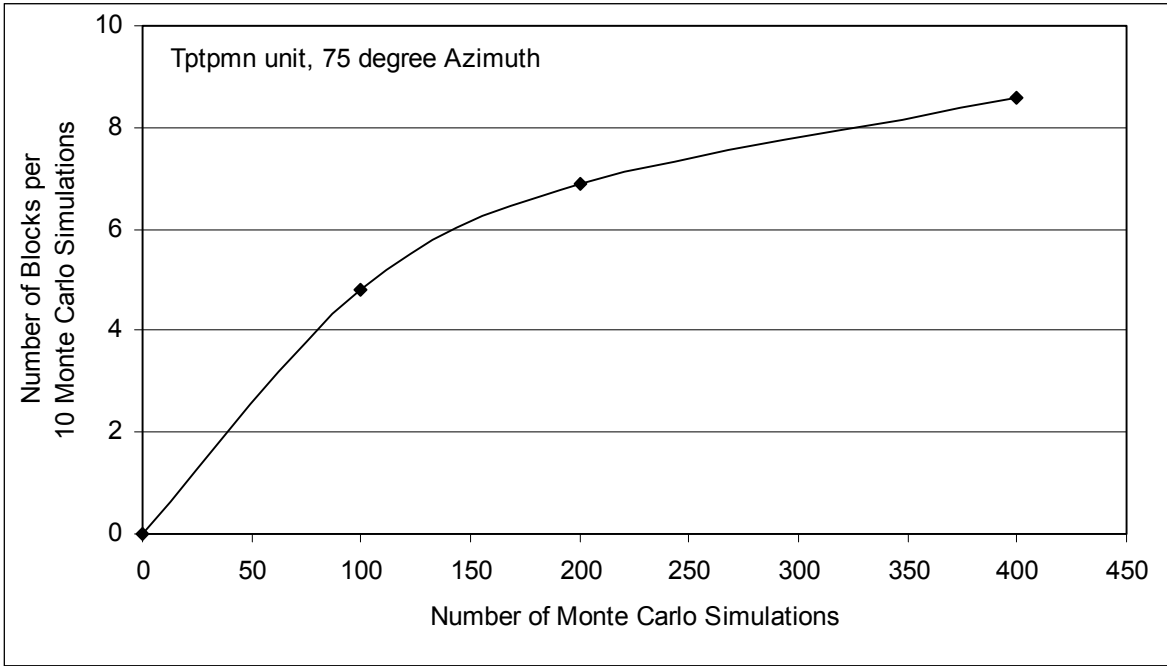


Figure IV-5. Predicted Number of Key Blocks Per 10 Monte Carlo Simulations, Tptpmn Unit

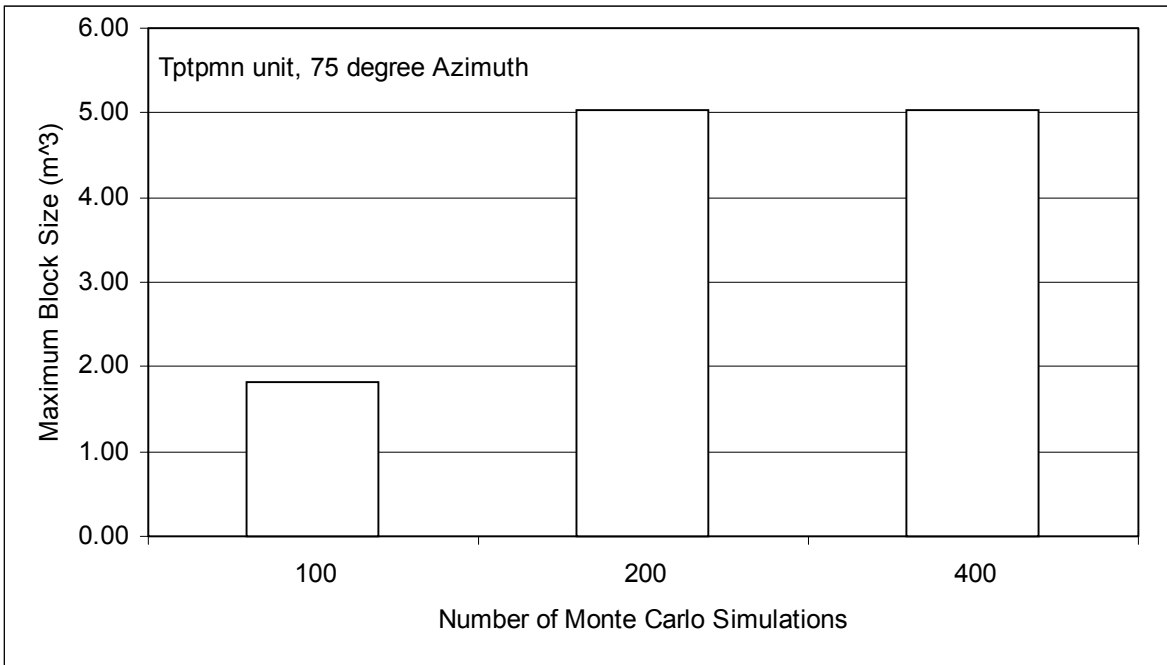


Figure IV-6. Predicted Number of Maximum Block Size, Tptpmn Unit

ATTACHMENT V
QUASI-STATIC APPROACH FOR SIMULATION OF SEISMIC EFFECT

QUASI-STATIC APPROACH FOR SIMULATION OF SEISMIC EFFECT

The probabilistic key block analysis code DRKBA considers only gravity load in its assessment of mechanical stability of key blocks. Due to this limitation, seismic loads can not be directly applied to the opening in the DRKBA analysis. An alternative method that applies a reduction of joint strength parameters was used to account for the seismic effect.

The following equation was used to calculate the reduced friction angle in the alternative method:

$$\Delta\phi = a \tan(PGA/1g) \quad (\text{Eq. V-1})$$

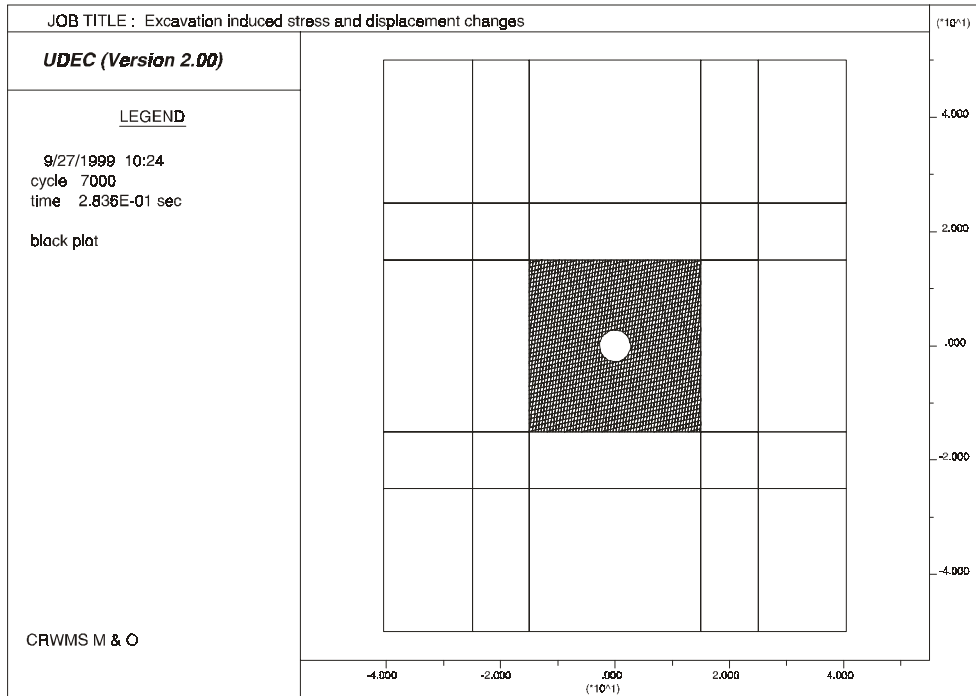
where PGA is the peak ground acceleration with unit in g .

This method is illustrated by the simple examples presented in [Figure V-1](#). The stable joint plane example is presented in [Figure V-1a](#). In this example, the alternative method (i.e., with a reduced friction angle) predicts a stable condition, which is the same as the approach with the seismic load included. The unstable joint plane example is presented in [Figure V-1b](#). The alternative reduced friction angle method is capable of predicting the unstable joint condition as shown.

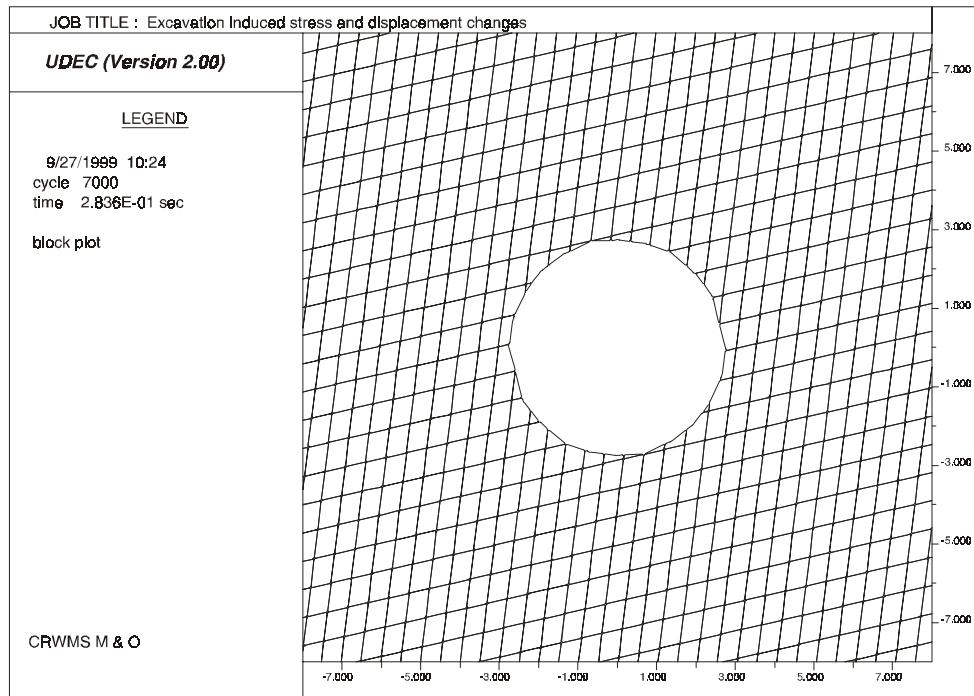
The alternative method was also verified using numerical simulation of a dynamic analysis against a quasi-static analysis. The numerical simulation was completed using the distinct element code UDEC (CRWMS M&O 1994). The mesh used for the UDEC analysis is presented in [Figure V-2](#). The fracture geometry resembles a typical cross section in the highly fractured Tptpmn unit. Two joint sets, one near horizontal and one near vertical, are simulated. The joint spacings for the near horizontal joint set and the near vertical joint set are 0.7 m and 0.5 m respectively. The dip angle for these two sets are 83° and 13° respectively. Due to the dynamic and static nature of the analysis, the boundary conditions differ for these two analyses. The boundary conditions imposed for these two analyses are listed in [Table V-1](#). The material properties used in the analysis and their sources are listed in [Table V-2](#).

The initial consolidation and excavation were first simulated as a typical static analysis. The dynamic boundaries were then imposed for the dynamic analysis with a 10 Hz sinusoidal shear wave at the bottom boundary. The peak particle velocity of 34 cm/sec (10,000-year event) was simulated as the peak velocity in the sinusoidal wave. The block movements around the opening after one full cycle of shear wave (duration of 0.1 second) are shown in [Figure V-3a](#). Blocks over the upper-right hand corner show large movement downward, also the lower-left hand corner show floor heaving due to blocks' upward movement.

As for the quasi-static analysis using the alternative method, joint cohesion and friction angle were reduced from 0.86 MPa and 41° to 0.1 MPa and 18° to account for seismic effect. The reduction of friction angle was calculated based on Equation V-1 with $PGA = 0.43 g$ for a 10,000-year event earthquake. The reduction of cohesion is included to ensure a conservative result, and is based on the time-dependent analysis described in [Attachment VI](#). The cohesion versus time relationship is shown in [Figure 8](#). A cohesion value at year 1,000 was selected based



(a) UDEC Mesh



(b) Blow-out of the mesh around opening

Figure V-2. Distinct Element Mesh for UDEC Analysis

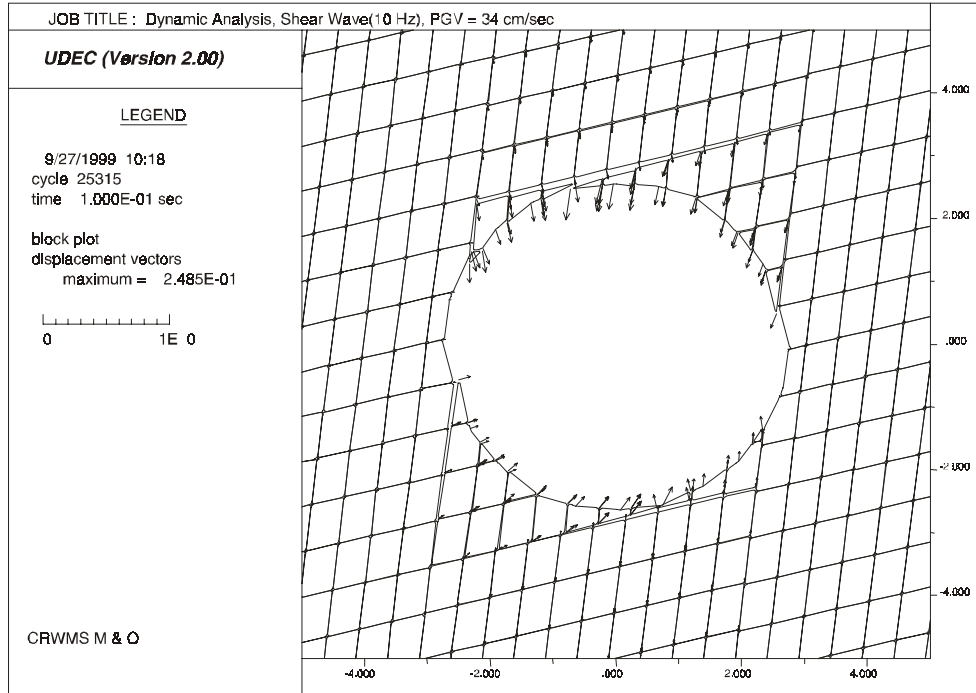
Table V-1. Boundary Conditions for UDEC Analyses

Boundary	Dynamic Analysis	Quasi-Static Analysis
Left	X free, Y fixed	X fixed
Right	X free, Y fixed	X fixed
Top	X and Y Viscous with overburden surcharge	Pressure boundary with overburden surcharge
Bottom	X and Y Viscous with shear wave velocity imposed	Y fixed

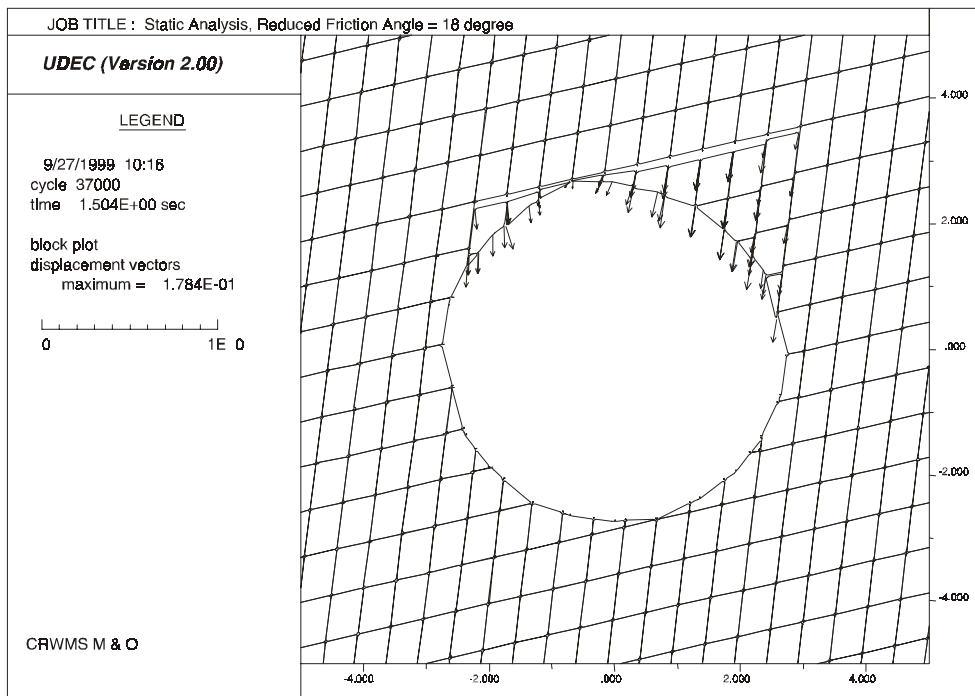
Table V-2. Material Properties Used in UDEC Analyses

Material Property and Unit	Value	Source ¹
Rock Mass Elastic Modulus (GPa)	33.03	CRWMS M&O 1997c, p. 5-88
Rock Mass Poisson's Ratio	0.21	CRWMS M&O 1997c, p. 5-96
Rock Mass Density (g/cc)	2.27	CRWMS M&O 1997c, p. 5-10
Joint Cohesion (MPa)	0.86	CRWMS M&O 1997c, p. 5-143
Joint Friction Angle (degree)	41	CRWMS M&O 1997c, p. 5-143

¹DTNs for the source data are provided in Table 2.



(a) Dynamic Analysis Result



(b) Quasi-Static Analysis Result

Figure V-3. Prediction of Block Movements from UDEC Analysis

ATTACHMENT VI
TIME-DEPENDENT AND THERMAL EFFECTS ON JOINT COHESION

TIME-DEPENDENT AND THERMAL EFFECTS ON JOINT COHESION

The site-specific time-dependent behavior of joint strength parameters for the host rock is not available at this time. An approach based on the time-dependent degradation work by Kemeny (1991) is used in this study. The approach assumes that the degradation occurs mainly due to the reduction of joint cohesion. Joint cohesion exists due to the asperities along the joint surface. These asperities may shear off with time and they may shear off due to the increased shear stress caused by the thermal effect. By using the numerical analysis results for the thermally induced shear stress and some site-specific data, the joint cohesion degradation with time can be quantified based on the approach reported by Kemeny and Cook (1986).

The equation for the mode II stress intensity factor (K_{II}) for a single asperity under shear and normal stresses can be expressed in the following (Kemeny and Cook 1986):

$$K_{II} = \frac{(\tau - \sigma_n \tan(\phi))2w}{\sqrt{\pi a(t)}} \quad (\text{Eq. VI-1})$$

Where τ is the shear stress, σ_n is the normal stress, and ϕ is the friction angle. The geometrical parameters w and a are shown in [Figure VI-1](#).

Crack growth occurs when K_{II} is equal to K_{IIC} . Equation VI-1 can be re-written based on the Mohr-Coulomb relationship as:

$$C_0 = \frac{K_{IIC} \sqrt{\pi a(t)}}{2w} \quad (\text{Eq. VI-2})$$

where C_0 is the joint cohesion.

A cohesion of 0.1 MPa is predicted using the parameters $K_{IIC} = 0.5 \text{ MPa (m)}^{0.5}$ and a_0 is equal to 0.0127 m. These parameters are therefore used as the initial parameters before time-dependent crack growth occurs. As the asperity size decreases due to time-dependent crack growth, the cohesion will decrease as given by Equation VI-2.

The time-dependent crack growth can be expressed using the following equation (Kemeny 1991):

$$\frac{d(a(t))}{dt} = A \left[\frac{K_{II}}{K_{IIC}} \right]^n \quad (\text{Eq. VI-3})$$

Combining Equations VI-1 and VI-3, the time-dependent crack growth can be written as:

$$\frac{d(a(t))}{dt} = 2^n A \pi^{-n/2} \left[\frac{w(\tau - \sigma_n \tan(\phi))}{\sqrt{a(t)} K_{IIC}} \right]^n \quad (\text{Eq. VI-4})$$

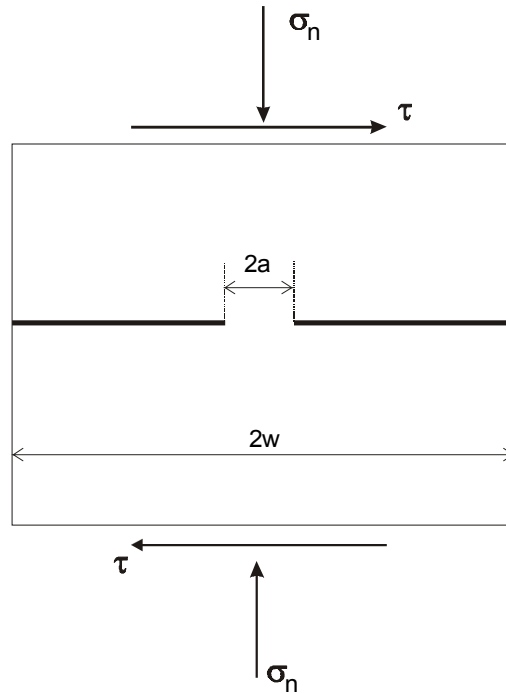


Figure VI-1. Parameters Used for Calculation of Mode II Stress Intensity Factor

Where A and n are subcritical crack growth parameters. Previous Yucca Mountain studies have used $n = 25$ and A ranging from 10^{-6} to 10^{-4} m/s (Kessler and McGuire 1996). A value for A of 10^{-5} m/s is used in this analysis.

The effective shear stress, $(\tau - \sigma_n \tan\phi)$, is time-dependent due to the thermal loading by the canisters. The thermal loading can cause horizontal stresses as high as 50 MPa in the backs of the underground drifts, decreasing the stability of some joints and increasing the stability of others. On average, it is found that the effective shear stress along the joints $(\tau - \sigma_n \tan\phi)$ increases by as much as 16% in the time period where heating of the rock occurs. The function used to describe the additional effective shear stress due to thermal heating is as follows:

$$f(t) = 1 + 0.00001044556 * e^{(120-t)/50} t^2 \quad (\text{Eq. VI-5})$$

This function is presented graphically in Figure VI-2. The figure shows that the shear stresses are increased by approximately 10% in the period between 50 and 200 years. Adding this function to Equation VI-4, the time-dependent crack growth expression is now:

$$\frac{d(a(t))}{dt} = 31536000 * 2^n A \pi^{-n/2} \left[\frac{w(\tau - \sigma_n \tan(\phi))(1 + 0.00001044556 * e^{(120-t)/50} t^2)}{\sqrt{a(t)} K_{IIc}} \right]^n \quad (\text{Eq. VI-6})$$

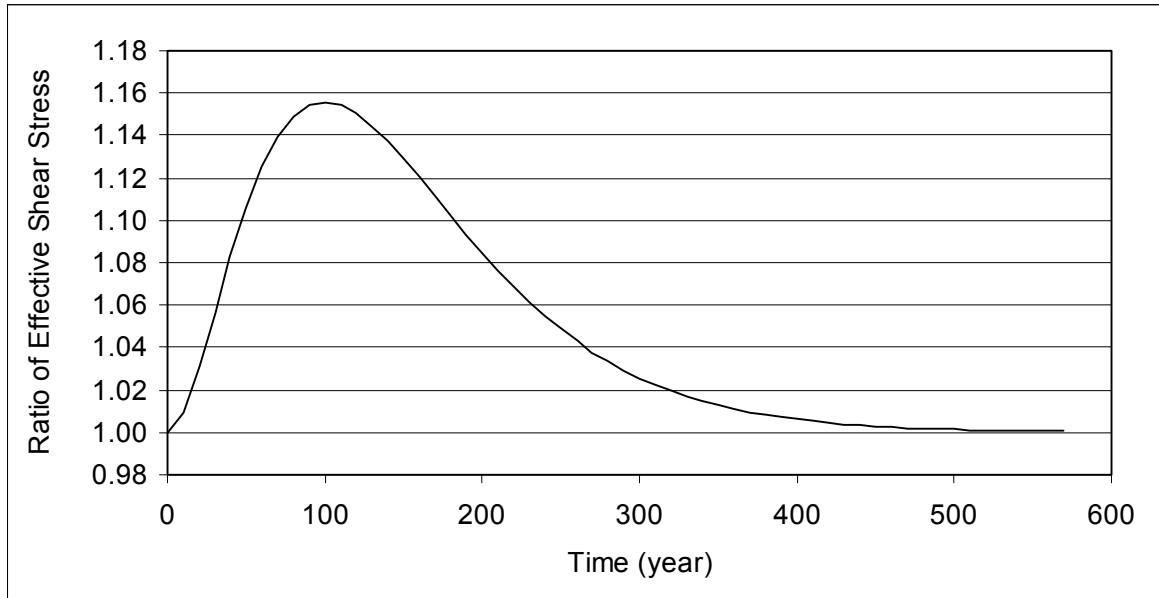


Figure VI-2. Function of the Additional Shear Stress Due to Thermal Loading

The nonlinear differential equation was solved numerically using MathCAD. The calculation results in an asperity vs. time relationship. This relationship is then used in conjunction with Equation VI-2 to obtain the cohesion values for various time.

Numerical analysis made for the in situ stress state give a range of effective shear stresses ($\tau - \sigma_n \tan\phi$) that range from 0.04 to 0.06 MPa. Calculations were made with effective shear stresses of 0.04, 0.0425, 0.045, 0.0475, 0.05, 0.0525, 0.055, 0.0575, and 0.06 MPa, and the results were averaged. This approach results in a stepped cohesion reduction over time as shown in Figure 8.